DEVELOPMENT OF NEW SENSITIVE THERMOLUMINESCENT MATERIALS FOR RADIATION DOSIMETRY

PhD Thesis

in

Engineering Physics

University of Gaziantep

Supervisor:

Assoc. Prof. Dr. A. Necmeddin YAZICI

Co-supervisor:

Prof.Dr.Ö.Faruk BAKKALOĞLU

By

Mehmet DOĞAN

January, 2008

GAZIANTEP UNIVERSITY
GRADUATE SCHOOL OF
NATURAL & APPLIED SCIENCES
Department of Engineering Physics

Name of the thesis : Development of New Sensitive Thermoluminescent Materials for Radiation Dosimetry
Name of the student **:** Mehmet DOĞAN
Exam date **: 18.01.2008**

Approval of the Graduate School of Natural and Applied Sciences

Prof. Dr. Sadettin ÖZYAZICI
Director

I certify that this thesis satisfies all the requirements as a thesis for the degree of Doctor of Philosophy.

Prof. Dr. Zihni ÖZTÜRK
Head of Department

This is to certify that we have read this thesis and that in our opinion it is fully adequate, in scope and quality, as a thesis for the degree of Doctor of Philosophy.

Prof. Dr. Ö.Faruk BAKKALOĞLU
Co.Supervisor

Assoc. Prof. Dr. A. Necmeddin YAZICI
Supervisor

Examining Committee Members	Signature
Prof. Dr. Zehra YEĞİNGİL	…….
Prof. Dr. Zihni ÖZTÜRK	…….
Assoc. Prof.Dr. A. Necmeddin YAZICI	……..
Assoc. Prof. Dr. İlyas EKER	…..…….…….……..
Assist. Prof.Dr. Metin BEDİR	.....…….

ABSTRACT

DEVELOPMENT OF NEW SENSITIVE THERMOLUMINESCENT MATERIALS FOR RADIATION DOSIMETRY

DOĞAN Mehmet

PhD in Engineering Physics Department

Supervisor: Assoc. Prof. Dr. A. Necmeddin YAZICI

Co. Supervisor: Prof. Dr. Ö. Faruk BAKKALOĞLU

18 January 2008, 146+XIII pages

In this work, the thermoluminescent properties of undoped, and rare earth and metallic elements doped some alkaline earth borates were studied. The following materials BaB_4O_7, LiB_3O_5, $Li_2B_4O_7$, MgB_4O_7 and CaB_4O_7 were synthesized by solid state and melting methods in air condition. The X-ray diffractometer method was firstly used to characterize and identify the products and then the various metals and rare earth elements were doped to enhance the thermoluminescence (TL) sensitivity of developed materials. Some of the TL properties of developed phosphors were studied in detail. Comparative TL studies of these compounds were shown that the Ce-doped BaB_4O_7 and Al-doped LiB_3O_5 compounds have higher TL sensitivity than the others. In addition, after the investigation of TL properties of Ce-doped BaB_4O_7 and Al-doped LiB_3O_5 samples, they seem as a good promising TL detector for different dosimetric applications owing to its simple glow curve structures with high sensitivity, the absence of thermal fading even at elevated temperatures, reduced light sensitivity, re-usability with excellent reproducibility and chemical stability. Therefore, it was assumed that the obtained Ce-doped BaB_4O_7 and Al-doped LiB_3O_5 crystal are quite suitable for use in high dose measurements in medical or industrial areas. The trap parameters namely the order of kinetics (b), activation energy (E) and frequency factor (s) associated with the glow peaks of some TL samples were also obtained by computer glow curve deconvolution (CGCD) method.

Keywords: Thermoluminescence, Dosimetry, Alkaline earth borates.

ÖZET

RADYASYON DOZİMETRİSİ İÇİN YENİ HASSAS TERMOLUMİNESANS MATERİYALLERİN GELİŞTİRİLMESİ

DOĞAN Mehmet
Doktora Tezi Fizik Mühendisliği Bölümü
Danışman: Doç. Dr. A. Necmeddin YAZICI
Yardımcı Danışman: Prof. Dr. Ö. Faruk BAKKALOĞLU
18 Ocak 2008, 146+XIII sayfa

Bu çalışmada; saf, metalik ve nadir toprak elementler katkılı bazı alkali toprak bor bileşiklerinin termoluminesans (TL) özellikleri çalışıldı. BaB_4O_7, LiB_3O_5, $Li_2B_4O_7$, MgB_4O_7, ve CaB_4O_7 borat bileşikleri, katıhal ve eritme metotları yöntemi kullanılarak sentezlendi. Öncelikle, geliştirilen ürünlerin, X-ışını yansıması metodu kullanılarak kristal yapısı analiz edildi ve sonra değişik metal ve nadir toprak elementler geliştirilen ürünlere katkılanarak onların TL hassaslıkları artırılmaya çalışılmıştır. Geliştirilen tüm malzemelerin bazı TL özellikleri detaylıca çalışılmıştır. Sentezlenen tüm malzemelerin karşılaştırmalı TL sonucunda, Ce-katkılı BaB_4O_7 ile Al-katkılı LiB_3O_5 bileşiklerinin daha fazla TL duyarlılığına sahip oldukları görülmüştür. Bununla birlikte oda sıcaklığında düşük ısısal sönümleri, basit ışıma eğrisi yapıları, kimyasal kararlılığı ve tekrar tekrar kullanabilirlikleri açısından bu iki ürünün tıp ve endüstriyel alanda yüksek doz ölçümlerinde TL dozimetresi olarak kullanılabilecekleri kanaatine varılmıştır. Son olarak, Bilgisayar İle Işıldama Eğrisi Ayrışımı (CGCD) metodu kullanılarak sentezlenen TL bileşiklerin tuzak parametreleri de bulunmuştur.

Anahtar Kelimeler: Termoluminesans, Dozimetre, Alkali toprak boratları.

ACKNOWLEDGEMENT

I would like to express my gratitude to all those who gave me the possibility to complete this thesis.

I am deeply indebted to my supervisor Assoc. Prof. Dr. A.Necmeddin YAZICI for his helps, stimulating suggestions and encouragement helped me in all the time of this research. I want to thank him for all his helps, support, interest and valuable hints.

I would like to thank my Ph.D thesis committee members Prof. Dr. Zihni ÖZTÜRK and Assoc. Prof. Dr. İlyas EKER for their valuable comments about my reports. I would also like to submit my thanks to Asst. Prof.Metin BEDİR, Res.Asst.Hüseyin TOKTAMIŞ and Res.Asst.V.Emir KAFADAR from the Department of Engineering Physics for supporting me in my research studies.

TABLE OF CONTENT

Page

LIST OF FIGURES

Page

LIST OF TABLES

CHAPTER I

INTROCUCTION

1.1. Basic Concepts of Luminescence in Solids

The process of emission by thermal stimulation from a crystalline solid after irradiations is called as “thermally stimulated luminescence” or simply “thermoluminescense (TL)’’ [1]. The TL belongs the class of phenomena involving light emission from solids (insulators or semiconductors) and then labeled as luminescence. The storage of radiation energy is an important feature for dosimetry which is generally favored by presence of activators namely impurity atoms and structural defects. The different kinds of luminescence phenomena are defined in literature according of the simulation method causing light emission. The most known of luminescence processes are [1]:

Thermoluminescence: released by increasing temperature;

Photoluminescence: obtained by stimulation with UV light;

Radioluminescence: stimulated by ionizing radiation;

Triboluminescence: stimulation due to mechanical stress;

Chemiluminescence: stimulated by chemical reactions;

Phosphorescence: excited by ionizing radiation, UV and visible light.

Thermoluminescence dosimetry (TLD) is based on materials which (after exposure to ionizing radiation) emit light while they are heated. The impurities in the TL material give rise to localized energy levels within the forbidden energy band gap which are crucial to the TL process. As a means of detecting the presence of these defect levels, the sensitivity of TL is unrivalled. The high TL sensitivity allows the determination of very low radiation doses. The sensitivity of thermoluminescent material varies depending on the type of dosimeter. On the other hand, it is known that there is a high relation between the luminescence and defects involved in this process [1].

The phenomena of thermoluminescence (TL) can be described as follows; a solid sample is excited by ionizing at a certain low temperature. The sample studied for its luminescence properties is usually insulator or semiconductor in which conduction is due entirely to the absorbed radiation energy. Radiation may take place in laboratory or environment. Another version is when it is a naturally occuring material irradiated by radiation field in its natural surrounding. A thermoluminescent material absorbs some energy which is stored during exposure to ionizing radiation. The storage capacity of a TL material makes it suitable for dosimetric applications. At the end of irradiation the sample is placed a suitable heater for heating. This period of heating is called as ‘’readout’’ stage. During this stage, the temperature of heater rose gradually at a constant heating rate. When the material is heated, the stored energy is released in the form of visible light as in shown Figure.1.1. The light emission is recorded as a function of temperature using the light sensitive detector called as photomultiplier tube. As a result; the graph of TL intensity is plotted against temperature.

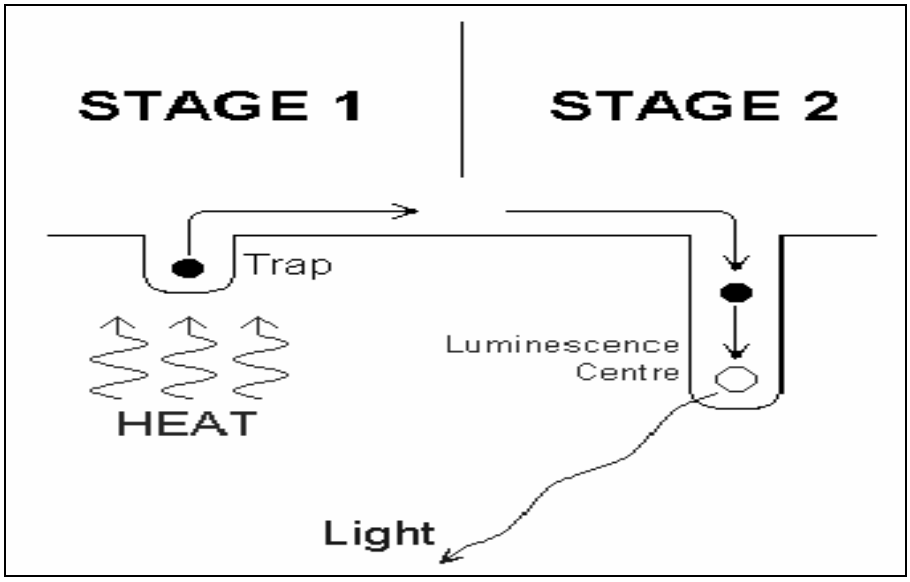

Figure 1.1. Phenomena of thermal excitation of luminescence

This graph, which is referred to as a *glow curve*, is a unique product of the TL measurement. A reference glow curve which was obtained from TLD-100 dosimeters is illustrated in Figure 1.2.

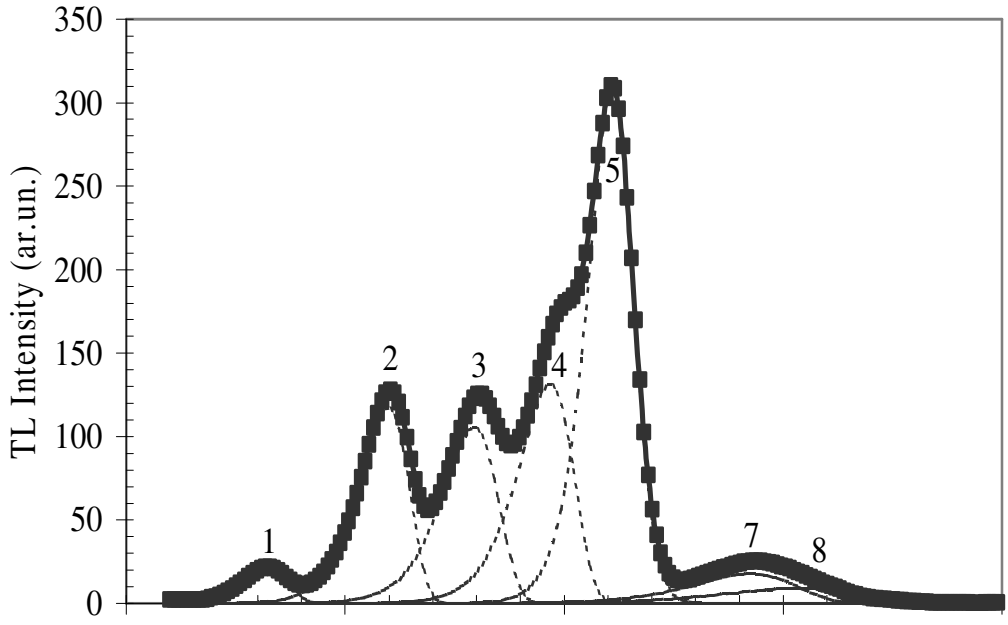

Figure 1.2. An analyzed glow curve of TLD-100 obtained at a linear heating rate of 2 ^{o}C/sec following β-ray exposure at room temperature for 1 min (Dots represent experimental points, solid line is the global fitting, dashed lines are fitted individual peaks).

A solid start to emit (infra) red radiation at higher temperatures (say in excess of 200 °C) which the intensity increases with increasing temperature. This is thermal or black body radiation. The TL material cannot emit light again by simply cooling the sample and reheating it another time. It should first be re-exposed to ionizing radiation before it produces light again. As a result, according to the TL phenomenon, the three essential ingredients are necessary to the production of TL intensity. Firstly, the material must be an insulator or semiconductor. It is necessary to mention that metals do not exhibit luminescent properties. Secondly, the material must have at some time absorbed energy during exposure to ionizing radiation. Thirdly, the TL emission is triggered by heating the material [2].

1.2. Principles of Thermoluminesce

In order to explain the occurrence of thermoluminescence single peak, there should be at least two kinds of imperfections existing in the crystal. When atoms of a crystal characterized by three-dimensional periodicity it is observed that there are some point defects within the crystal. Efficient thermoluminescent materials have a high concentration of traps, provided by structural defects and impurities [3]. A real crystal may contain defects which are basically of the following types;

1. Intrinsic defects; vacancies (or missing atoms), interstitials, aggregate forms of previous defects.
2. Defects induced by ionizing radiations: F centers, V centers, Vk centers…
3. Extrinsic (or impurity) defects: Substitutional impurities, interstitial impurities.

The traps are provided by lattice defects or impurities, the fixation between the conduction and valence band is energetically metastable. Upon irradiation of solids with ionising radiation, pairs of charge carriers (electrons and holes) are formed, which can move freely within the conduction and valence band, respectively. During the initial excitation, one of imperfection captures electrons and the other captures holes; the electrons and holes are produced in pairs by applied radition. As seen from Fig.1.3, the electron trapping state is often considered to be rather close the conduction and the hole trapping sate is far from valence band. In model, while heating the sample, the electrons are thermally released, usually to the conduction band, and then they may recombine with trapped holes, thus producing emitted photons. In this stuation, the hole trapping state is called the luminescence or recombination center and electrons trapping state termed the trap. In this case, during the heating, holes are raised (energetically) into the valence band and then recombine with trapped electrons. This band model is usually an oversimplification of more complex situation since it assumes the existence of only one trapping state and one kind of recombination center. It doesn't allow for any retrapping of free electrons. The lifetime of trapped electrons depends on the energy difference between conduction band and traps, therefore peaks occurring at higher temperatures are more stable. This effect of fading is influenced by the ambient temperature, but incident light can bleach TL traps as well. Furthermore, fast anomalous fading is assumed to be possible as tunnelling of the carriers through the potential barrier.

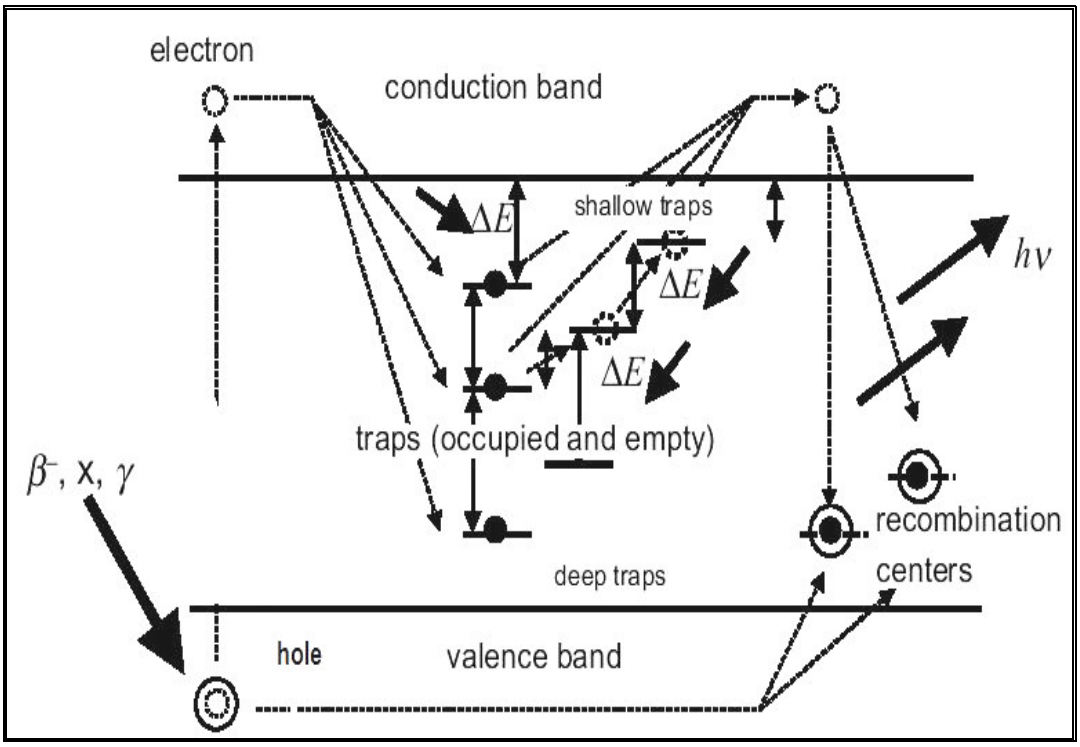

Figure 1.3. The scheme of luminescence excitation and emission in solids

1.3. Crystal Defects

Crystalline solids have a very regular atomic structure such that, the local positions of atoms with respect to each other are repeated at the atomic scale. These arrangements are called crystal structures, and their study is called ‘‘crystallography’’. The ideal crystal has an infinite 3D repetition of identical units, which may be atoms or molecules. Real crystals are limited in size, and they have some disorder in stacking which are called ‘‘defects’’. Crystal defects occur as points, along lines, or in the form of a surface, and they are called ‘‘point, line, plane defects, or volume defects’’ respectively [4].

1.3.1. Point defects

A point defect involves a single atom change to the normal crystal array. There are three major types of point defect: a) Vacancies, b) Interstitials and c) Impurities. They may be built-in with the original crystal growth, or activated by heat. They may be the result of radiation, or electric current etc. Point defects can be divided into Frenkel defects and Schottky defects, and these often occur in ionic crystals. The former are due to misplacement of ions and vacancies. Charges are balanced in the whole crystal despite the presence of interstitial or extra ions and vacancies. On the other hand, when only vacancies of cation and anions are present with no interstial or misplaced ions, the defects are called Schottky defects. Due to the defects, the ions have some freedom to move about in crystals, making them relatively good conductors [4].

a) Vacancies

A vacancy is the absence of an atom from a site normally occupied in the lattice (Fig.1.4a). The vacancies may be single or two (di-vacancy), three (tri-vacancy) or more.

b) Interstitials

An interstitial is an atom on a non-lattice site. There needs to be enough room for it, so this type of defect occurs in open covalent structures, or metallic structures with large atoms (Fig.1.4b).

c) Impurities

An impurity is the substitution of a regular lattice atom with an atom that does not normally occupy that site. The atom may come from within the crystal,

(e.g. a chlorine atom on a sodium site in a NaCl crystal) or from the addition of impurities (Fig.1.4c).

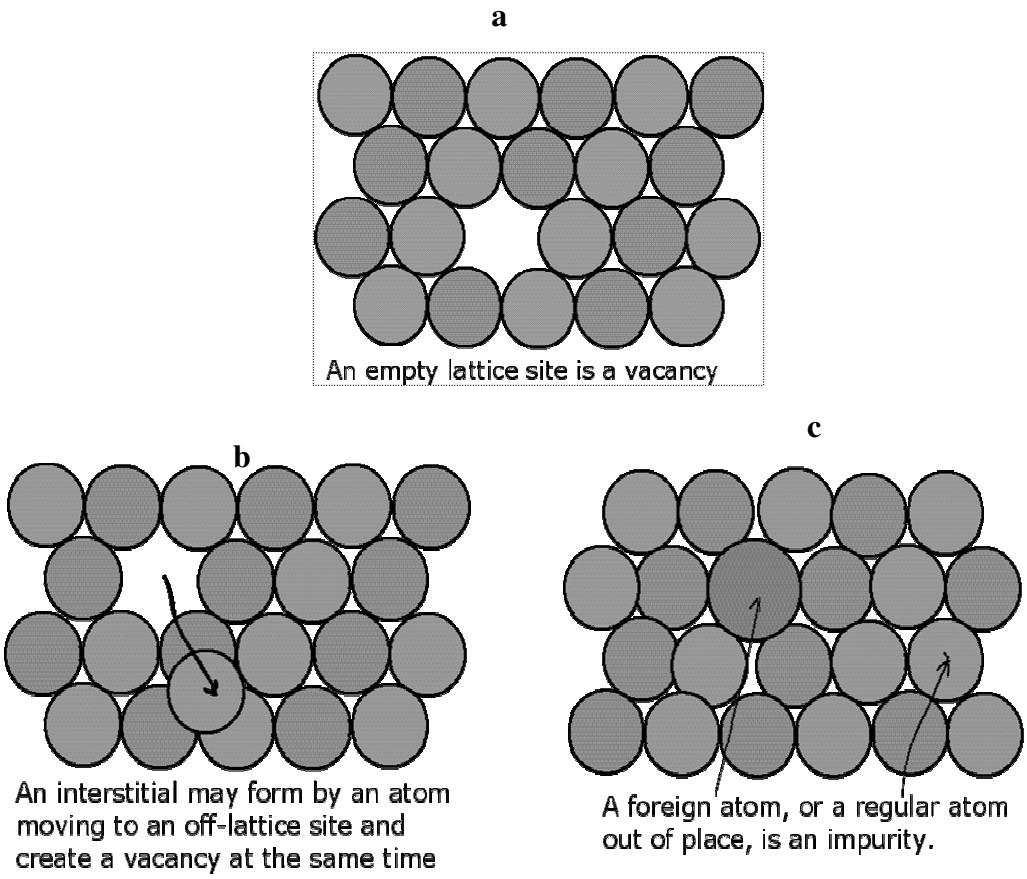

Figure 1.4. Point defects ; (a) vacancy, (b) interstitial, (c) impurity type defects

1.3.2. Line Defects

a) Dislocation

A dislocation is a line discontinuity in the regular crystal structure (Fig.1.5). There are two basic types: Edge dislocations, and Screw dislocations. An edge dislocation in a metal may be regarded as the insertion (or removal) of an extra half plane of atoms in the crystal structure. In ionic and covalent solids edge dislocations involve extra half planes of unit cells. The regions surrounding the dislocation line are made of essentially perfect crystal. The only severe disruption

to the crystal structure occurs along the dislocation line (perpendicular to the page). A screw dislocation changes the character of the atom planes. The atom planes no longer exist separately from each other. They form a single surface, like a screw thread, which "spirals" from one end of the crystal to the other. Combinations of edge and screw dislocations are often formed as edge dislocations can be formed by branching off a screw dislocation.

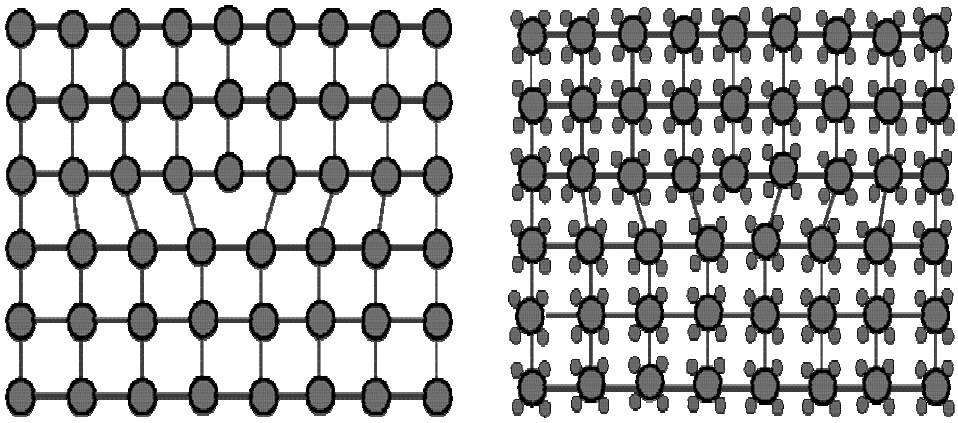

Figure 1.5. Line defects

1.3.3. Planar Defects

A planar defect is a discontinuity of the perfect crystal structure across a plane (Fig.1.6).

a) Grain Boundaries

A grain boundary is a general planar defect that separates regions of different crystalline orientation (i.e. grains) within a polycrystalline solid (Fig.1.6(a)). The atoms in the grain boundary will not be in perfect crystalline arrangement. Grain boundaries are usually the result of uneven growth when the solid is crystallising. Grain sizes vary from 1 μm to 1 mm [4].

b) Tilt Boundaries

A tilt boundary, between two slightly mis-aligned grains appears as an array of edge dislocations (Fig.1.6b).

c) Twin Boundaries

A twin boundary happens when the crystals on either side of a plane are mirror images of each other (Fig.1.6c). The boundary between the twinned crystals will be a single plane of atoms. There is no region of disorder and the boundary atoms can be viewed as belonging to the crystal structures of both twins. Twins are either grown-in during crystallisation, or the result of mechanical or thermal work.

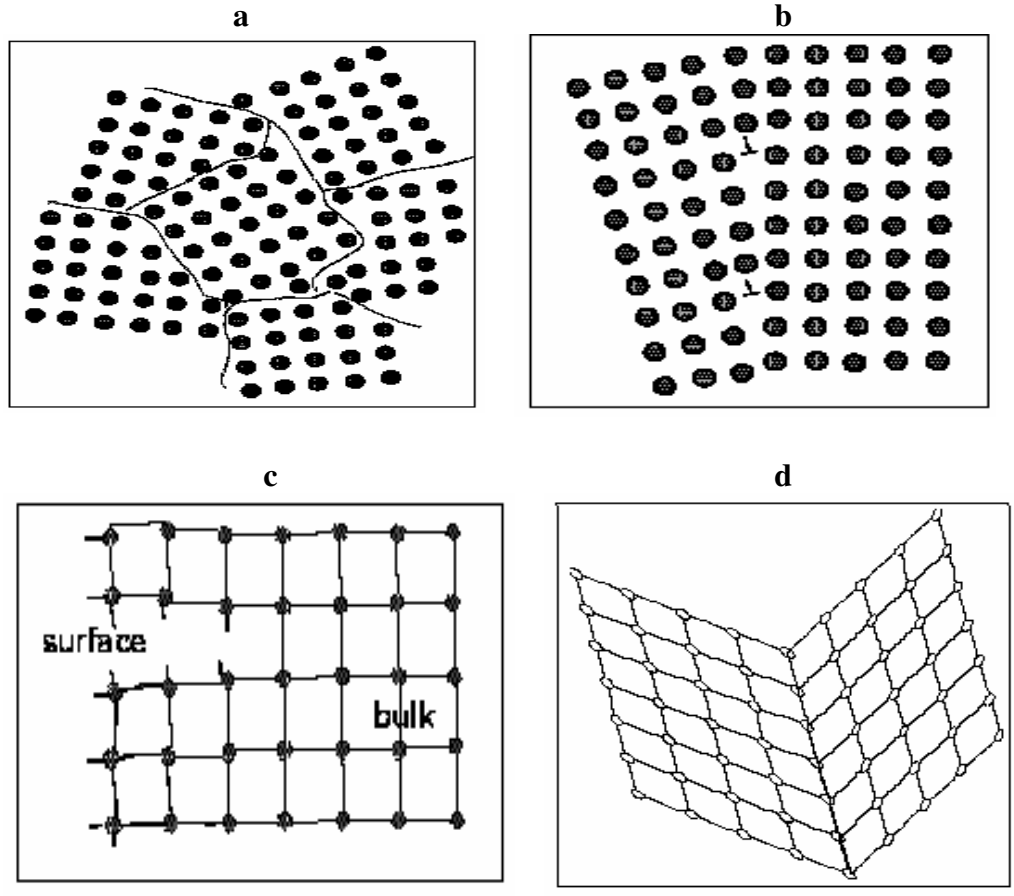

Figure 1.6. Planar defects. (a) Grain boundaries, (b) Tilt boundaries, (c) Twin boundaries, and (d) Microcracks

d) Microcracks

A microcrack occurs where internal broken bonds create new surfaces. They are about 10 μm in size and there is a tendancy to form on the surface of a solid rather than in the bulk. They also form at grain boundaries and other regions of disorder. The region across which the bonds are broken is known as the ‘‘separation plane’’. Microcracks are formed when there is abrasion (or impacts) with dust particles. When a crystal has more than one type of atom, there will be chemical as well as physical disorder in the grain-boundaries (Fig.1.6d).

1.3.4. Volume defects

Volume defects are voids, i.e. the absence of a number of atoms to form internal surfaces in the crystal. They have similar properties to microcracks because of the broken bonds at the surface. Microcracks and Voids can exist in both crystalline and amorphous solids.

1.4. Applications of Thermoluminescence

The thermoluminescence phenomena has many applications in human life. Some possible applications of TLD -measurements are [5].

In radiation monitoring:

Personnel monitoring: the primary objective of personnel dosimetry is to monitor the radiation dose delivered to personnel during routine occupational exposure. Examples include workers at nuclear reactors, hospital radiotherapy technicians or naval person on nuclear powered vessels. A personnel dosimetry also includes the determination of observed doses caused by accidental exposure to radiation.

Environmental monitoring: the continuous monitoring of radiation released to environment has become a major concern for industrialized nations and TLD usage in an important factor in this type of activity. The interest is increased exposure to harmful radiations that people can expect on long-term, manned space flights. Additional concern lies in the prolonged exposure of electronic components where the decreasing scales of the active regions in these devices.

In nuclear medicine:

The small size and high sensitivity of TLD materials has long been exploited in clinical studies since the TLD samples can be inserted into appropriate openings in human body before exposing the patient to ionizing radiations during diagnosis and/or therapy; a) Therapy monitoring, b) Measurement of doses in sensitive organs and areas, c) Internal emitter dosimetry, and d) Phantom dosimetry.

In experimental dosimetry:

a) Natural background studies, b) source calibrations, c) high energy physics studies

In geology:

One of important application of thermoluminescence is its use in the dating or archaeological and geological samples. For example thermoluminescence could also be used for estimating the age of rocks [6-7].

1.5. The General Characteristics of TL Dosimeters

A radiation dosimeter is a device, instrument or system that measures or evaluates, either directly or indirectly, the quantities exposure, kerma, absorbed dose or equivalent dose, or their time derivatives (rates), or related quantities of

ionizing radiation. A dosimeter along with its reader is referred to as a dosimetry system. In order to be useful, radiation dosimeters must exhibit several desirable characteristics. For example, in radiotherapy exact knowledge of both the absorbed dose to water at a specified point and its spatial distribution are of importance, as well as the possibility of deriving the dose to an organ of interest in the patient. In this context, not all of the numerous known TL phosphors are suitable for radiation dosimetry. For a suitable radiation dosimeter, TL phosphor is expected to show following characteristics [5]:

1. Relatively simple glow curve structure, temperature of main peak T_m at about 180-250 ^{o}C. At higher temperature the infrared emission from the hot sample and sample holder increasingly interferes with the measurement of low doses.
2. High sensitivity, which consists of both high efficiency of light emission and low threshold dose. The desirable properties of TLD materials include a linear response to absorbed dose and an adequate sensitivity. The dose response of most TL materials is far from linear, however, displaying a variety of non-linear effects depending upon the dose range and irradiation.
3. High resistance against environmental factors as humidity, solvents, light long term stability of stored information at room temperature (low fading). A sufficient storage stability of electrons (or holes) in traps to cause no desirable fading even during extended storage at ambient or slightly increased temperatures or in biomedical implantation studies, or body temperature.

4. Low photon energy dependence of response and a linear response over a range of doses are, for most application, the desirable features. Depending on the particular use, high or low thermal neutron sensitivity or a certain LET response may also be the desirable characteristic.
5. Effective atomic number Z_{eff} closes to that of biological tissue, in order to deal with a tissue equivalent material.
6. The phosphor should not be very expensive. It is preferred to be easier and cheaper to work with a ‘‘one way’’ dosimeter and nontoxic. It should be possible to use a small sample only. It may be advantageous if the material can easily be prepared with reproducible properties in a normally equipped chemical laboratory [2,8].
7. The TL samples should not contain any toxic substances which are harmful to human body.
8. Wavelenght of a released light from the TL materails should be in visible region.
9. Simple annealing procedure for reuse.

In fact only a few of materials match to these properties. In general nominally pure compounds, such as salts and oxides show weak TL signals and they are not considered as efficient dosimetric materials. But when they are doped with proper impurities, which act as activators of host materials, much higher efficiencies can be obtained after the doping.

1.5.1. Dose response curves

The TL signal is a function *(F)* of the absorbed dose *D*. Ideally *F(D)* shows a linear dose response over a wide dose range at least over the range of interest of application. The most of materials used in practical dosimetry show a variety of non-linear effects. A pattern that is found frequently as the dose is increased is first a linear response, then a supralinear and finally during the approach to saturation a sublinear response. The normalized dose response function (also called the supralineary index) *f (D)* is defined as [9];

$$f(D) = \frac{F(D)/D}{F(D_1)/D_1} \tag{1.1}$$

where *F(D)* is dose response at dose *D* and D_1 is a low dose at which the dose response is linear. The ideal TLD material has $f(D) = 1$ in a wide dose range. If $f(D) \rangle 1$ the response is called supralinear, if $f(D) \langle 1$ is called sublinear. These features are illustrated in Figure 1.7.

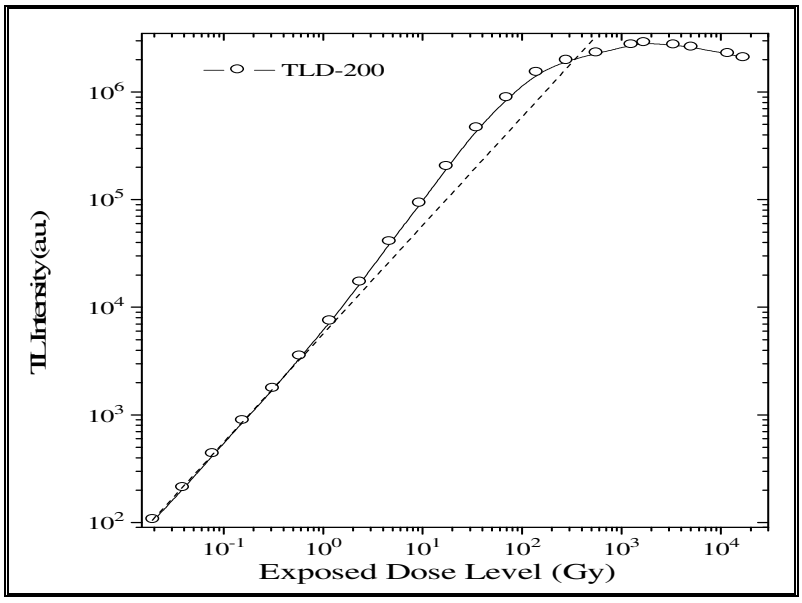

Figure 1.7. Example of dose response curve of dosimetric peak of CaF_2:Dy (TLD-200) material

1.5.2. Energy response

In many TLD applications, the main response is to determine the dose absorbed in human tissue. Due to this reason it is desirable that the TLD has an energy response equal or at least proportional to that of human tissue. If a TL materail is exposed to photons with a certian fluence Φ and energy *E,* so the absorved dose in that TL materail D_{TL} can then be written as;

$$D_{TL} = \Phi E(\mu_{en}/\rho)_{TL}, \tag{1.2}$$

where $(\mu_{en}/\rho)_{TL}$ is the mass energy absorption coefficient of the TL material.

If the TL material is replaced by tissue, i.e. exposed to photons with the same Φ and *E* then for the absorbed dose in tissue a similar equation follows;

$$\frac{D_{TL}}{D_{tissue}} = \frac{(\mu_{en}/\rho)_{TL}}{\mu_{en}/\rho)_{tissue}}, \tag{1.3}$$

where $(\mu_{en}/\rho)_{tissue}$ is the mass energy absorption coefficient of tissue. In Fig.1.8, this ratio has been plotted for several TL materials as a function of the energy [10]

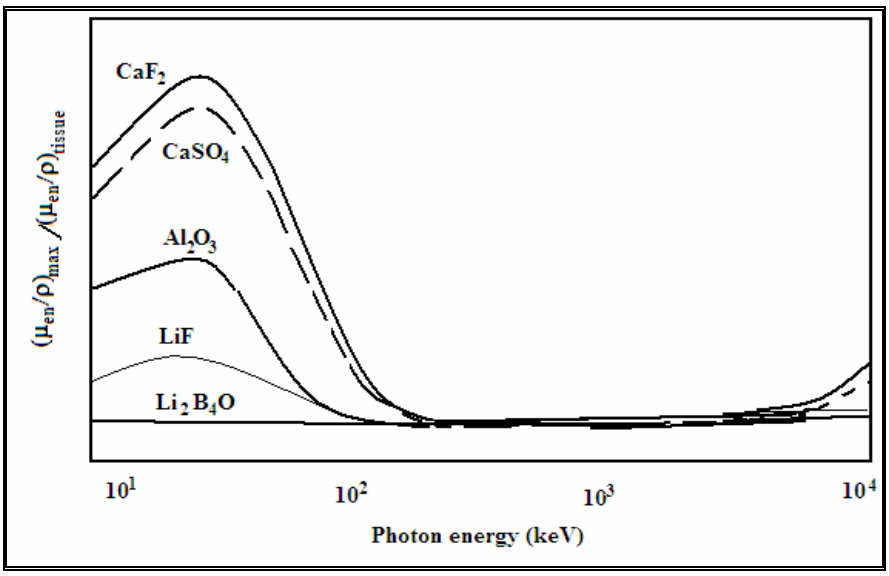

Figure 1.8. Photon energy response for a few indicated TLD materials. (The reference material is soft tissue with Z_{eff}=7.35)

As seen from the Fig.1.8, the ratio is constant above 200 keV for all materails. In the mentioned energy region the photoelectric effect is dominant. The photoeelectric component of mass energy absorption coefficient of certain element varies approxiametly as $Z^3 - Z^4$. In order to characterise the energy response with one number instead of whole curve the concept of effective atomic number Z_{eff} has been introduced as [11];

$$Z_{eff} = \sqrt[m]{\sum_i a_i Z_i^m} , \tag{1.4}$$

where a_i is the fractional electron content of element *i* with atomic number Z_i. The value of *m* will be typically range from 3 to 4, with 3.5 a reasonable value. Tissue is defined as Z_{eff}=7.35. The TL material is called tissue equivalent material if its Z_{eff} value is the same or near the Z_{eff} of human body. As seen from Fig.1.8, $Li_2B_4O_7$ is almost tissue equivalent.

1.5.3. Sensitivity

The sensitivity of a particular TLD material is defined as the TL signal (peak height or TL intensity integrated over a certain temperature region) per unit absorbed dose and per unit mass. As defined where, it depends upon the read-out system used in the measurement. This includes many parameters such as heating rate and light detection system, etc. Especially the efficiency of the light detection system (including the geometrical light collection efficiency, optical filters and detector efficiency) is difficult to measure in an absolute sense. Therefore, one normally defines a relative sensitivity by comparing the TL signal from the material of interest with the TL signal from LiF (TLD-100), since this latter material is

widely used. Apart from the TL reader equipment properties and the read-out conditions the TL signal will, of course, depend on the TL material itself. The sensitivity depends on the type and energy of the ionizing radiation. In general low LET radiation (photons, beta particles) shows a higher TL signal than high LET radiation (alpha particles, neutrons). The gamma radiation of the decay of β is widely used as reference radiation [9].

1.5.4. Annealing behaviour

One of the attractive points of TLD is the possibility to reuse the TL material many times. The TL material has precisely the same properties as before a thermal annealing procedure is required to reuse. This pre-irradiation annealing consists of holding the sample at an elevated temperature for some time followed by a cooling to room temperature at a certain cooling rate α. Sometimes this is followed by a low temperature anneal. The annealing procedure serves for several purposes. Firstly, it empties all the traps as far as this has not happened during the read-out, i.e. it resets the TL signal to zero. Secondly, it re-establishes the thermodynamic defect equilibrium which existed in the material before irradiation and read-out. During irradiation and the read-out this equilibrium is disturbed and the reaction is pushed back in the opposite direction by thermal annealing. Finally, it resets the occupancy of the deep, thermally disconnected, traps. They are not always present but, if so, they influence the TL sensitivity of a given peak since they act as competitors [3].

CHAPTER II

LITERATURE SURVEY

2.1. Historical Overview of Thermoluminescence

The first TL observations were performed on natural minerals, as diamonds or fluorspar, and were first described for diamonds by Robert Boyle in 1663 [3]. A much more spectacular TL effect of a green fluorspar known as false emerald was used for scientific entertainment, and then the powdered mineral was dusted as letters or figures on a metal plate and heated. In the 18th century, a TL of minerals such as rock crystal, amethyst, topaz and of calcite, had ben described. By the end of the 18th century, a relationship of thermoluminescence and phosphorescence as well as triboluminescence was evident. In the early 19th century, the electric spark was observed to induce TL by exposure to its light. Calcareous biominerals, as mother of pearl, scallop shells and egg shells, gave spark-irradiated an orange-red TL. A colouration of fluorspar by spark irradiation was observed to vanish after heating [3].

Finally in 1888, Wiedemann introduced the term luminescence for the observation of excess light emission over the thermal background. Wiedemann and Schmidt (1895) were the first to detect thermoluminescence (TL) of substances irradiated with cathode rays and they were also the first to investigate TL activators

systematically [12]. Cathode rays, X-rays and the detection of natural radioactivity opened the way to induce TL experimentally in natural and synthetic minerals. The role of luminescence activators, especially manganese, iron and rare earth elements, has since then been a subject of intense studies supported by the availability of artificial irradiation sources and refined analytical methods. The first glow curves (measured light intensity vs. temperature) were recorded by Przibram and his co-workers [13] (1922-23) at the Radium-Institut in Vienna. Various minerals, as alkali halides, calcium carbonates, silicates, and of course the wide variety of fluorites, were usually exposed to radium sources or X-rays, and the resulting luminescence investigated visually, recorded spectrographically or measured by photoelectric detectors.

The first theoretical model of TL was proposed by Randall and Wilkins (1945) for first order kinetics [14] and later extended by Garlick and Gibson (1948) for second order kinetics [15]. Meanwhile, work concentrated on geological materials, trace impurities, and development of dosimeter substances doped with such metal traces. First attempts to apply TL on biogenic calcium carbonates were performed by Johnson (1960) showed that calcitic mollusc shells are suitable, whereas aragonitic shells do not emit TL [16]. In the subsequent years, TL was adapted as a method of geological, paleontological and archaeological dating of rocks, soils, sediments, weathering deposits, fossil bones, shells, pottery and other ceramic materials. Thermoluminescence as a method for the detection of food irradiation has been developed after 1985 for irradiated spices, herbs, fruits, vegetables, and mushrooms, using the TL of mineral particles. Such particles were also isolated from the intestines and legs of marine crustaceans.

The first application of this phenomenon for dosimetric purposes was from Daniel and his friends [17]. Since then much research has been carried out for a better understanding and improvement of the material characteristics as well as to develop new TL materials. Nowadays, the TLD is a well-established dosimetric technique with applications in areas such as personnel, environmental and clinical dosimetry [18].

The TL is a widespread phenomenon. About three quarters of 3,000 natural minerals exhibit TL effect; some minerals as fluorite (CaF_2) from certain areas in Iceland, Brazil, Turkey and India are among the most sensitive phosphors known [19-20]. The TL effect is not restricted to inorganic crystals and glasses, but TL from organic compounds such as various polymers [21-22]; and others including Teflon [23], polyethylene, and polypropylene [24] usually occurs below room temperatures. They aren't interesting for practical dosimetry.

Early investigations of artificially activated TL phosphors such as $CaSO_4$:Mn date back to the turn of the century [25]. This material was used in 1935, and again since 1949 in rocket experiments for UV dosimetry [26-27], and 1954 was employed in the first medical dosimetry studies with TLD [28]. The effect of X-ray on CaF_2 was firstly studied by Wick and Slattery in 1928 [29]. Mangenese-activated CaF_2 was introduced in mid-1950's as a sensitive and stable material which has one major glow peak [30-31-32].

Lithium fluoride dates back to the late 1940's and early 1950's, when Daniels and his students [17] at university of Wisconsin studied the TL of alkali halides [33]. They used pressed pellets of lithium fluoride powder for dosimetry experiments. Lithium fluoride that is activated with magnesium and titanium, called

‘‘TLD-100,’’ dominated the low *Z* detector market for following years and is still the most used TL phosphor [34-35]. Manganese-activated lithium borate and beryllium oxide [36,37] have been the most successful more recent low Z_{eff} materials so far.

Considerable efforts have been devoted during the past 50 years to the improvement of sensitivity and stability of high Z_{eff} materials [38,39]. Natural fluorites [40-41] turned out to be not too successful, and TL glasses [42,43] could never seriously compete with crystalline phosphors. High sensitive phosphors such as $CaSO_4$:Mn, CaF_2:Dy turned out to be not stable enough for long-term experiments, but other, equally stable and more sensitive materials ($CaSO_4$:Dy, $CaSO_4$:Tm) became available [17]. This field is still progressing rapidly with new detector materials or modified old ones.

A big volume of information has been published on the thermoluminescence in general and specific applications, including dosimetry. Total number of publications on the TLD is approaching 3000 and is increasing at rate of 200 papers per a year.

2.2. General Characteristics of Borates

There are literally hundreds of forms and uses of borate products in industry and science. The following are the most frequent uses areas of the borates: In agriculture, ceramics**,** detergents**,** fiber glass, glass, flame retardants, wood treatment, cellulose insulator, plastics, textiles, paper, metallurgy, and pharmaceutical products. Borates are important materials due to their wide usage in glass, abrasives, refractories, cleaning compounds, fibres and composites to flame

retardants, fuels, glazes, frits etc [44]. They can be used in medical nuclear applications, agriculture and TL dosimetery. Borates reduce the thermal expansion of glass; provide very good resistance to vibration, high temperature and thermal shock. About 230 natural occouring minerals of borates were defined in the world. Turkey has the world's largest borates reserves. The Kırka borate deposit, in western Turkey, the most important B_2O_3 producer at present in the world, exhibits a symmetrical zonation in a lateral sense; it is comprised of: a central body of sodium borate (borax), an intermediate zone of Na–Ca borate (ulexite), and a marginal zone of calcium borate (colemanite). This mineral zonation is also developed in a vertical sense, although it is somewhat asymmetrical because of the presence of a discontinuous magnesium borate horizon overlying the central body of borax. The genesis of such a mineral zonation in the Tertiary lacustrine borate deposits of the world has been attributed to a number of diagenetic processes.

Many materials are today used in radiation dosimetry as the TL phosphors, which may show different sensitivies as well as large differences in the linearity to the response to dose. The most widely used thermoluminsecent materials consist of salts or oxides of alkaline or alkaline earth metals, activated by rare earth or metal ions impurities. In general, all TL phospors can be roughtly classified, depending on their effective atomic number Z_{eff} , into two main groups; The first one includes tissue-equivalent materails (Z_{eff} close to 7.4), while the second one is given by systems with higher atomic numbers. Due to growing interest in radiation dosimetry in environmental, personal and clinical applications, several efforts are in progress in order to produce new and high performance TL materials [45,46]. Our attempt is to research alkaline earth borats activated by rare earth and or metal

ions impurities. Due to their great importance, this work has been aimed to research, design and study novel crystalline materials for high-efficient TLDs of radiation.

In the framework of this thesis, the following objectives are introduced;

1. To develop and optimize borate base TL materials doped with rare earth and metallic elements in high temperature conditions;

2. To study and test the TL and dosimetric properties of them;

Very few results have been published on the thermoluminescence of alkaline earth borates. Because of the important features of alkaline earth borates, it is thought useful to undertake a further study on of these materials. Thermoluminescence studies of borate compounds were started in 1974 by studies of Kazanskaya [47]. Since then, detailed TL studies on various alkaline earth borates were reported [38,48,49,50].

2.3. Literature Survey on the Thermoluminescence Properties of BaB_4O_7

Manam and S. K. Sharma firstly reported in 2004 thermally stimulated luminescence (TSL) studies of BaB_4O_7 compound [48]. The polycrystalline sample of BaB_4O_7 was prepared by a melting method and the formation of the BaB_4O_7 compound was confirmed by an X-ray diffraction study. The compound has orthorhombic structure at room temperature. The TSL glow curves of BaB_4O_7 compound when heated at a constant heating rate of 4 $^oC/s$ exhibit two thermoluminescence (TL) glow peaks at 110 and 150 ^oC followed by a shoulder around 210^oC.

Sangeeta and S.C. Sabharwal reported the kinetics of thermally stimulated emission (TSL) from XB_2O_4 (X= Ca, Sr, Ba) has been investigated employing both isothermal decay and peak shape analysis methods in 2004 [49]. For BaB_2O_4 the emission was observed to lie in the visible region and the kinetics of TL emission could be determined without any ambiguity. However, the emission spectra of CaB_2O_4 and SrB_2O_4 were found to consist of two broad emissions: one in the UV and the other in the blue green regions. Consequent to the presence of two emission bands, the determination of TL kinetics required collection of TL data for the two components of emission separately [49].

Juan Li and his friends had an experimental study such that they have prepared the polycrystalline powder of dysprosium-doped BaB_4O_7 phospor by solid-state reaction in air with high temperature [50]. The TL glow curves and three-dimentional (3D) TL emission spectrum was studied in 20-130 kGy dose range The emission bands about at 480, 575, 660 and 750 nm were observed in the three-dimensional (3D) emission spectrum.

2.4. Literature Survey on the Thermoluminescence Properties of MgB_4O_7

This phosphor is a near tissue equivalent material with an effective atomic number for photoelectron absorption equal to 8.4. The preparation of polyscrystalline magnesium borate activated by dysprosium has been reported at first in 1971 by Hitom *et al* [51], it was improved by Prokic is reported by different authors as having one dosimetric peak whose temperature varies from 158 ^{o}C to 217 ^{o}C as obtained with different heating rates [52].

T. Karali and his team mates presented X- ray excited TL spectra of magnesium borate doped with either single rare earth ions Dy or Tm, or co-doped with Dy/Tm, Tm/Mn or Dy/Tb [53]. Intrinsic emission from the host material was found in the UV/blue region at approximately 375 nm, with a tail extending to 200 nm. The main dosimetric peak is detected at approximately 180 ^{o}C but slight differences are noted between the glow peak maxima from the different rare earth ions and there were changes following thermal treatments.

Environmental radiation monitoring in the vicinity of coal-fired power plants which are used primarily to determine the variability in measured background exposures were presented by F. Adrovic [54]. Measurements have been done using a multi-element, high sensitive dosemeter system composed of three solid, properly filtered, sintered $CaSO_4$:Dy thermoluminescent detectors, and one low-atomic number MgB_4O_7:Dy,Na thermoluminiscencent detector produced at the Vinca Institute .

Thermoluminescent dosimetric characteristics of MgB_4O_7:Dy,Na were presented by Furetta [55]. The following TL dosimetric properties of this material were examined in that study; the shape of glow curve, TL sensitivity, annealing procedure, photon dose response, and minimum detectable dose, precision of TL measurements, reproducibility, and energy response and fading characteristics.

Sensitivity and fading characteristics of thermoluminescence magnesium borate was reported by C.M.H. Driscoll et al [56]. The new tissue equivalent magnesium borate has been studied and compared with those established materials.

Furetta was reported some thermoluminescence characteristics of magnesium borate activated by Dy and Na, namely the thermoluminescence (TL)

response of absorbed dose and the fading behavior [57]. Magnesium borate activated by Dy and Na shows a very good linear range of the TL response as a function of the absorbed dose as well as a low threshold dose.

Pradhan has investigted the general characteristics of MgB_4O_7:Dy, $Li_2B_4O_7$:Cu,Ag, $Li_2B_4O_7$:Cu as promising TL dosimeters due to their tissue equivalent effective atomic number [58].

A thermoluminescent material based on MgB_4O_7:Dy was also developed at the Boris Kidric Institute of Nuclear Sciences and characterized by L.L Campos and O.O. Ferando Filho [59] .

J.H. Souza et al [60] done two sets of experimental studies followed by computer analysis of more than 200 glow curves indicate that a combination of at least eleven peaks of first order kintetics is necessary to describe the glow behavior of MgB_4O_7:Dy. It was found that for a heating rate of 1 $^oC.s^{-1}$ the maximum intensity of individual peaks are situated the following temperatures: 101, 110, 126,142, 155, 160, 173,192, 224, 231 and 304 ^oC.

2.5. Literature Survey on the Thermoluminescence Properties of CaB_4O_7

The TL characteristics of glass containing divalent copper were studied by Fukuda *et al* [61]. The TL of X-ray irradiated borate containing copper (0.01 to 1.0 mol %) has ben studied. Thermally stimulated current (TSC) for X-ray irradiated glass showed maxima in temperature region 90-100 ^oC.

The TL in sintered CaB_4O_7 doped with activators Eu, Dy, Pb and Cu was investigated bu Y.Fukuda and his friends [62].

The effect of lithium co-dopant on the thermoluminescence of some TL phosphors has been studied by Mirjana Prokic [63]. Results show that lithium co-dopant when present in $CaSO_4$:Dy, $CaSO_4$:Tm, CaF_2:Mn, MgB_4O_7:Dy, MgB_4O_7:Tm, MgB_4O_7:Tb, MgB_4O_7:Mn, CaB_4O_7:Dy and CaB_4O_7:Tm thermoluminescent phosphors induces higher luminescence efficiency either due to better incorporation of activator ions or due to improvement in energy transfer processes.

Glass compositions with calcium tetraborate (CaB_4O_7) and calcium metaborate (CaB_2O_4), such as the $x CaB_4O_7 - (100-x)\ CaB_2O_4$ system ($0 \leqslant x \leqslant 100$ wt%) were obtained by the traditional melting/quenching method by S.S. Rojas [64]. The Dy doped and Li co-doped $80CaB_4O_7–20CaB_2O_4$ (wt%) glass samples were studied by the thermoluminescence technique. The addition of Dy improved the signal sensitivity in about three times with respect to the undoped glass sample. The addition of Li as a co-dopant in this glass caused a shift to a lower temperature of about 20 °C in the main glow peak.

2.6. Literature Survey on the Thermoluminescence Properties of LiB_3O_5 and $Li_2B_4O_7$

Lithium Triborate (LiB_3O_5) is a non-linear optical (NLP) crystal. Mazzetti and Carli proved the existence of LiB_3O_5 compound in 1926 [65] and followed by Rollet and Bouaziz [66].

In 1999, Moryc and Ptak studied the infrared spectra of LBO [67]. The samples were made from lithium carbonate, natural boric acid, boric acid

containing isotope ^{10}B (94.4%) and ^{11}B (98.4) and hydrated lithium hydroxide with ^{6}Li isotope .

Ogorodnikova and his colleague have studied the recombination processes and lattice defects in crystals of alkali metal borate LiB_3O_5 (LBO) by the means of the TL and electron spin resonance (ESR) techniques [68]. N. Senguttuvana and his collogues reported crystal growth of LBO doped with Ce, In, Ni, Cu and Ti and some studies on their luminescent properties. Crystals were grown by the Bridgman method. The Ce-doped compound showed strong emission at 375 nm for two excitation peaks at 270 and 320 nm [69].

El-Faramawy *et al* reported the dosimetric properties of Cu-doped lithium borate [70]. The temperature at wich the TL is observed to be most intensive is at 178 ^{o}C. This study indicated that that material has low fading and wide linear dose response. Different concentrations from copper were added to lithium borate, as a doping material to get a good dosimeter compatible with the commercial one.

C. Furetta *et al* investigated the thermoluminescence properties of $Li_2B_4O_7$ polycrystaaline powder undoped and doped with Cu or Eu impurities in 1996 [71]. In the case of $Li_2B_4O_7$:Eu, a high temperature thermoluminescence peak caused by the impurity is observed at any dopant concentration. Comparison with data concerning undoped $Li_2B_4O_7$ allows for idetification of the contributions of impurities to the glow curves.

M. Danilkina *et al* were investigated the false-dose effects in the thermoluminescent detectors of ionizing radiation based on $Li_2B_4O_7$:Mn,Si. To reveal the mechanism of daylight sensitivity, thermoluminescence, EPR, and luminescence excitation studies and technological experiments were undertaken. A

400 nm light was shown to be most effective to store the dose and to excite the luminescence band near 600 nm [72].

X. Zhengye and his colleagues have prepared $Li_2B_4O_7$:Cu,Ag,Mg phosphors by the sintering technique. The roles of Ag and Mg dopants in the phosphors have been studied using the methods of TL glow curves and 3D TL spectra. The results indicated that proper concentrations of Ag and Mg can enhance the TL of $Li_2B_4O_7$:Cu. It was also indicated that the intensity of TL peak at 130 °C is reduced with the increasing Ag concentration, and enhanced with the increasing Mg concentration [73].

The main dosimetric characteristics are presented of newly prepared tissue-equivalent, highly sensitive thermoluminescent detector, $Li_2B_4O_7$:Cu,Ag,P in the form of sintered pellets, developed at the Institute of Nuclear Sciences, Vinca by M. Prokić [74]. As a result of an advancement in the preparation procedure by the sensitising of basic copper activated lithium borate TL material, significant improvement in the TL sensitivity of $Li_2B_4O_7$:Cu,Ag,P was gained.

Key characteristics of a newly prepared tissue-equivalent, highly sensitive TLD, $Li_2B_4O_7$:Cu,Ag,P are also presented by N Can and his friends. The material was again developed at the Institute of Nuclear Sciences, Belgrade, in the form of sintered pellets. A new preparation procedure has greatly increased the sensitivity of the basic copper activated lithium borate and the glow curve of $Li_2B_4O_7$:Cu,Ag,P consists of a well-defined main dosimetric peak situated at about 460–465 K with a sensitivity which is about four to five times higher than that of LiF:Mg,Ti (TLD-100).

The thermoluminescence properties of three different prepartion of lithium borate have been studied with specific reference to their use in medical dosimerty by B.F Wall his colleogues [75]. The properties of lithium borate powder with copper make it more attractive for low dose measurements than the more conventional phosphor doped with manganese.

Recently, two new types of tissue equivalent thermoluminescent detectors have aroused attention: LiF:Mg,Cu,Na,Si and $Li_2B_4O_7$:Cu,Ag,P by S.Miljanica and his colleogues [76]. In that work, the characteristics of both detectors were compared with the characteristics of the well-known type LiF:Mg,Ti detector (TLD-100). The results confirmed tissue equivalency of both new types in the investigated range of photon energies. LiF:Mg,Cu,Na,Si detector has very high sensitivity (approximately 75 times higher than that of TLD-100) and is convenient for use in a very low range of doses. $Li_2B_4O_7$:Cu,Ag,P detector shows some improvements in comparison with the previously prepared types of lithium borate. The most important is the five times higher sensitivity than that of TLD-100.

$Li_2B_4O_7$:Cu TLD phosphor radiation dosimetry characteristics was also investigated by A.R. Lakshmanan et al [77]. The major peak in that phosphor occurred at 230 ^oC and its TL sensitivity to gamma radiation is two three times higher than that of LiF TLD-100.

CHAPTER III

THEORY

3.1. Basic Concepts of Thermoluminescence of Solids

The theoretical explanation of thermoluminescence is based on the electron band theory. TL materials are insulators or semiconductors with a crystalline structure. According to the simplest model, the one trap-one centre model, in an ideal crystal the electrons occupy the valence bands, which are separated from the conduction band by the so-called forbidden band gap. In real crystals various defects occur as a consequence of ionizing radiation or of impurities in the lattice. In both cases the electrons can possess “forbidden” energies. Thermoluminescence (TL) method is relatively complex process since it involves a trap and a luminescence center. When an insulator or semiconductor is exposed to ionizing radiation at room or at low temperature, electrons are released from the valence band to the conduction band. This leaves a hole in the valence band. Both types of carriers become mobile in their respective bands until they recombine or until they are trapped in lattice imperfections in the crystalline solids. These lattice imperfections play very crucial role in the TL process. Some of the electrons and holes can recombine under emission of light (radioluminescence), while the others will be trapped at the level LT in the “forbidden” energy gap [78]. The trapped

electrons may remain for a long period when the crystals are stored at room temperature. They can be released due to the sufficient energy given to the electron when the crystal is heated. These electrons may move in the crystalline solid until they recombine with suitable recombination centers that contain hole with the emission of TL light. This process of light emission by stimulation from a crystalline solid after irradiations is called as "thermally stimulated process" or simply "thermoluminescence".

3.2. The One Trap–One Centre Model

The energy band theory of solids explains the observed TL properties. In an ideal semiconductor or insulator crystalline most of the electrons reside in the valence band. The next highest band that the electrons can occupy is the conduction band, separated from the valence band by the so-called forbidden band gap. The energy difference between the valence band and conduction band is denoted as E_g. However, whenever structural defects occur in a crystal, or if there are impurities within the lattice, there is a possibility for electrons to possess energies which are forbidden in the perfect crystal. In a simple TL model two levels are assumed, one situated below the bottom of the conduction band and the other situated above the top of the valence band (Fig.3.1). The highest level indicated by T is situated above the equilibrium Fermi level (E_f) and thus empty in the equilibrium state, i.e. before the exposure to radiation and the creation of electrons and holes. It is therefore a potential electron trap. The other level (indicated by R) is a potential hole trap and can function as a recombination centre. The absorption of radiant energy with $h\nu > E_g$ results in ionization of valence electrons, producing energetic electrons and

holes which will, after thermal ionization, produce free electrons in the conduction band and free holes in the valence band (transition a). The free charge carriers recombine with each other or become trapped. In the case of direct recombination an amount of energy will be released which may excite a luminescent centre. The luminescent centre relaxes (returns to the ground state) under the emission of light. However, in semiconductors and insulators a certain percentage of the charge carriers are trapped: the electrons at T and the holes at R (transition b). The probability per unit time of release of an electron from the trap is assumed to be described by the Arrhenius equation, where p is the probability per unit time, s is the frequency factor, k is the Boltzmann's constant, and T is the absolute temperature [79].

$$p = se^{\frac{-E}{kT}} \tag{3.1}$$

In the simplified model s is constant. E is called the trap depth or activation energy, the energy needed to release an electron from the trap into the conduction band. If the trap depth $E>>kT_o$, with T_o the temperature at irradiation, trapped electrons will remain for a long period of time, until exposure to the radiation there will exist a substantial population of trapped electrons. There must be an equal population of trapped holes at level R, due to the free electrons and holes are created and annihilated in pairs. Because the normal equilibrium Fermi level E_f is situated below level T and above level R, these populations of trapped electrons and holes represent a non-equilibrium state. The reaction path for return to equilibrium is always open, but because the perturbation from equilibrium (during exposure to ionising radiation) was performed at low temperature (compared to E/k), the

relaxation rate as determined by Eq. (3.1) is slow. Thus, the non-equilibrium state is metastable and will exist for an indefinite period, governed by the rate parameters *E* and *s* [80].

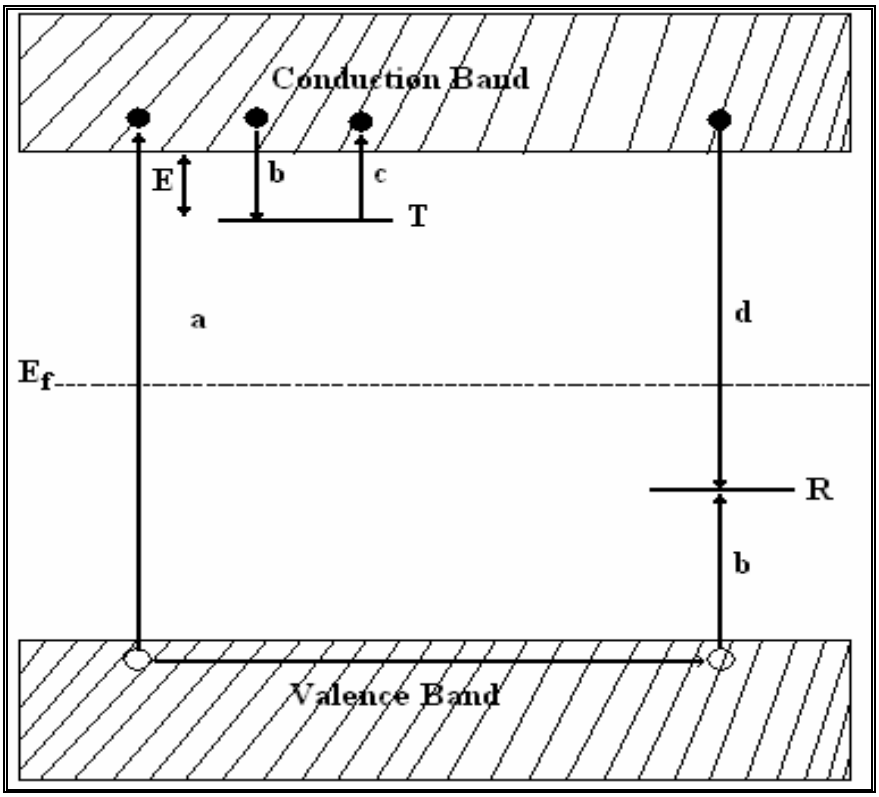

Figure 3.1. (a) Generation of electrons and holes; (b) electron and hole trapping; (c) electron release due to thermal stimulation; (d) recombination. (●) shows electrons, (○) shows holes. Level T is a electron trap, level R is a recombination centre, E_f is Fermi level

The return to equilibrium can be speeded up by raising the temperature of the TL material above T_o. This will increase the probability of detrapping and the electrons will now be released from the trap into the conduction band. The charge carrier migrates through the conduction band of the crystal until it undergoes recombination at recombination centre R. In the simplified model this

recombination centre is a luminescent centre where the recombination of the electron and hole leaves the centre in one of the higher excited states. Return to the ground state is coupled with the emission of light quanta, i.e. TL. The intensity of TL $I(t)$ in photons per second at any time t during heating is proportional to the rate of recombination of holes and electrons at R. If m (m^{-3}) is the concentration of holes trapped at R the TL intensity can be written as;

$$I(t) = -\frac{dm}{dt} \tag{3.2}$$

Here, it is assumed that each recombination produces a photon and that all produced photons are detected. The rate of recombination is proportional to the concentration of free electrons in the conduction band n_c and the concentration of holes m [79],

$$I(t) = -\frac{dm}{dt} = n_c m A \tag{3.3a}$$

with the constant A the recombination probability expressed in units of volume per unit time which is assumed to be independent of the temperature. The rate of change of the concentration of trapped electrons n is equal to the rate of thermal release minus the rate of retrapping [79],

$$-\frac{dn}{dt} = np - n_c(N-n)A_r \tag{3.3b}$$

with N the concentration of electron traps and A_r the probability of retrapping (m^3/s). The rate concentration of free electrons is equal to the rate of thermal release minus the rate of retrapping and the rate of recombination, Eqs.(3.3a)–

(3.3c) described the charge carrier traffic in the case of release of a trapped electron from a single-electron trap and recombination in a single centre.

$$-\frac{dn_c}{dt} = np - n_c(N-n)A_r - n_c mA. \tag{3.3c}$$

For TL produced by the release of holes the rate equations are similar to Eqs. (3.3a)–(3.3c). These equations form the basis of many analyses of TL phenomena. There is no general analytical solution. Perhaps the most important of all the assumptions introduced into the rate equations is that called the quasiequilibrium assumption by Chen and Mc Keever in order to develop an analytical expression. An important assumption is that at any time [81].

$$\left|\frac{dn_c}{dt}\right| \langle\langle \left|\frac{dn}{dt}\right|, \quad \left|\frac{dn_c}{dt}\right| \langle\langle \left|\frac{dm}{dt}\right| \tag{3.4}$$

It requires that the free electron concentration in the conduction band is quasistationary. The trapped electrons and holes are produced in pairs during the irradiation. Charge neutrality dictates therefore;

$$n_c + n = m \tag{3.5}$$

which for $n_c \approx 0$ means that $n \approx m$ and since $dc_c/dt \approx 0$ one gets from eq.3.3a and equation (3.3b):

$$I(t) = -\frac{dm}{dt} \approx -\frac{dn}{dt} \tag{3.6}$$

$$I(t) = \frac{mAns \exp\left\{-\frac{E}{kT}\right\}}{(N-n)A_r + mA} \tag{3.7}$$

3.3. First-Order Kinetics (Slow Retrapping)

By assuming [82-83] negligible retrapping during the heating stage, i.e. and assuming $mA>>(N-n)A_r$, if we solving Eq. (3.7) analytically without additional simplifying assumptions and Eq. (3.7) can be written as;

$$I(t) = -\frac{dn}{dt} = sn\exp\left\{-\frac{E}{kT}\right\} \tag{3.8}$$

Equation (3.8) describes the charge transport in the lattice as a first-order process and the glow peaks calculated from this equation are called first-order glow peaks [84]. Solving the differential Equation (3.8) yields;

$$I(t) = -\frac{dn}{dt} = n_o s\exp\left\{-\frac{E}{kT}\right\}\exp\left\{-s\int_0^t \exp\left\{-\frac{E}{kT(t')}\right\}dt'\right\} \tag{3.9}$$

where n_o is the total number of trapped electrons at time t=0. Usually the temperature is raised as a linear function of time according to with β the constant heating rate and T_o the temperature at t=0.

$$T(t) = T_0 + \beta t \tag{3.10}$$

This gives the intensity as function of temperature;

$$I(t) = -\frac{1}{\beta}\frac{dn}{dt} = n_o\frac{s}{\beta}\exp\left\{-\frac{E}{kT}\right\}\exp\left\{-\frac{s}{\beta}\int_{To}^{T}\exp\left\{-\frac{E}{kT'}\right\}dT'\right\} \tag{3.11}$$

This is the well-known Randall–Wilkins first-order expression of a single low peak. The peak has a characteristic asymmetric shape being wider on the low temperature side than on the high temperature side. On the low temperature side, i.e. in the initial rise of the glow peak, the intensity is dominated by the first exponential *(exp(-E/kT))*. If I is plotted as function of 1/T, a straight line is expected

in the initial rise temperature range, with the slope of -*E*/*k*, from which the activation energy *E* is readily found.

The Randall–Wilkins equation properties are illustrated in Fig.3.2. In Fig.3.2a it is shown how $I(T)$ varies if n_o varies from n_o=0.25 m^{-3} till n_o=2 m^{-3} while E=1 eV, s=1×10^{12} s^{-1} and β=1 K/s are kept constant. It can be noted that the temperature at the peak maximum, T_m, stays fixed. This is a characteristic of all first-order TL curves. The condition for the maximum can be found by setting *dI/dt=0* (or, somewhat easier from *dlnI(T)/dt=0*). From this condition one gets in this equation No does not appear which shows that T_m does not depend on N_o. From Fig.(3.2a) it can be seen that not only the peak height at the maximum but each point of curve is propoertional to N_o.

$$\frac{\beta E}{kT_m^2} = s\exp\left\{-\frac{E}{kT_m}\right\}, \tag{3.12}$$

In the application in dosimetry, N_o is the parameter of paramount importance since this parameter is proportional to the absorbed dose. Under the conditions of area under the glow peak is equal to;

$$\int_0^\infty I(t)dt = -\int_0^\infty \frac{dn}{dt} = -\int_{n_0}^{n_\infty} dn = n_0 - n_\infty \tag{3.13}$$

n_0 since, and n_∞ is zero for $t\rightarrow\infty$ [79].

.

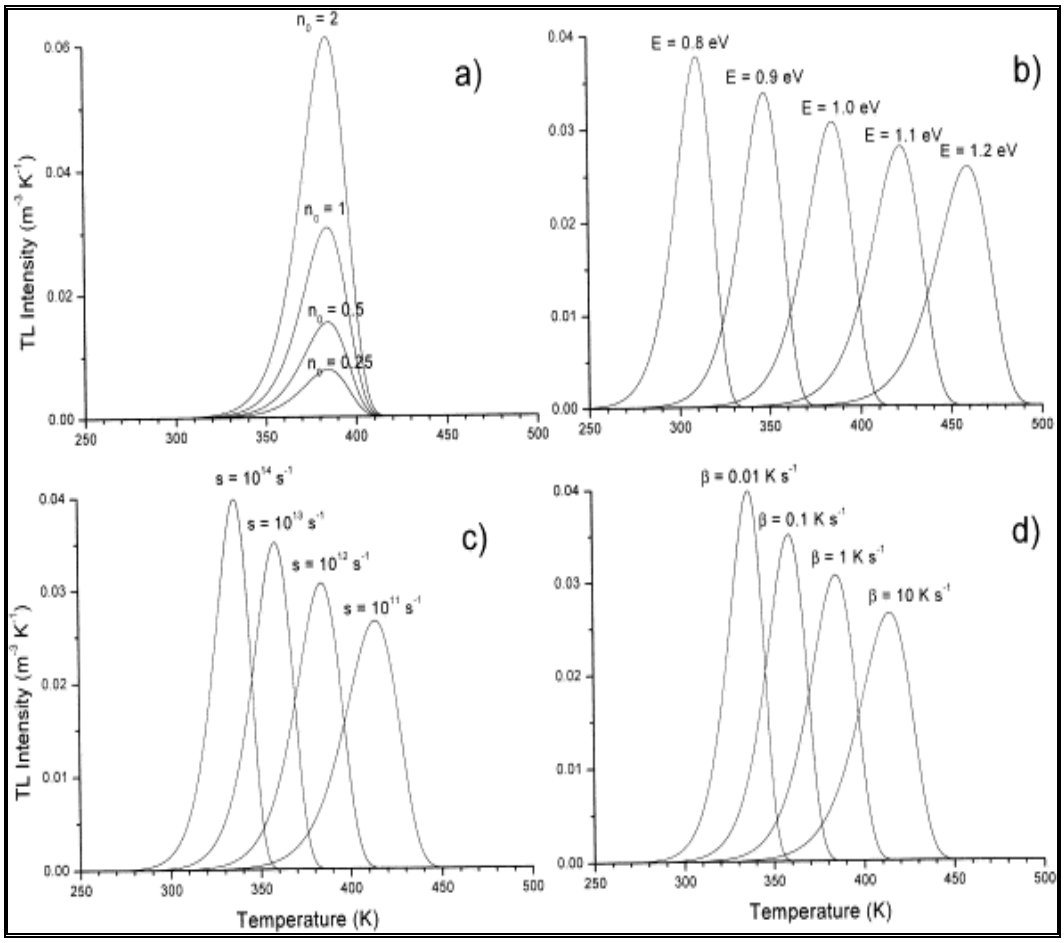

Figure 3.2. Properties of the Randall-Wilkins first order TL equation, showing (a) variation with n_o, the concentration of trapped charge carriers after irradiation; (b) the variation with E, the activation energy; (c) the variation with s, the escape frequency; (d) the variation with β, the heating rate

In Fig. (3.2b) the activation energy *E* has been varied from 0.8 to 1.2 eV. As *E* increases the peak shifts to higher temperatures with a decrease in the height and an increase in the width keeping the area (i.e. n_o) constant. Similar changes can be noticed as *s* is varied (see Fig. (3.2c) but now in the opposite way: as *s* increases the peak shifts to lower temperatures with an increase of the height and a decrease in width. In Fig.(3.2d) the heating rate has been varied. As β increases the peak shifts to higher temperatures while the height decreases and the width increases just as in

the case of decreasing *s*. The activation energy *E* and the frequency factor *s* are the main physical parameters called the trapping parameters and are fixed by the properties of the trapping centre. The other two parameters can be chosen by the experimenter by choosing a certain dose (n_o) and by read-out of the signal at a certain heating rate β. Investigation of a new TL material will therefore start with studying the glow peak behaviour under variation of the absorbed dose and the heating rate.

In practical applications, it is convenient to describe the glow peak in terms of parameters which are easy to derive experimentally, namely the intensity of peak at the maximum I_m and the temperature at the maximum T_m. Kitis et al. [85] have shown that Eq. (3.11) can be quite accurate approximated by, with $\Delta=2kT/E$ and $\Delta_m=2kT_m/E$. Recently Pagonis et al. [86] have shown that a Weibull distribution function also accurately describes the first-order TL curve.

$$I(T) = I_m \exp\left[1+\frac{E}{kT}\frac{T-T_m}{T_m}-\frac{T^2}{T_m^2}\exp\left\{\frac{E}{kT}\frac{T-T_m}{T_m}\right\}(1-\Delta)-\Delta_m\right] \tag{3.14}$$

These expressions may be convenient for peak fitting purposes.

3.4. Second-Order Kinetics (Fast Retrapping)

Garlick and Gibson [87] assumed negligible retrapping during thermal excitation period i.e. they assumed $mA<<(N-n)A_r$ and the trap is far from saturation, i.e. $N>>n$ and $n=m$. Under these assumptions, Eq.(3.7) becomes;

$$I(t) = -\frac{dn}{dt} = s\frac{A}{NA_r}n^2 \exp\left\{-\frac{E}{kT}\right\}, \tag{3.15}$$

We see that now *dn/dt* is proportional to n^2 which means a second-order reaction. With the additional assumption of equal probabilities of recombination and retrapping, $A=A_r$, integration of Eq. (3.15) gives Eq.(3.16)

$$I(T) = \frac{n_0^2}{N}\frac{s}{\beta}\exp\left\{-\frac{E}{kT}\right\}\left[1+\frac{n_0 s}{N\beta}\int_{T_0}^{T}\exp\left\{-\frac{E}{kT'}\right\}dT'\right]^{-2} \qquad (3.16)$$

This is the Garlick–Gibson TL equation for second-order kinetics [86]. The main feature of this curve is that it is nearly symmetric, with the high temperature half of the curve slightly broader than the low temperature half. The initial concentration n_o appears here not merely as a multiplicative constant as in the first-order case, so that its variation at different dose levels change the shape of the whole curve. From Fig. (3.3a) it can be seen that T_m decreases as n_o increases. Fig. (3.3b) and (c) shows the variation in size and position of a second-order peak as function of *E* and *s/N* respectively and in Fig.3.3(d) as function of the heating rate. The area under the curve is, proportional to the initial concentration n_o but the peak height is no longer directly proportional to the peak area, although the deviation is small [79].

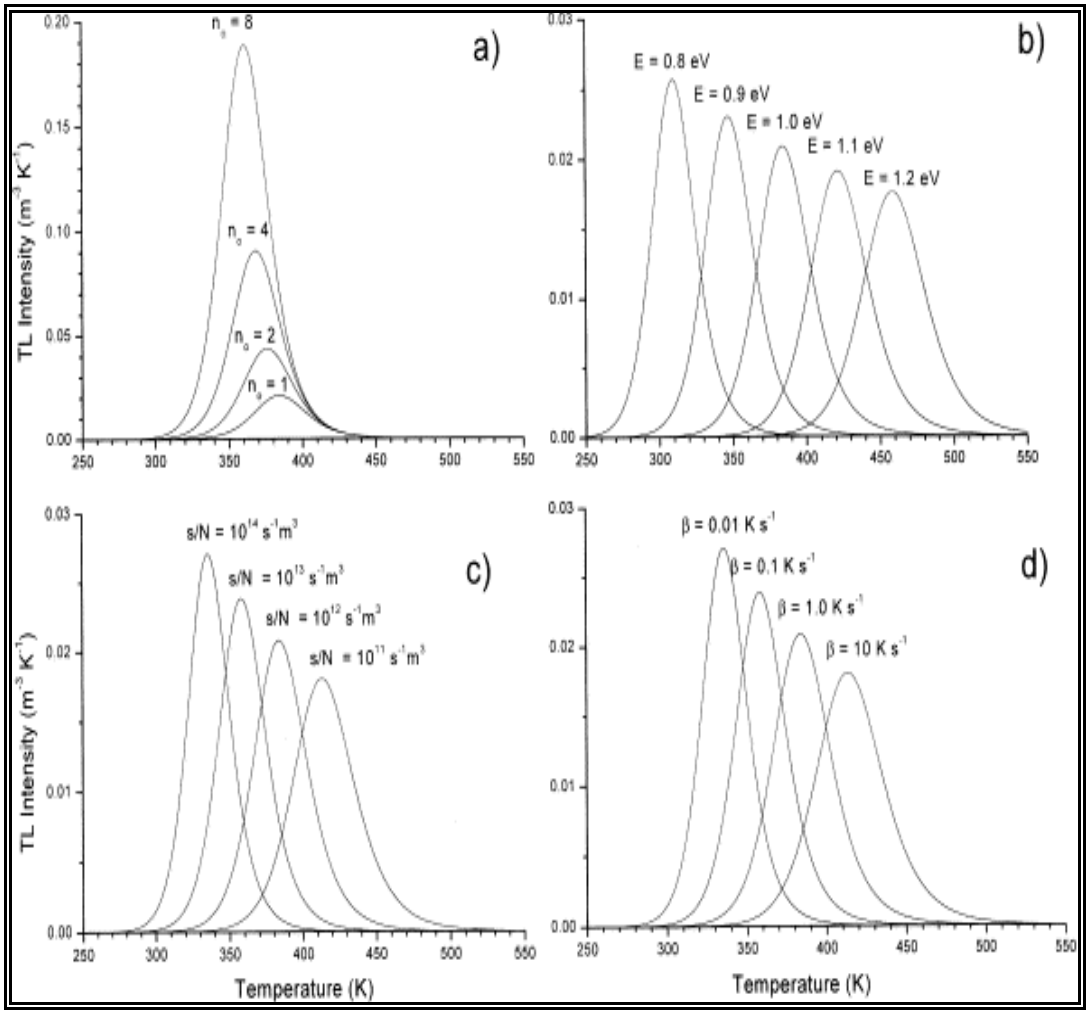

Figure 3.3. Properties of the Garlick–Gibson second-order TL equation, showing: (a) variation with n_o; (b) the variation with E; (c) the variation with s/N; (d) the variation with β

It can be derived that the temperature shift can be approximated by

$$T_1 - T_2 \approx T_1 T_2 \frac{k}{E} \ln f \tag{3.17}$$

where T_1 is the temperature of maximum intensity at a certain dose and T_2 the temperature of maximum intensity at f times higher dose. With the parameter values of Fig.3.3 (a) the shift is 25 K. When E=1 eV, T_1=400 K and the absorbed

dose is increased by a factor 1000, which is easy to realise experimentally, a temperature shift of 77 K can be expected.

It can be seen that, similarly to the first-order case, the term dominating the temperature dependence in the initial rise is *exp(-E/kT).* So the `initial rise method' for the determination of the trap depth can be applied here as well. Also for second-order kinetics the glow peak shape, Eq. (3.16), can be approximated with a function written in terms of maximum peak intensity I_m and the maximum peak temperature T_m,with Δ and Δ_m the same meaning as in Eq. (3.14) [88].

$$I(T) = 4I_m \exp\left(\frac{E}{kT}\frac{T-T_m}{T_m}\right) X\left[\frac{T^2}{T_m^2}(1-\Delta)\exp\left\{\frac{E}{kT}\frac{T-T_m}{T_m}\right\} + 1 + \Delta_m\right]^{-2} \qquad (3.18)$$

3.5. General-Order Kinetics

The first- and second-order forms of the TL equation have been derived with the use of specific, simplifying assumptions. Without any simplifying assumptions, the TL peak will fit neither first- nor the second-order kinetics. For this case May and Partridge, used an empirical expression for general-order TL kinetics, namely where s' has the dimension of $m^{3(b-1)}s^{-1}$ and b is defined as the general-order parameter and is not necessarily 1 or 2 [89].

$$I(t) = -\frac{dn}{dt} = n^b s' \exp\left\{-\frac{E}{kT}\right\} \qquad (3.19)$$

Integration of Eq. (3.19) for $b\neq1$ produces where now $s''=s'n_0^{b-1}$. Eq. (3.20) includes the second-order case (b=2) and reduces to Eq. (3.11) when $b\rightarrow1$.

$$I(T) = \frac{s''}{\beta} n_0 \exp\left\{-\frac{E}{kT}\right\}\left[1+(b-1)\frac{s''}{\beta}\int_{T_0}^{T}\exp\left\{-\frac{E}{kT'}\right\}dT'\right]^{-b/b-1} \qquad (3.20)$$

The general- order case is useful since intermediate cases can be dealt with and it smoothly goes to first- and second-orders when $b \rightarrow 1$ and $b \rightarrow 2$ respectively (Fig.3.4) [90].

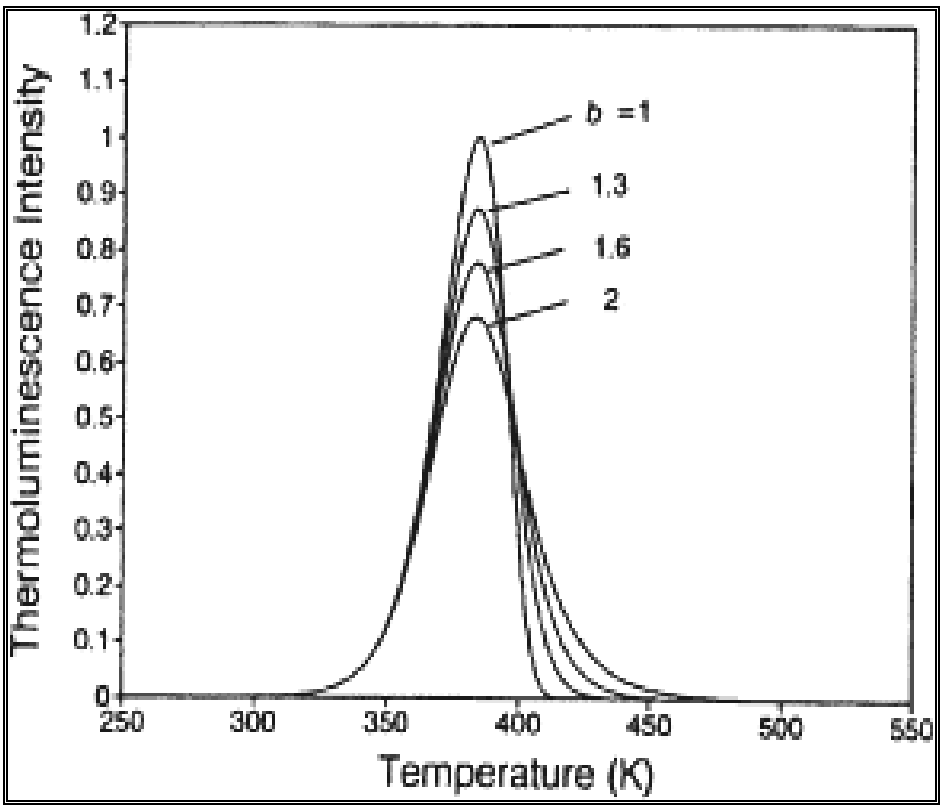

Figure 3.4. Comparison of first-order (b=1), second-order (b=2) and intermediate-order (b=1.3 and 1.6) TL peaks, with E=1 eV, s=1×10^{12} s^{-1},n_0=N=1 m^{-3} and β =1 K/s

3.6. Advanced Models

The one trap–one centre model shows all the characteristics of the phenomenon TL and explains the behaviors of the glow peak shape under variation of the dose and heating rate. However, there is no existing TL material known that

accurately is described by the simple model. In general, a real TL material will show more than one single electron trap. Not all the traps will be active in the temperature range in which the specimen is heated. A thermally disconnected trap is one which can be filled with electrons during irradiation but which has a trap depth which is much greater than the active trap such that when the specimen is heated only electrons trapped in the active trap (AT) and the shallow trap (ST) (Fig.3.5(a)) are freed [91]. Electrons trapped in the deeper levels are unaffected and thus this deep electron trap (indicted in Fig.(3.5a) with DET is said to be thermally disconnected. But its existence has a bearing on the trapping filling and eventually on the shape of the glow peak [92].

Another process which might happen is a recombination without a transition of the electron into the conduction band (Fig.3.5c). Here the electron is thermally stimulated into an excited state from which a transition into the recombination centre is allowed. This means that the trap has to be in the proximity of a centre. The transition probability may strongly depend on the distance between the two centers. Finally, the another possibility is that the defect which has trapped the electron is not stable but is involved in a reaction with another defect (Fig. 3.5d).

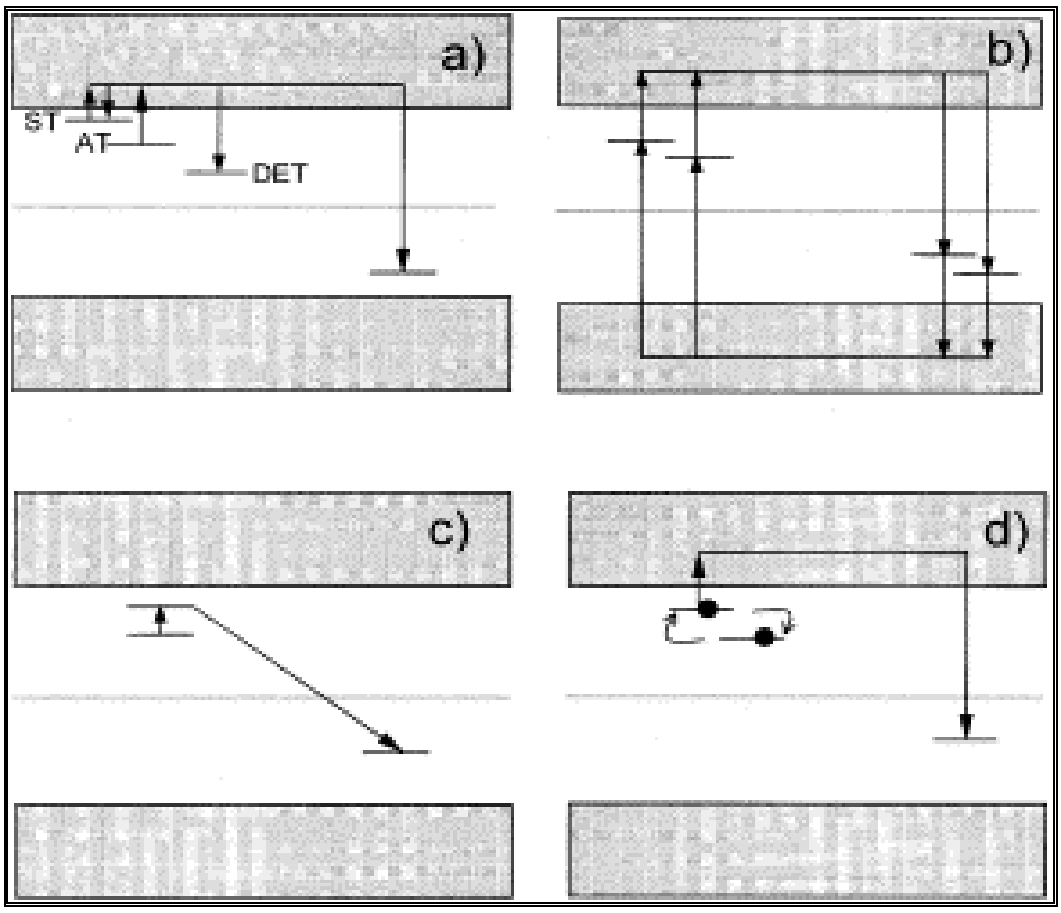

Figure 3.5. Advanced models describing the thermally stimulated release of trapped charged carriers including: (a) a shallow trap (ST), a deep electron trap (DET), and an active trap (AT); (b) two active traps and two recombination centres; (c) localised transitions; (d) defect interaction (trapping centre interacts with another defect)

It may be conluded that at low temperature the trap depth is changing while the trapped electron concentration is stable. At higher temperatures electrons are involved in two processes: the escape to the conduction band and the defect reaction. It appears that the simulated glow curves can be very well fitted by Eq. (3.11). It is clear that (again) the fitting parameters do not have the simple meaning of trap depth and escape frequency [93].

3.7. Trapping Parameter Determination Methods

The determination of trapping parameters from thermoluminescence glow curves has been a subject of interest for half a century. There are various methods for evaluating the trapping parameters from the glow curves [80, 82,87, 94,95,96]. When one glow peak is highly isolated from the others, the experimental methods such as initial rise, variable heating rates, isothermally decay, and peak shape methods are suitable methods to determine these parameters. However in most materials, the glow curve consists of several peaks. In case of overlapping peaks there are essentially two ways to obtain these parameters, the first one is the partial thermal cleaning method and the second one is the computer glow curve deconvolution program. In most cases, the partial thermal cleaning method can not be used to completely isolate the peak of interest without any perturbation on it. Therefore, the computer glow curve deconvolution program has become very popular method to evaluate trapping parameters from TL glow curves in recent years [97].

3.7.1. Peak shape method

Evaluation of E from the shape of the peak utilising parameters such as T_m, full width at half-maximum $\omega = T_2 - T_1$, half width on the high temperature side of the maximum $\delta = T_2 - T_m$, half width on the low-temperature side of the maximum $\tau = T_m - T_1$, and $\mu_g = \delta/\omega$ called the shape parameter. The order of kinetics b can be estimated by means of shape parameters. Chen found that μ_g is not sensitive to changes in E and s, but it changes with the order of kinetics b [90]. It has been shown that the ranges of μ_g varies from 0.42 for b=1 to 0.52 for b=2 in

case of linear heating. The first peak shape method was developed by Grossweiner [96]; later Chen [90] modified Halperin and Braner's equations [98] for calculating *E* values;

$$E_\tau = \left[1.51 + 3(\mu_g - 0.42)\right]\frac{kT_m^2}{\tau} - \left[1.58 + 4.2(\mu_g - 0.42)\right]2kT_m$$
$$E_\delta = \left[0.976 + 7.3(\mu_g - 0.42)\right]\frac{kT_m^2}{\delta} \qquad (3.21)$$
$$E_\omega = \left[2.52 + 10.2(\mu_g - 0.42)\right]\frac{kT_m^2}{\omega} - 2kT_m$$

After determination of the activation energy and the order of kinetics, using the following expressions the frequency factor *s*, it must be noted that this parameter called as pre-exponential factor in the general order kinetic, can be estimated for first and general order kinetics respectively.

$$s = \frac{\beta E}{kT_m^2}\ \exp\left[\frac{E}{kT_m}\right]$$
$$s = \frac{\beta E}{kT_m^2}\left[\exp(-\frac{E}{kT_m})(1 + (b-1)\frac{2kT_m}{E})\right]^{\frac{b}{b-1}} \qquad (3.22)$$

3.7.2. CGCD method

The studies of thermally stimulated processes like thermoluminescence yields information on defect centers in solids. TL has been recognized that information about the trapping levels can be extracted from the glow curve [99-100]. Computerized glow curve analysis is now used not only for extraction of physical parameters but also for dosimetric purposes. However, it can be noted that different models, approximations and minimization procedures are used for the glow curve analysis. As a consequence one may wonder whether the results of the glow curve analysis reflect properties of the TL material and/or irradiation

conditions or should be ascribed to artifacts of the analysis procedure used in the computerized glow curve fitting.

In this study, the TL glow curves and were analyzed using a computerized glow curve technique (CGCD) developed at the IRI, Delft, Netherlands [101]. This method has become very popular to obtain these parameters for the last two decades [102-103]. It has great advantages over the experimental methods (i.e. initial rise, peak shape and etc) owing to simultaneous determination of trapping parameters of all peaks without additional thermal treatments and experimental repetitions. Also, this method uses all data points in the whole glow curve rather than just a few points during the curve fitting procedures. Each peak in the glow curve is fitted to the first-order Randal-Wilkins model. The used CGCD program, which is based on the least square minimization procedure, was developed at the Reactor Institute at Delft, The Netherlands [101]. In this program, the first-order kinetics were approximated for all CGCD evaluations by the expression

$$I(T) = n_0 s \exp(-\frac{E}{kT}) \exp\left[-\frac{s}{\beta} \frac{kT^2}{E} \exp(-\frac{E}{KT}) * (0.992 - 1.620 \frac{kT}{E}) \right] \qquad (3.23)$$

and the general-order kinetics were approximated by the expression

$$I(T) = n_0 s \exp(-\frac{E}{kT}) \left[1 + \frac{(b-1)s}{\beta} \frac{kT^2}{E} \exp(-\frac{E}{kT}) * (0.992 - 1.620 \frac{kT}{E}) \right]^{\frac{b}{1-b}} \qquad (3.24)$$

where n_0 (m^{-3}) is the concentration of trapped electrons at t=0, T (K) is the absolute temperature, k (eVK^{-1}) is Boltzmann's constant, β ($^oCs^{-1}$) is heating rate.

The computer program is based on the Marquardt algorithm to obtain minimum chi-squared. A computerized curve fitting program constructs a glow

curve using the initial values of the input parameters and compares the computed curve with the experimental curve. The values of parameters are then sequentially varied until a best fit is obtained.

3.7.3. Initial rise method

The simplest, and most generally applicable method for evaluating the activation energy *E* of a single TL peak is the initial rise method. The basic premise upon which this method is based is that at the low temperature end of the peak, all the relevant occupancies of the states, the trap, and the recombination center and, in some cases, other interactive states can be considered as being approximately constant. The rise of the measured intensity as a function of temperature in this region is, therefore, very close to exponential, and given as;

$$I(T) = C\exp(-E/kT) \tag{3.25}$$

where the constant C includes all the dependencies on the other parameters and occupancies, *E* is the activation energy (eV), *k* is the Boltzmann`s constant (eV/K^{-1}) and *T* is the temperature (K). Plotting ln(*I*) against *1/T* a linear plot is obtained with slope equal to *–E/k*. Hence it is possible to evaluate *E* without any knowledge of the frequency factor *s* given by;

$$E = -kd(\ln(I))/d(1/T) \tag{3.26}$$

Once the value of *E* was determined, the frequency factor (*s*) was obtained from the Eq.(3.22). This method can only be used when the glow peak is well defined and clearly seperated from the other peaks.

3.7.4. Heating rating method

Another important method is various heating rates for the determination of activation energies. If a sample is heated at two different linear heating rates β_1 and β_2 the peak temperatures will be different. Eq.(3.22) can therefore, be written for each heating rate and dividing the equation for β_1 (and T_{m1}) by the equation for β_2 (and T_{m2}) and rearranging, one gets an explicit equation for the calculation of *E;*

$$E = k\frac{T_{m1}T_{m2}}{T_{m1}-T_{m2}}\ln[(\frac{\beta_1}{\beta_2})(\frac{T_{m2}}{T_{m1}})^2] \tag{3.27}$$

Here the calculation of *E* is not affected by problems due to thermal quenching, as with the initial rise method. When various heating rates for the first-order kinetics are used, the following expression is obtained:

$$\ln(\frac{T_m^{\ 2}}{\beta}) = (\frac{E}{k})(\frac{1}{Tm}) + cons\tan t \tag{3.28}$$

A plot of ln (T_m^2/β) versus ($1/ T_m$) should yield a straight line with a slope *E/k*, and then *E* is found. Additionally, extrapolating to $1/T_m = 0$, a value for *ln(sk/E)* is obtained from which s can be calculated by inserting the value of *E/k* found from the slope. The variable heating rate methods can also applicable for general-order kinetics which includes the second-order case. For the general order, one can plot $ln\left[I_m^{\ b-1}(T_m^{\ 2}/\beta)^b\right]$ versus $1/T_m$, whose slope is equal to *E/k* [6].

CHAPTER IV

SAMPLE PREPARATION METHODS

Since investigation of the TL, many new TL materials with much higher sensitivity have been introduced [6,17,38,47]. However, as mentioned in previously, a few of TL materials have stood out as promising and attracted a lot of attention. Efficient thermoluminescent materials have a high concentration of traps, provided by structural defects and impurities. Although there are several available dosimetric TL materials presently, a few of them were mentioned here. These materials can be grouped into two main categories; tissue equivalent phosphors, which in general show poor sensitivity (such LiF, $Li_2B_4O_7$, BeO, $MgO.nB_2O_3$, etc) and compounds with high sensitivity but no tissue equivalence (such $CaSO_4$, CaF_2, $SrSO_4$, Mg_2SiO_4, etc).

In literature, there are many TLD sample preparation methods [17,38,47,52]. But a few of them are useable. Some of them are expensive, and some of them require much effort during sample development so, a few of methods can use sample growth. The most used methods are listed below.

4.1. Lithium Fluoride (LiF) Preparation Method

The success story of lithium dates back to late 1940's and early 1950's, when Daniels and his students studied alkali halides. They used pressed of lithium fluoride powder manufactured by the Harshaw Chemical co., for dosimetry experiments [104]. The Harshaw patent describes two preparation methods for LiF: Mg, Ti TL phosphor: a) The solidification Method, b) Single Crystal Method.

In the solidification method, lithium fluoride (10^6 parts by weight), magnesium fluoride (400 pars by weight), lithium cryolite (200 pars by weight) and lithium titanium fluoride (55 parts by weight) are mixed in graphite crucible. The mixture is homogeneously fused in vacuum and the product slowly cooled, then crushed and sieved between 60 and 200 μm.

In the single crystal method, above mixture is placed in a vacuum or inert-atmosphere oven to grow a single crystal by the Czochralski method at temperature sufficiently high to obtain a homogeneous fusion mixture. The mixture is then slowly moved to lower temperature zone to allow progressive solidification (about 15 mm/h). Once the material was cooled, it is crushed and sieved between 60 and 200 μm [105,106]. In both cases the resulting TL phosphor powders are annealled at 400 ^{o}C during some hours and then at 80 ^{o}C during 48 h.

4.2. Aluminum Oxide (Al_2O_3:C) Preparation Method

Single crystal α-Al_2O_3 is commonly known as sapphire or corundum, with the last name being used generically for the type of structure. It has already been known as TL material for a long time [107]. Interest in the material has increased

considerably since the improvement of the dosimetric properties by intentional inclusions of oxygen vacancies into its structure. Such a modification of the oxide is possible by annealing and melting under strongly reducing conditions in the presence of graphite [108,109]. Nowadays the material is produced in different forms: single crystals, powders and thin layers on substrates and in a number of different laboratories. The crystal growth of aluminum oxide α-Al_2O_3:C is performed in highly reducing atmosphere in presence of graphite. The sample is grown from melt at 2050 ^{o}C [80]. Silica is widely used in glass-making because the quenching rates are much lower, but researchers would like to make glass from alumina as well because of its superior mechanical and optical properties. Alumina can form glass if it is alloyed with calcium or rare-earth oxides, but the required quenching rate can be as high as 1000 degrees per second, which makes it difficult to produce bulk quantities.

Rosenflanz and colleagues started by mixing around 80 mole % of powdered alumina with various rare-earth oxide powders -- including lanthanum, gadolinium and yttrium oxides [110]. Next, they fed the powders into a high-temperature hydrogen-oxygen flame to produce molten particles that were then quenched in water. The resulting glass beads, which were less than 140 microns across, were then heat-treated or sintered at around 1000°C. This produced glass samples in which nanocrystalline alumina-rich phases were dispersed throughout a glassy matrix. The new method avoids the need to apply pressures of 1 gigapascal or more, as is required in existing techniques.

4.3. Calcium Sulphate ($CaSO_4$) Preparation Methods

$CaSO_4$: Dy is phosphor first introduced by Yamasahita and his colleagues for using in TLD of ionized radiation [111]. This phosphor finds applications for its high sensitivity and ease preparation. Several efforts have been made to increase sensitivity of this phosphor by co-doping. The most popular $CaSO_4$ phosphors are doped with Dy and Tm. The $CaSO_4$:Dy and The $CaSO_4$:Tm phosphors can be prepared by technique of Yamashita et al [112]. Natural mineral gypsum $CaSO_4.H_2O$ crystals, Dy_2O_3 and Tm_2O_3 and sulpheric acid are used as preferred base materials. The procedure utilized included:

- The transparent crystals of gypsum $CaSO_4.H_2O$ are subjected to a thermal treatment at 110 ^oC for 24 hour to remove the crystalline water. They are then ground and sieved to produce fine grain powder.
- The powder are washed a few times, with boiling distilled water to remove non-activator content mainly sodium. Then powder is dried.
- The required amount of Dy_2O_3 or Tm_2O_3 are dissolve in a diluted hot acid, followed by the addition of a known amount the treated powder to the concentrated hot acid. The heating continues until the acid is completed evaporated and the polycrystalline appeared.
- The materials prepared are washed repeatedly and then dried by a high temperature heat treatment, ground a sieved to get grains with sizes between 70 and 200μm [113,114].

4.4. Alkaline Earth Borates Preparation Methods

Pure borate as well as alkali borate has attracted interest as thermoluminesecence dosemeter materials because their effective atomic numbers are very close to that of tissue. They are usually used with doped impurities because the TL response of material without impurities is very low compared with commercial phospors. The most used sample prepration methods for alkaline earth boartes are melting point and solid state diffusion methods.

4.4.1. Melting point method

In melting point method, each phosphor was obtainted by reaction between boric acid (H_3BO_3) and corresponding carbonate $MgCO_3$, $CaCO_3$, or $BaCO_3$ and Boric acid are mixed in the stoichiometric ratio and sufficient solution of desired dopant (in form of chlorides, nitrates, or oxides) is added, to obtain impurity content ranging form 0.01 to 10 wt%. After stirring and desiccation, the mixture is melted at 950 ^{o}C in silica or platinum crucible, and then rapidly cooled to room temperature. The resultant glassy mass is reheated at 650 ^{o}C for 0.5 hour, which assures crystallization, and then ground and sieved to obtain a 100 to 200 mesh crystalline powder.

4.4.2. Solid state diffusion method

In solid state diffusion method, the corresponding alkaline borates in carbonate forms (99%, Merck) and H_3BO_3 (99.5%, Merck) were mixed in the stoichiometric ratio in desired amount. The mixture was ground finely in an agate mortar. Homogenized mixture was transferred into a convenient porcelain crucible and preheated at 300 ^oC for 4 h to obtain CO_2 and H_2O release. Then the desired amount of impurities is added mixture. The resultant mixture is ground in an agate mortar for 1.5h to get a good homogeneity. After that, the mixture was heated in at 750 ^oC for 16 h in an oven [115]. The resultant material rapidly cooled to room temperature in desicator and sieved to select particles of homogenous size (100-200 μm).

CHAPTER V

EXPERIMENTAL EQUIPMENTS AND PROCEDURES

The experimental procedure, equipments and materials utilized in this work are described below:

5.1. Materials

This work has two main stages; namely synthesis and characterization of TL materials. The aim of first stage is to synthesize some of new TL crystals, undoped or doped with rare earth and metalic ions under high conditions. Following solid powders were used in synthesis of products: Li_2CO_3, $MgCO_3$, $CaCO_2$, $BaCO_3$ (99%, Alrich) and boric acid (H_3BO_3 (99.5%), CeO_2(98%, Alrich), MnO_2, Al_2O_3.....

The polycrystalline samples of undoped and Ce-doped BaB_4O_7, CaB_4O_7 were prepared by a melting method. After a series of attempts we successed to prepare the samples with melting point method. The preparation of barium borate sample was made by mixing barium carbonate ($BaCO_3$) (99%, Alrich) and boric acid (H_3BO_3 (99.5%,) in stoichiometric ratio and the mixture was melted at 900^oC in a quartz tube for 4.5 hour then cooled samples rapidly to 650 ^oC and we get out the sample from the oven then cooled to room temperature. The resultant glassy mass was ground and sieved to obtain 100-200 mesh powder. Ce-doped BaB_4O_7

samples were prepared in a similar manner by taking the starting material in stoichiometric ratio and adding desired amount of CeO in the mixture. The sample materials was ground and sieved to a grain size of 200 µm. After 1 h annealing at 400 ^{o}C, the phosphors were cooled rapidly to room temperature and ground in an agate mortar again.

The preparation of calcium borate sample was made by mixing barium carbonate ($CaCO_3$) (99%, Merck) and boric acid (H_3BO_3 (99.5%, Merck) in stoichiometric ratio and the mixture was melted at 950 ^{o}C in a platinum crucible for 4.5 hour then rapidly cooled to room temperature. The resultant glassy mass was ground. The glassy mass is reheated at 650 ^{o}C for 0.5 h, which assures a complete crystallization, and then ground and sieved to obtain 100-200 mesh powder [116,117].

MgB_4O_7, $Li_2B_4O_7$, LiB_3O_5 samples were prepared with solid-state reaction methods. Even though melting point method is simple and provide good homogeneity in sample due to sticking of sample to platinum crucible is useless for those samples.

Impurities doped $Li_2B_4O_7$, CaB_4O_7 and LiB_3O_5 and undoped TL compounds were synthesized with solid state method as follows. Li_2CO_3 (99%, Merck) and H_3BO_3 (99.5%, Merck) were mixed in the stoichiometric ratio in desired amount. The mixture was ground finely in an agate mortar. Homogenized mixture was transferred into a convenient porcelain crucible and preheated at 300^{o}C for 4 h to obtain CO_2 and H_2O release. Then, the mixture was heated in platinum crucible the at 750 ^{o}C for 16 h. Sufficient aqueous solution of desired dopant (Mn, Al, Ce in form of oxides) weighted separately, were mixed with $Li_2B_4O_7$, LiB_3O_5 and

CaB_4O_7 and finely powdered in an agate mortar and then mixture heated for 10 h in porcelain crucible. The resultant material rapidly cooled to room temperature in desicator and sieved to select particles of homogenous size (100-200 μm). The expected reaction is given below:

$$Li_2CO_3 + 4H_3BO_3 \rightarrow Li_2B_4O_7 + CO_2 + 6H_2O,$$

$$CaCO_3 + 4H_3BO_3 \rightarrow CaB_4O_7 + CO_2 + 6H_2O,$$

$$Li_2CO_3 + 6H_3BO_3 \rightarrow 2LiB_3O_5 + CO_2 + 9H_2O,$$

Al, Mn, Ce impurities doped LiB_3O_5, CaB_4O_7, $Li_2B_4O_7$ TLDs were synthesized with same manner by taking base materials Li_2CO_3, $CaCO_3$ and H_3BO_3 mixed with desired ratio of impurities [112]. Normal TL materials are in bulk or powder form. The solid form may be composed entirely of single crystals or polycrystalline extrusions or as a homogeneous composite of the phosphor. The powder dosimeter has some special advantages, e.g. good flexibility of the dosimeter size and shape. The grain size affects the sensitivity and influences its handling in dispensers. A good compromise is to use powders with grain sizes between 75 and 200 μm. Hot-pressed forms of TL detectors are produced by compression of polycrystalline material at elevated temperature. Another solid form is obtained by extrusion of the fused polycrystalline material through a shapped die, and by cutting and polishing the resultant extrusion. Sintered dosimeters are prepared by high temperature sintering of pressed phosphor powder. Samples of impurities doped and undoped BaB_4O_7, MgB_4O_7, CaB_4O_7, $L_2B_4O_7$ and LiB_3O_5 dosimeters were produced in this way but physical fragility limits their use, particularly in large and thin form powder form [118].

5.2. Equipments in Laboratory

The thermoluminescence laboratory has two main rooms. In the first room, there are a furnace, a sieve, a digital balance, and etc. They are used to prepare the samples to the experimental applications. The irradiation and reading process are carried out in the other room called as darkroom. Radiation source and TL reader are present in this room.

Figure 5.1. Thermoluminescence laboratory

5.2.1. Equipments used before irradiation process

Samples growth heating processes and annealing stages were done at different temperatures with a micro-processor controlled electrical oven for different periods range between 1 min to 24 hours. One of the attractive points of TLD is the possibility to reuse the TL material many times. To be sure that in the reuse the TL material has precisely the same properties as before a thermal annealing procedure is required. Therefore, the heating and annealing process were also done by this oven to remove any trapped defect centers which can interfere

with subsequent irradiations. The temperature was measured by chromel-alumel thermocouple placed in close proximity to the samples. The temperature sensitivity of the oven is estimated to ±1 ^{o}C. They were also used a digital balance to estimate the weight of the used samples, sieves to sieve crushed samples for wanted dimensions (50 μm to 2 mm) and some chemicals to clean samples (Fig.5.2).

Figure 5.2. Some of the used equipments: oven, chemicals, sieves and digital balance

5.2.2. Radiation source and irradiation procedure

The samples are irradiated at room temperature immediately by a ^{90}Sr-^{90}Y β (beta)-source (Fig.5.3). The activity of this source is about 100 mCi. It is calibrated by manufacturer on March, 10, 1994. The recommended working life-time is about 15 years. Stronium-90 emits high energy beta particles from their daughter products (^{90}Sr β-0.546 MeV together with ^{90}Y β-2.27 MeV). Beta radiation is absorbed by air, so its intensity declines with distance much more rapidly than inverse square law calculations would indicate. The typical strength of a 100 mCi Sr-90-^{90}Y β-source

installed in a 9010 Optical Dating System is 1.42 Gy/minute=0.0238 Gy/sec for fine grains on aluminium, or 1.5 Gy/min=0.025 Gy/sec for 100 mg quartz on stainless still. The irradiation equipment is an additional part of the 9010 Optical Dating System which is purchased from Little More Scientific Engineering, UK (Fig.5.4). The irradiation source equipment is interfaced to a PC computer using a serial RS-232 port [119].

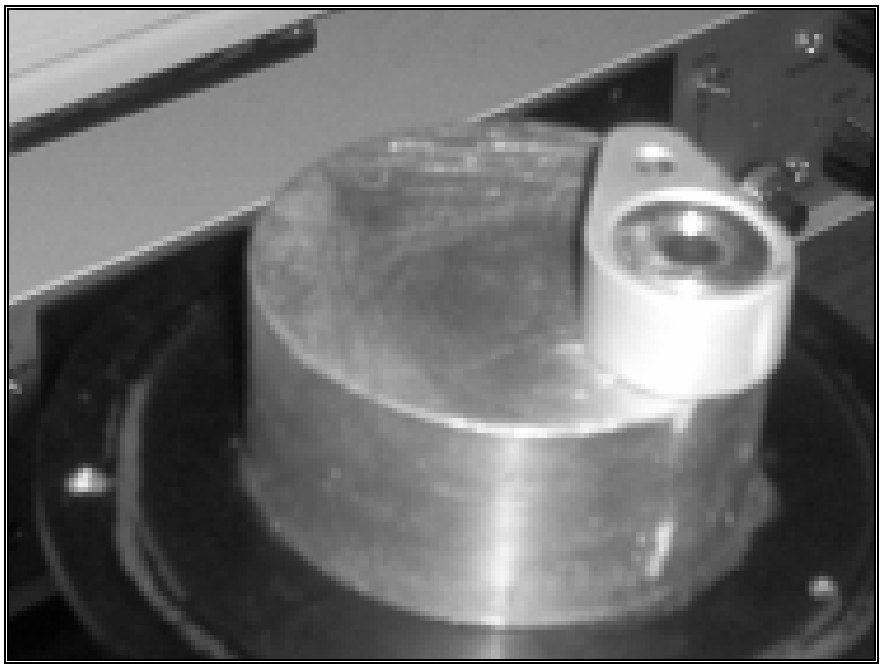

Figure 5.3. ^{90}Sr-^{90}Y β-source

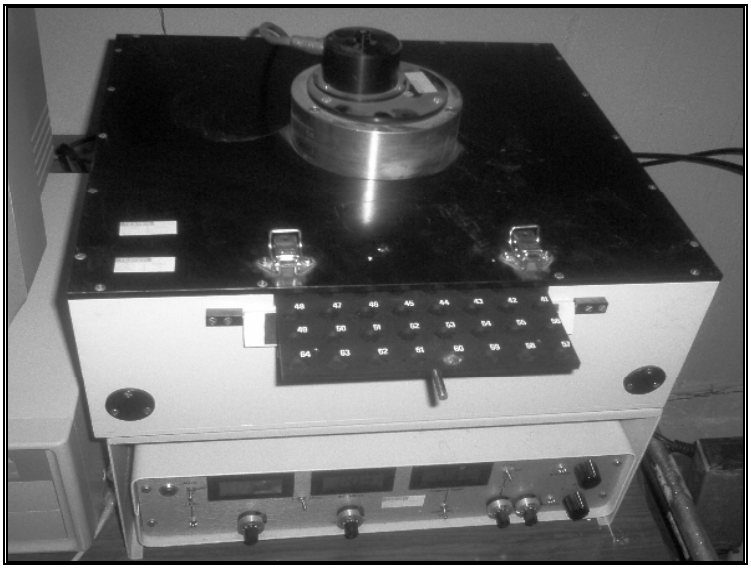

Figure 5.4. 9010 Optical Dating System (irradiator)

5.2.3. TL analyzer and TL measurements

A Harshaw TLD System 3500 Manual TL reader is used in this work (Fig.5.5). The device consists of a separate thermoluminescence detector and an automatic integrating picoammeter. The dosimeter is placed on a metal planchet in a sample drawer. The dosimeter is heated by electrically heating the planchet.

Figure 5.5. Harshaw TLD System 3500 Manual TL Reader

The technical architecture of the system includes both the Reader and a personal computer (PC) connected through a standard RS-232 serial communication port to control the 3500 Reader. The basic block diagram of reader is shown in Fig .5.6. All functions are divided between the reader and the specialized TLD Shell software that runs on the PC. Signal acquisition and conditioning are performed in the reader. In this way, each glow curve can be analyzed using a best-fit computer program based on a Marquardt algorithm minimizations procedure, associated to first-order and general-order kinetic expressions. The instrument includes a sample change drawer for inserting and removing the TLD elements. The reader uses contact heating with a closed loop feedback system that produces adjustable linearly ramped temperatures from 1 ^{o}C to 50 ^{o}C per second accurate to within ± 1 ^{o}C to 400 ^{o}C in the standard reader.

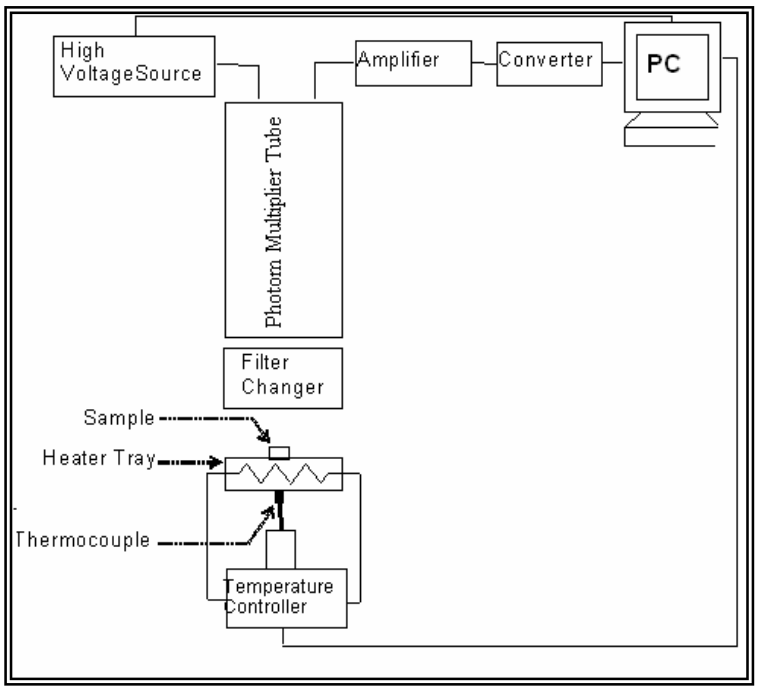

Figure 5.6. Basic block diagram of TL reader

The Time Temperature Profile (TTP) is user defined in three segments: Preheat, Acquire, and Anneal, each with independent times (Pre-read anneal: adjustable from 0 to 1000 sec between room temperature to 200 ^{o}C, Linear ramp: adjustable from 1 ^{o}C to 50 ^{o}C per second, Post-read anneal: from 0 to 1000 sec between 300 ^{o}C and 400 ^{o}C. The typical time temperature profile is shown in Figure .5.7.

To improve the accuracy of low-exposure readings and to extend planchet life, the 3500 provides for nitrogen to flow around the planchet. By eliminating oxygen in the planchet area, the nitrogen flow eliminates the unwanted oxygen-induced TL signal. Nitrogen is also routed through the photo-multiplier tube (PMT) chamber to eliminate moisture caused by condensation.

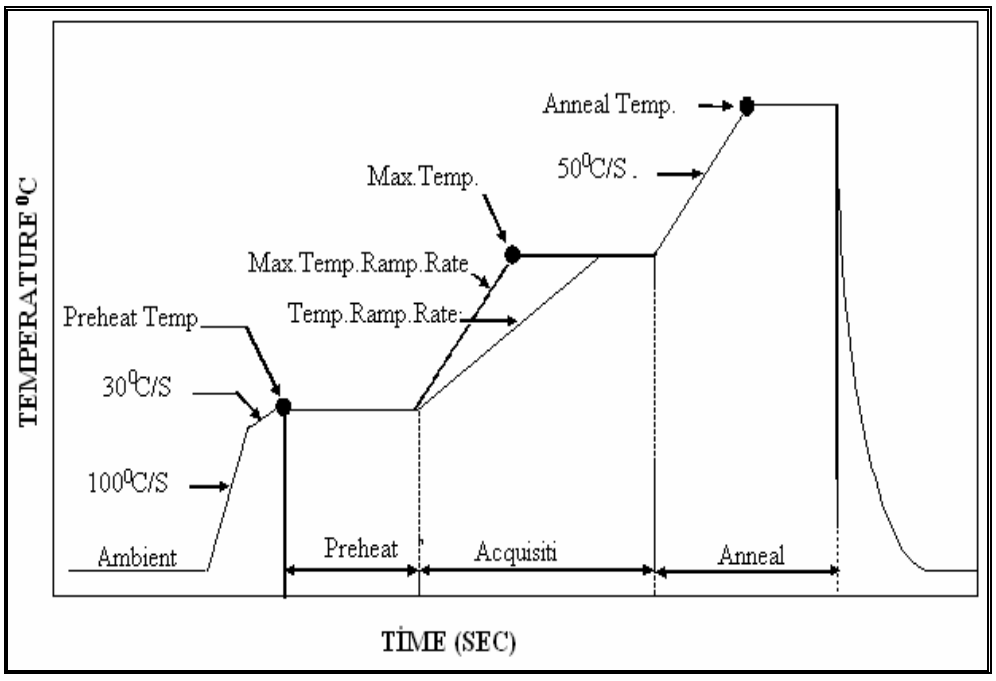

Figure 5.7. Typical time temperature profile (TTP)

5.2.4. X-ray difractometer and X-ray measurements

The analysis of crystal structures is normally performed by using X-ray diffraction technique. X-rays are form of electromagnetic radiation with wavelengths in the range 0.1-10 Å. X-rays produce in the X-rays production tube. A basic diagram of X-rays tube is seen in Fig. 5.8. X-ray diffraction technigue are used to analyse crystalline structures.

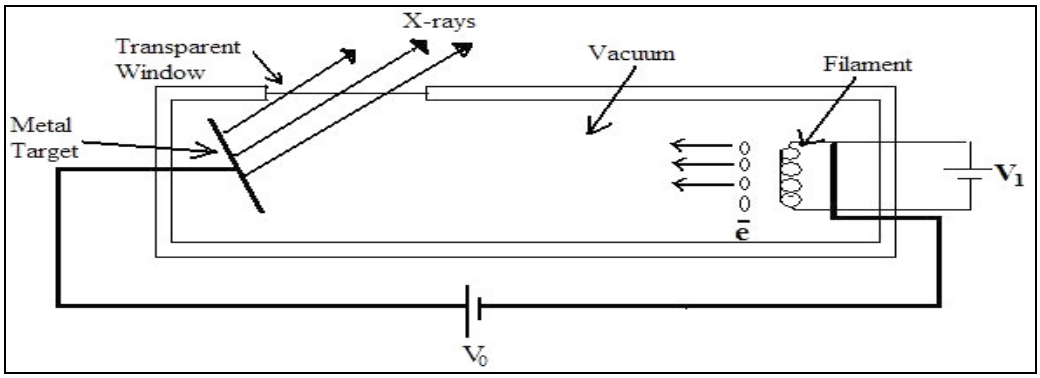

Figure 5.8. Basic block diagram of a X-ray tube

X-Ray diffraction (XRD) examinations were performed to identify the produced samples. XRD patterns were recorded from $10^o<2\theta<80^o$ at a scanning rate of 4^o min^{-1} at RT by using a Rigaku MiniFlex X-ray Diffractometer with a Cu Kα (λ=1.5405 Å) radiation source (Fig. 5.9). Inter plane spacing *(d),* lattice parameters of unit cell and miller indexes are found from 2θ values by using a computer program package called ‘‘POWD’’ [120]. This program is designed to interpret and index the powder diffractions patterns. This programme is based on Bragg’s law given in Eq.(5.1) Inter plane spacing (*d*), lattice parameters of unit cell and miller indexes are found by using previously explained computer program.

Crystal's systems are tired and when $\sum \Delta d(=d_{obs}-d_{cal})$ value found to be minimum, it is decided that this system is the best choice for selected crystal. Conformations were performed by comparing evaluated values with characteristics *d* values of International Centre for Diffraction Data (ICDD) cards of appropriate materials using;

$$n.\lambda=2.d.\sin\theta \tag{5.1}$$

where *n* is an integer such as 1,2,3, and etc; λ is the wave length (λ=1.54056 Å for Cu anode, *d* is the distance between successive parallel planes in Å, θ is the angle of incidence and reflection of the x-ray beam from the given atomic plane.

Figure 5.9. Rigaku MiniFlex X-ray Diffractometer

5.2.5. Aminco-Bowman series 2 luminescence spectrometer

An Aminco-Bowman Series 2 Luminescence Spectrometer was used to measure the TL emission spectra between 200-600 nm using a linear heating rate of 20 ^{o}C/min and a scan rate of 30 nm/s (see Fig. 5.10). The recorded spectra have been corrected for the photomultiplier response. Spectrophotometers usually have a photomultiplier tube that amplifies the signal for accurate measurement.

Figure 5.10. Aminco-Bowman Series 2 Luminescence Spectrometer

CHAPTER VI

EXPERIMENTAL RESULTS AND DISCUSSIONS

As indicated in previous chapters, in this work, the alkaline earth borate samples were prepared with melting points and solid state diffusion methods due to their easily handling, simple usage feacture and provide good homogeneity in samples.

6.1. Investigation of TL Properties of Undoped and Ce-Doped BaB_4O_7 Samples

As mentioned previously, the TL studies of borate compounds are started in 1974 by work of Kazanskaya [121]. These compounds found several interesting applications e.g., in TLD [122,123]. Barium borate is also used as a non-linear optical material for laser harmonic generation. Many researchers [124,125] carried out the TL studies of magnesium borate compounds. However, so far no work has been reported on the thermally stimulated luminescence studies of Ce doped barium borate compound. Keeping this in view, we have firstly studied the TSL dosimetric properties of undoped and Ce-doped BaB_4O_7 compounds. The findings reported below show that it may be a promising material for personal dosimetry.

The polycrystalline samples of undoped and Ce-doped BaB_4O_7 were prepared by a melting method. The preparation of undoped BaB_4O_7 sample was made by mixing barium carbonate ($BaCO_3$) (99%, Aldrich) and boric acid (H_3BO_3

(99.5%, Aldrich) in stoichiometric ratio and the mixture was melted at 900 ^{o}C in a quartz crucible for 4.5 hour and then rapidly cooled to room temperature. Ce-doped BaB_4O_7 sample was prepared in a similar manner by taking the starting material in stoichiometric ratio and adding 10 mol % of CeO_2 in the mixture. The resultant glassy material was again heated at 400 ^{o}C for 1 hr and then ground in an agate mortar and sieved to select particles of homogenous size (100-200 μm). All the heat treatments were performed with an electrical furnace in TL laboratory, which is able to control the temperature within ±1 ^{o}C. All irradiations were carried out at room temperature with ^{90}Sr-^{90}Y beta (β) source delivering about 0.9 Gy/min in nowadays. The glow curves were obtained by using our Harshaw QS 3500 Manual type TL reader. Glow curve readout was carried out on a platinum planchet at a linear heating rate of 1 ^{o}C/sec up to 400^{o}C. A continuous flux of N_2 was used during the readouts to reduce chemiluminescence in the heated samples. A standard clear glass filter was always installed in the reader between the planchet and photomultiplier tube to eliminate the emitted infrared lights from the reader plus samples. The irradiated samples were kept in the dark in order to avoid any influence of the environment light. An Aminco-Bowman Series 2 Luminescence Spectrometer was used to measure the TL emission spectra between 200 nm and 600 nm using a linear heating rate of 20^{o}C/min and a scan rate of 30 nm/s. The recorded spectra have been corrected for the photomultiplier response.

In order to determine the identity of produced samples, a Rigaku D/Max-I IB X-ray diffractometer at 40 kV and 20 mA with CuK_1 (λ=1.5405Å) radiation were used. The X-ray diffraction measurements were taken at the interval of Bragg angle 2θ ($5^{o} \leq 2\theta \leq 80^{o}$) at scanning rate of 4 ^{o}min^{-1} at room temperature. The

recorded glow curves were analyzed using computer glow curve deconvolution (CGCD) program. X-ray diffraction pattern of Ce-doped BaB_4O_7 sample is shown in Fig. 6.1. By using a computer program [120], the lattice parameters of unit cell *a*, *b*, *c* and *d*-values were calculated and it was determined that the barium borate prepared by melting method has monoclinic crystal structure.

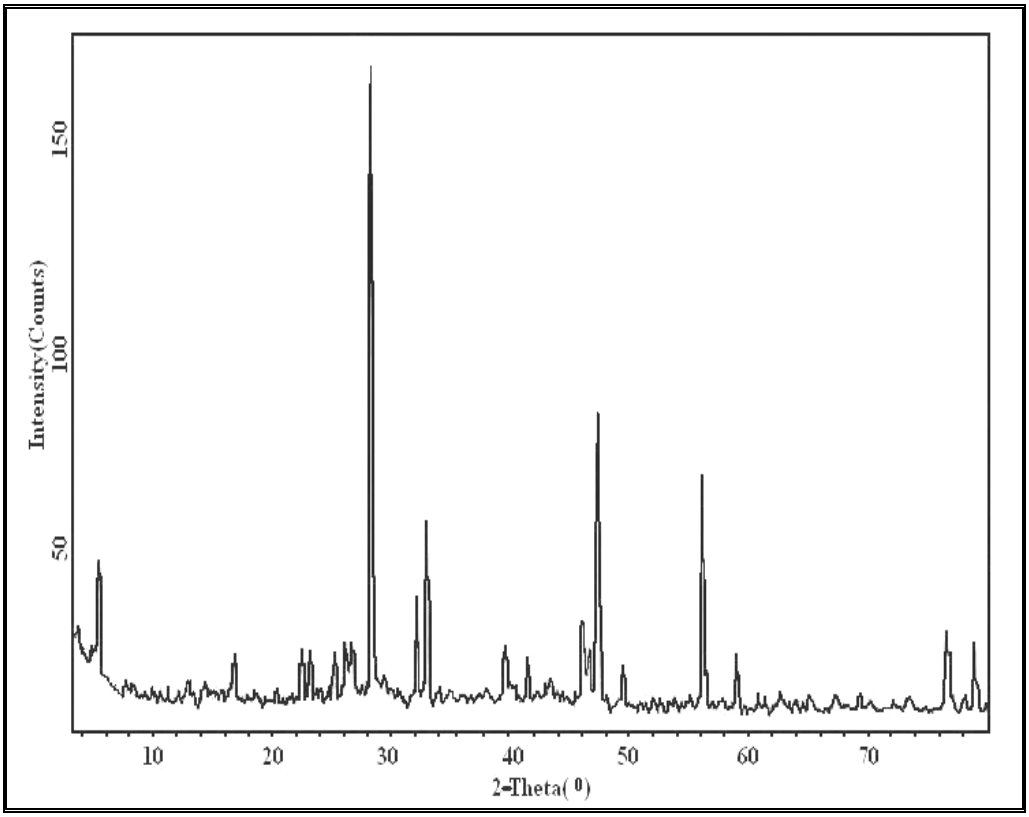

Figure 6.1. XRD pattern of Ce-doped BaB_4O_7 sample at room temperature

Figure 6.2 shows one of the analyzed glow curves of undoped BaB_4O_7 powder sample after irradiating the samples for 300 secs (≈4.5 Gy) by beta-rays. The TSL glow curves of undoped BaB_4O_7 sample exhibits one strong TL glow peak at around 195 ^oC with low intensity shoulders at about 117, 255 and 365 ^oC when heated at a constant heating rate of 1 ^oC/sec. The peak temperature (T_m) of main peak at around 195 ^oC depends on the applied dose and it shifts to low

temperature sides with increasing dose levels. The peak at 117 ^{o}C is not clear, being superimposed by the 195 ^{o}C peak and it fades quickly and completely disappears in a few days after irradiation.

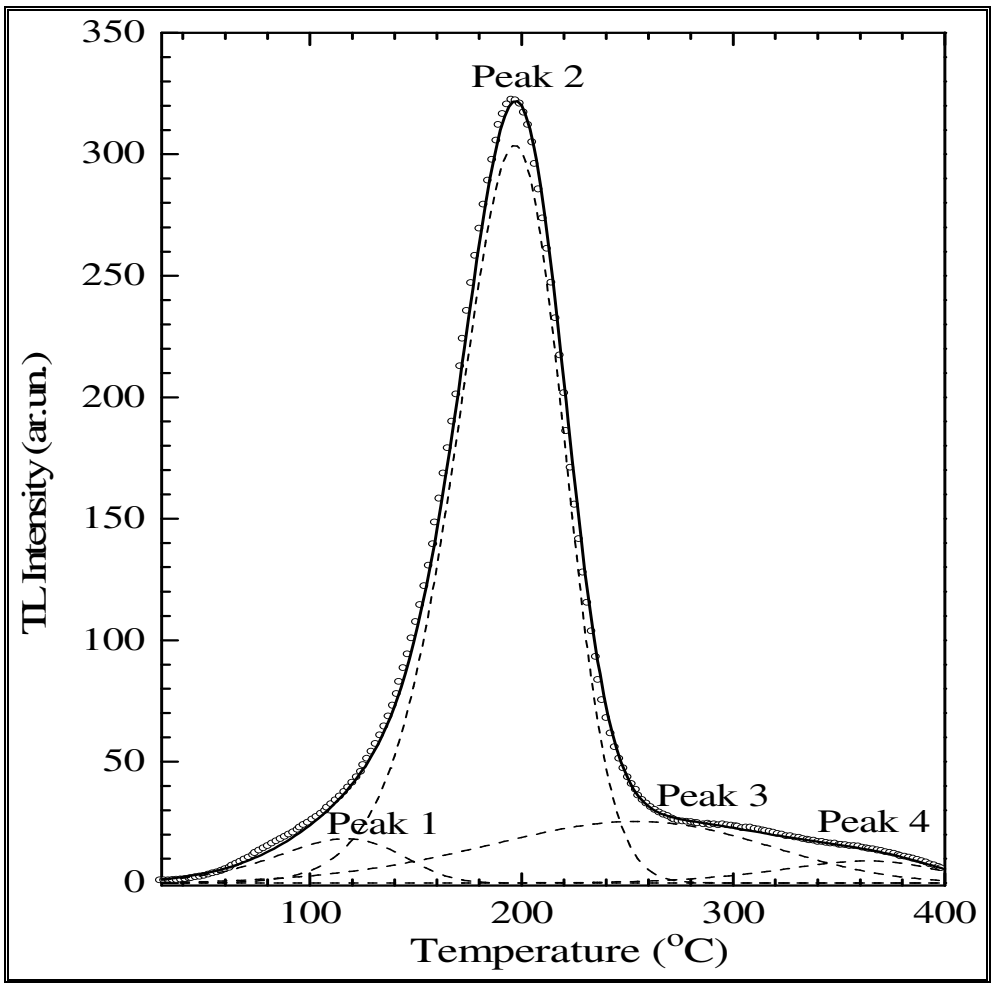

Figure 6.2. An analyzed glow curve of undoped BaB_4O_7 obtained at a heating rate of 1^{o}C/sec following β-ray exposure at room temperature for 300 secs (≈4.5 Gy). (The open circles represent the experimental points, the full curve is the global fitting and broken curves represent fitted individual glow peaks)

On the other hand, the TSL glow curves of beta-irradiated BaB_4O_7:Ce exhibit three prominent glow peaks at 195, 250, 331^{o}C and two shoulder peaks at around 90 and 135 ^{o}C on the low temperature sides of peak 3. An analyzed glow

curve of Ce-doped BaB_4O_7 phosphor obtained at a heating rate of 1 $^oC/s$ following beta ray exposure for 30 min (≈27 Gy) is shown in Fig. 6.3.

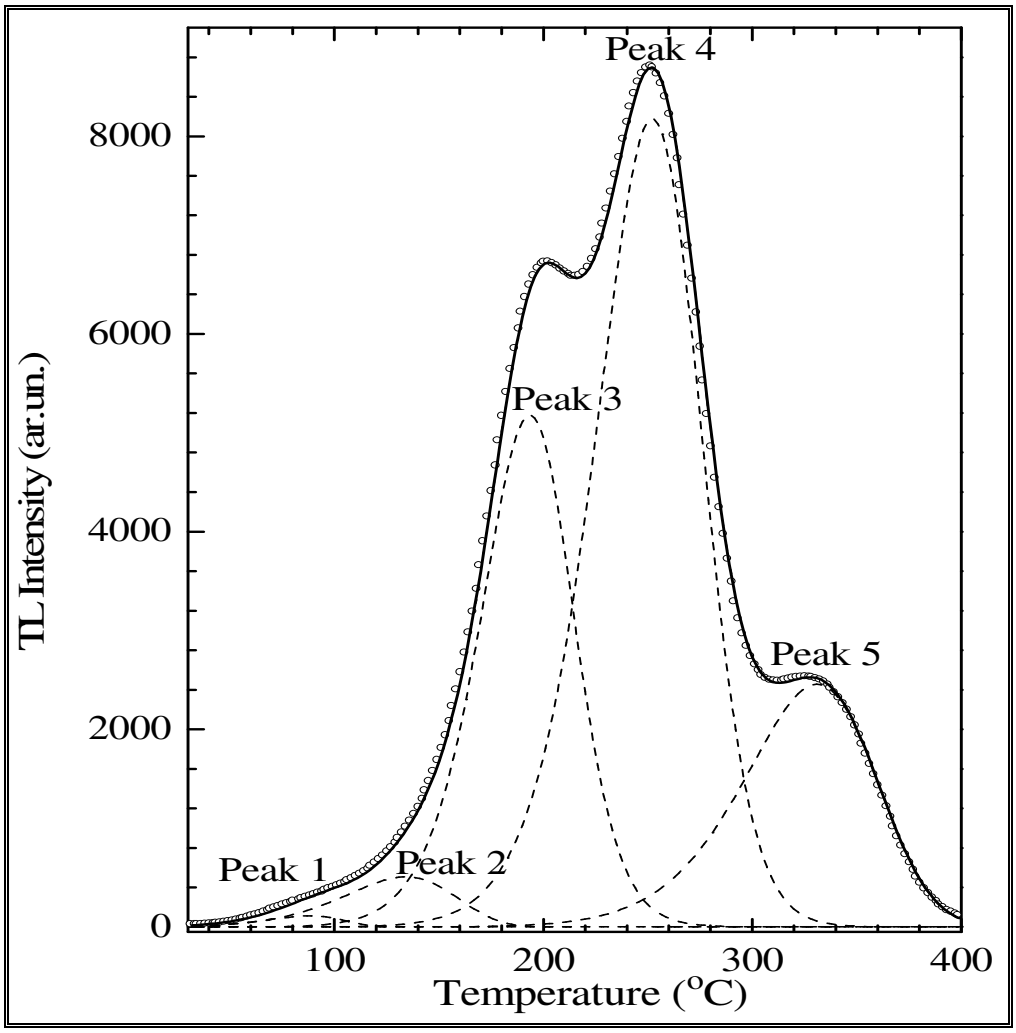

Figure 6.3. An analyzed glow curve of Ce-doped BaB_4O_7 obtained at a heating rate of 1^oC/sec following β-ray exposure at room temperature for 30 min (≈27 Gy)

One of the first problems investigated in the given study is the annealing procedure of Ce-doped BaB_4O_7 to be used in order to eliminate the effects of the previous irradiations. The experiment was carried out using different annealing temperatures and for each temperature, different annealing times ranging from 15 min to 1 hr was used. The temperatures used were ranging from 400 ^oC to 500 ^oC in

steps 50 ^{o}C. The whole experiment was repeated at various dose levels. The obtained results confirmed that an annealing treatment at 400 ^{o}C for 30 min was found sufficient to erase TL signal completely and restore the original TL sensitivity of the TL dosimeters. However, during routine applications of TL detectors for dose levels less than 2 Gy, readout anneal appeared to be an optimal and very convenient procedure. For this reason, the comparison of TL sensitivity of TL detectors after oven and readout anneal was performed. Some samples after their normal oven anneal, were irradiated to a test dose 0.9 Gy. The samples were subsequently readout up to 400 ^{o}C with a linear heating rate of 1 ^{o}C/s, and their glow curves were recorded. After this readout the samples were irradiated again at the same test dose and then readout. The glow curve shapes were seen to be identical in both cases, where the TL sensitivities were the same within less than 2%. However, for doses above 2 Gy, it was found that readout annealing is insufficient to completely remove the TL peak at 332 ^{o}C and therefore the oven annealing at 400 ^{o}C for 30 min is the best thermal treatment for getting a stable TL response and the lowest background.

In order to assess the reproducibility of the dose measurements attainable using Ce-doped sample, the TL stability after repeated cycles of the two procedures was also tested at two different dose levels (0.9 Gy and 27 Gy). Repeated cycles of (i) oven annealing, irradiation, readout and (ii) irradiation, readout, were carried out (Fig. 6.4). The results showed that both procedures show a very good stability within less than 2% based on standard deviation over more than 10 repeated cycles for the dose levels below 2 Gy. However, when the dose levels increased above 2 Gy (i.e for 27 Gy), it was observed that the readout annealing is not sufficient to

erase TL signal completely and restore the original TL sensitivity of the TL dosimeters (Fig. 6.4).

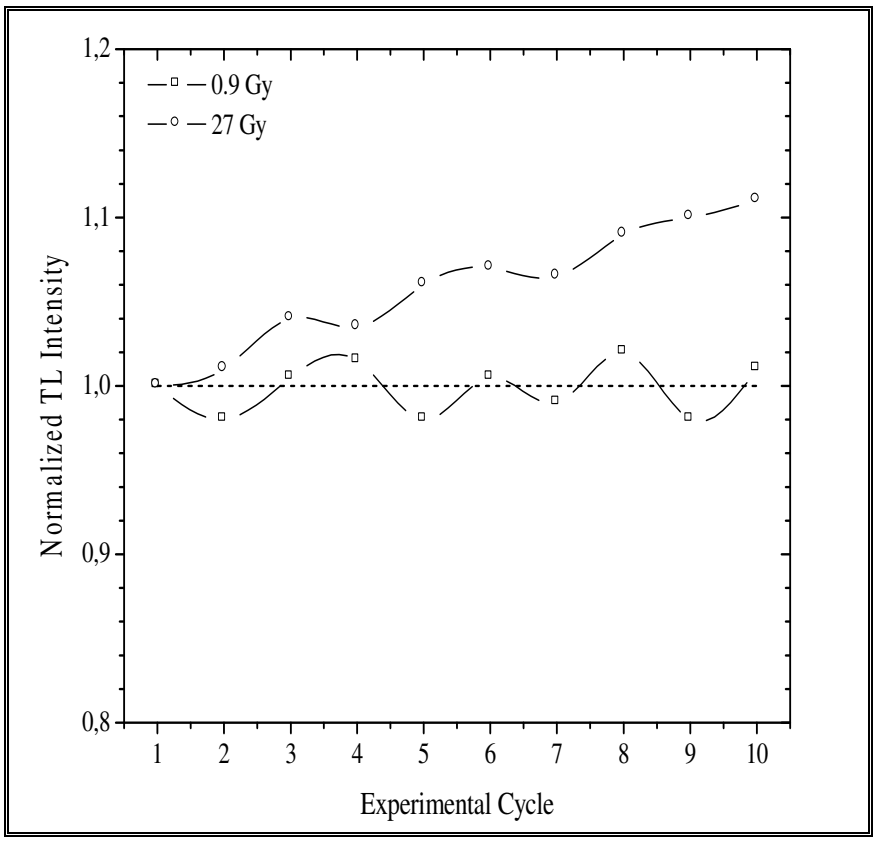

Figure 6.4. Reproducibility of deconvoluted peak areas of Ce-doped BaB_4O_7 through ten repeated cycles of irradiation-readout annealing

As a result, if the previous history of the material is unknown, it is thus advantageous to anneal the sample at 400 ^oC for 30 min before putting it to any dosimetric use. It has been stressed that most of the commercially produced TL samples change color after repeated annealing and readout procedures and thus they lose their initial sensitivity. On the contrary, the studied material (BaB_4O_7:Ce) in the given study stayed unchanged in its color after annealing and/or readout treatments.

The dose response of undoped and Ce-doped BaB_4O_7 were studied as a function of irradiation time between 1 sec (1.5 mGy) and 24 hr (1.3 kGy) using beta-rays. Figure 6.5 shows some of the selected glow curves of both undoped and Ce-doped samples after different dose levels. Samples were read immediately after irradiation and it is seen that there are no great differences in the glow curve structures of both samples with increasing dose levels.

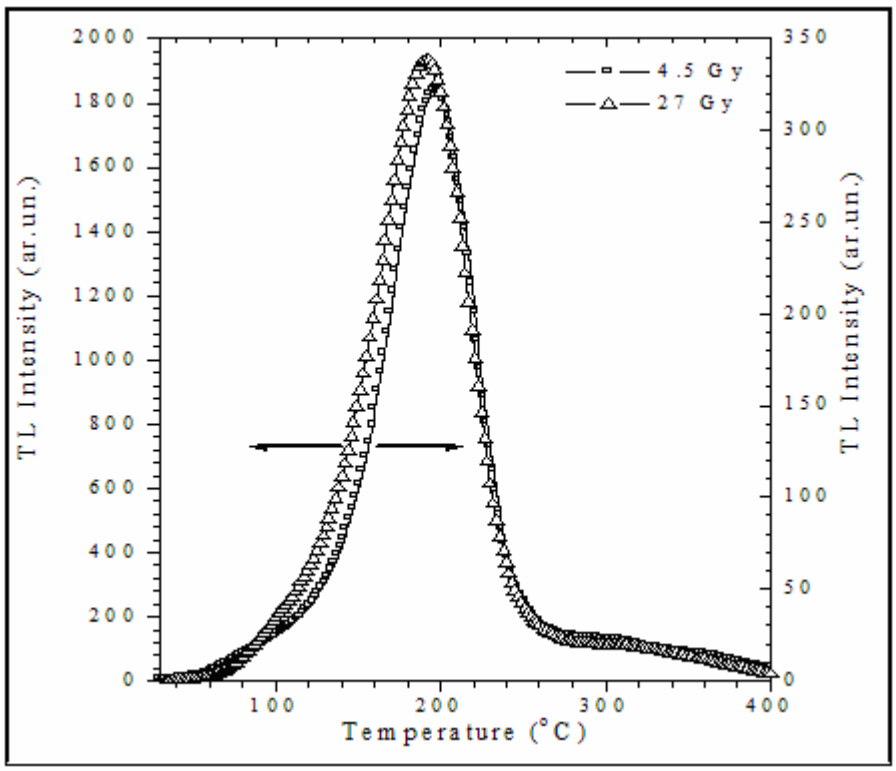

Figure 6.5. Some of the selected glow curves of undoped BaB_4O_7 measured at 1 $^oC/s$ after different dose levels

The resulting dose response curve is shown in Figure 6.6 and all TL response values reported are an average of three measurements. As seen from figure 6.6, the main glow peaks of both samples were linearly increased with increasing beta-ray dose up to 1.3 kGy and no saturation trend is observed in them

up to the applied maximum dose levels. It should be mention that the last peak at 332 ^{o}C in BaB_4O_7:Ce is also increases linearly but its slope is slightly less than 1. These results were obtained from the peak height measurements but peak area measurements were also given similar results. So, in contrast to other common TL materials, undoped and Ce-doped barium borate compounds show extremely useful TL feature of perfect linearity in its TL response with dose up to 1.3 kGy. Generally supralinearity is a characteristic of a large variety of TL materials, so TL linearity in the high dose region, over 10 Gy, is exceptionally rare.

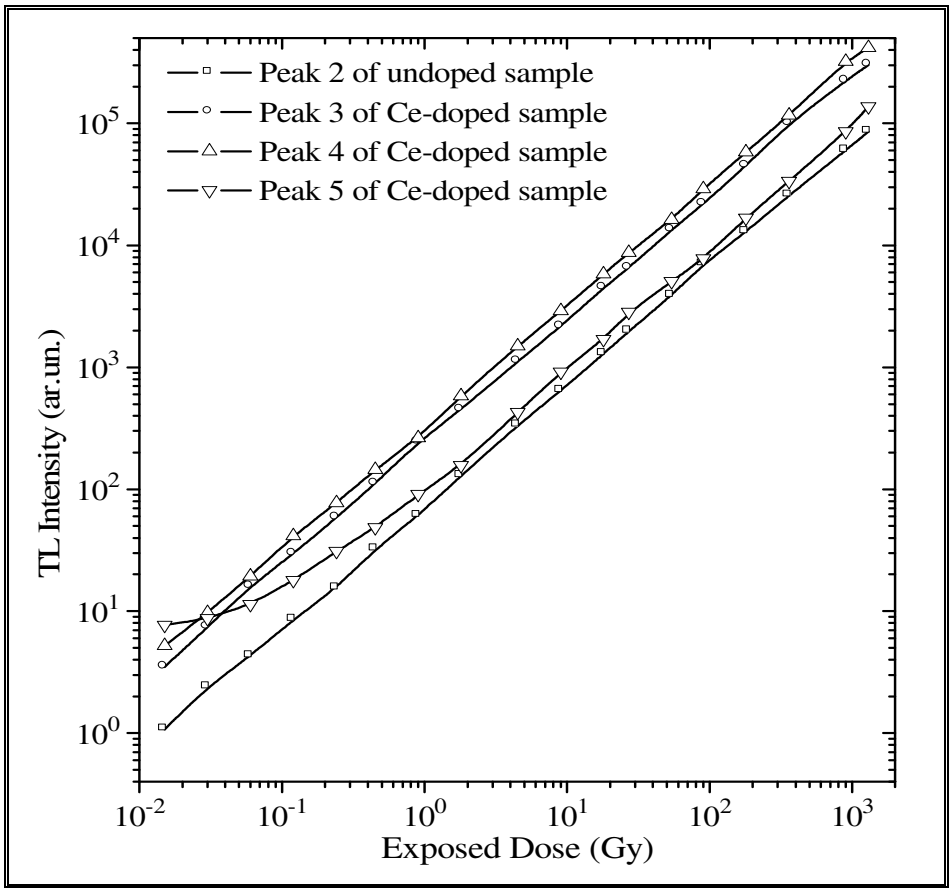

Figure 6.6. The TL dose response curve of main dosimetric peaks in the glow curves of both undoped and Ce-doped BaB_4O_7 samples

The typical glow curve intensity of TLD-100 was also compared with the intensity of Ce-doped BaB_4O_7 after a test beta dose of 0.9 Gy. It was observed that the third peak at 250 ^oC is most intense of the all peaks in Ce-doped BaB_4O_7 and hence it is important for dosimetric studies. Therefore, after the normalization to the same mass of all samples, the TL intensity of peak 4 of Ce-doped sample was compared with intensity of peak 5 in TLD-100 and it was found that the TSL intensity is enhanced by about 5 times when compared with the TSL intensity of undoped BaB_4O_7 compound whereas is approximately 1.8±0.1 of TLD100.

For sample to be useful in dosimetry, the TL intensity of its dosimetric peaks should be stable and no fade upon storage after exposure. In order to investigate the fading characteristics of all peaks in both samples, the TLD samples were stored in dark conditions at room temperature, between 25-30 ^oC over a period of one month after beta-ray exposure. Figure 6.7 shows two of the selected glow curves from the glow curves of fading experiment of Ce-doped sample. The results demonstrated a very small decrease of the TL response during the elapsed period of time in the main peaks (peaks 4 and 5) of BaB_4O_7:Ce (Fig. 6.8).

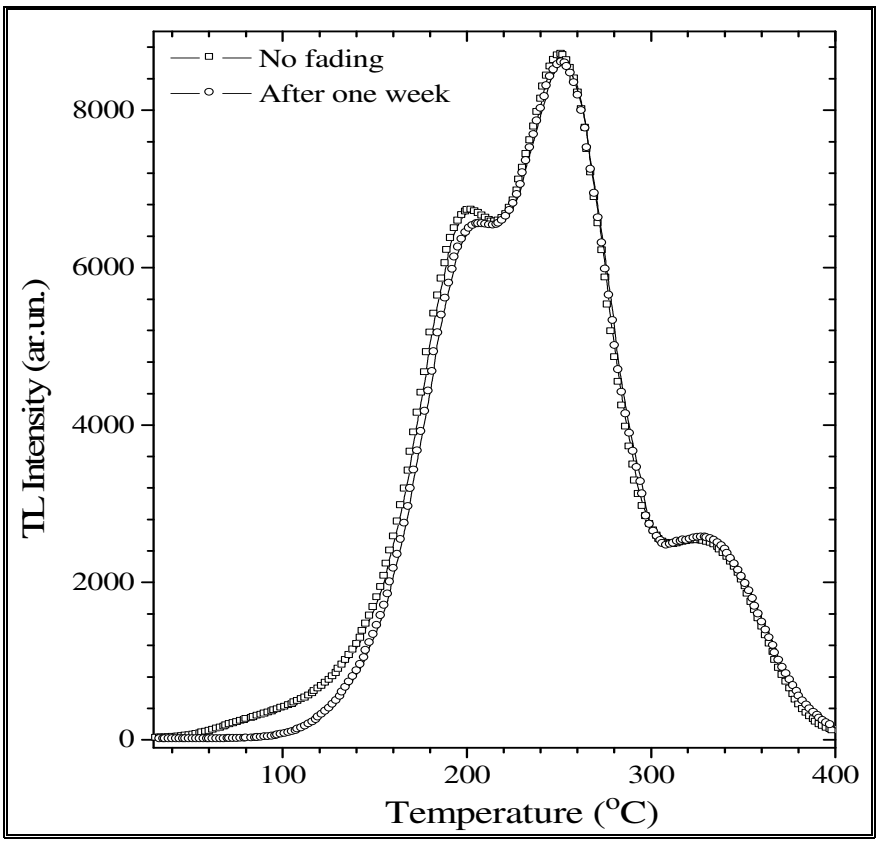

Figure 6.7. The recorded two glow curves of Ce-doped BaB_4O_7 after some storage times at room temperature in the dark condition

The fading of the peak 4 at around 250 °C of BaB_4O_7:Ce is less than 4% for one months if the dosimeters were protected from direct room light. It is seen that the first peaks at 90 and 135 °C fades completely after one week irradiation hence it is no dosimetric value. So, the influence of this peak in dosimetric measurements can be easily eliminated by making the TL measurements after a post-irradiation interval of one week or by incorporating a pre-read anneal at about 100 °C for a few seconds in the TL reader system. It is known that most of the common TL materials are very sensitive to light. However, it was observed that room temperature fading of Ce-doped BaB_4O_7 phosphor is less than 10% in one month even though the phosphor was not protected from room light. On the other hand, the fading rate of

main peak (T_m=195 ^oC) in undoped BaB_4O_7 is quite high from the main peaks of Ce-doped samples (Fig. 6.8).

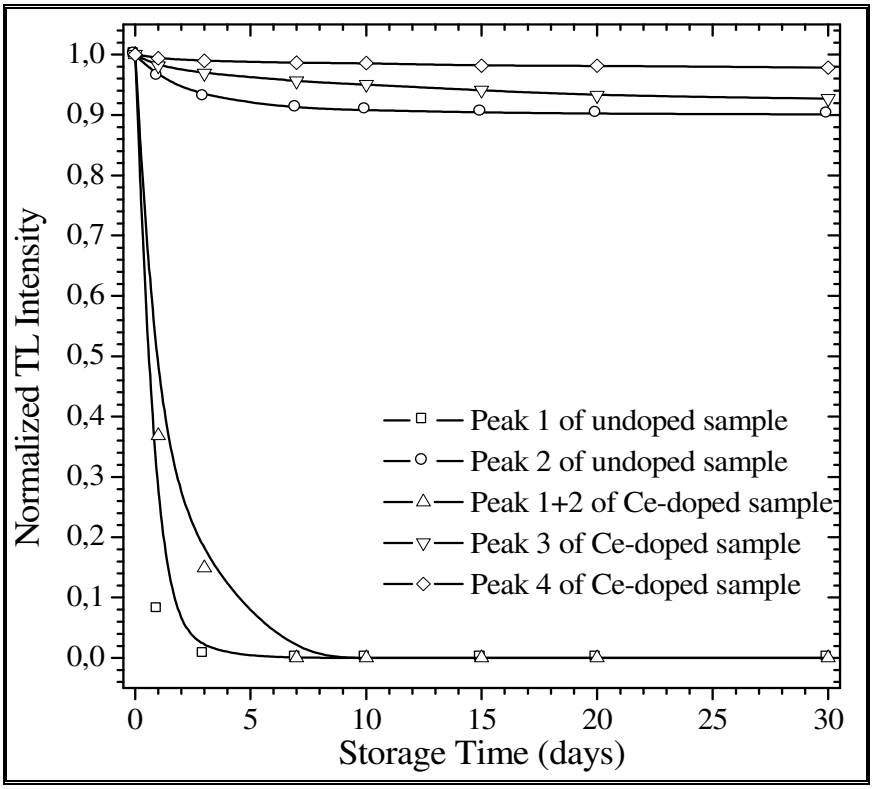

Figure 6.8. The obtained fading characteristics of glow peaks of undoped and Ce-doped BaB_4O_7 using the CGCD program

The usable dose range of many phosphors is limited at the lower end of doses by the variability in the background signal from the undosed samples. In the given study, the experimentally determined minimum detectable dose defined as that dose which gives three times the standard deviation of the zero reading of the Ce-doped BaB_4O_7 phosphors, is also estimated and it is found to be approximately 300 μGy.

The spectral composition of the TSL was also investigated for both samples. In general, Ce incorporation in the dosimetric materials gives an efficient emission

in the blue to green region of the spectrum and it acts as very efficient radiative recombination centre. An analyzed TL emission spectrum of BaB_4O_7:Ce samples recorded at 250 ^oC TL peak is shown in Figure 6.9. It shows a main emission in a wavelength range centered at around 360 nm and the other weaker band at around 425 nm (Fig. 6.9) that is convenient for conventional TLD readers. The property that violet and blue emissions are dominant is useful in TL dosimetry. The emission thus occurs in the most sensitive region for the common photomultiplier tubes. The spectral composition of the TSL emission leads to identify the recombination centers with Ce-ions.

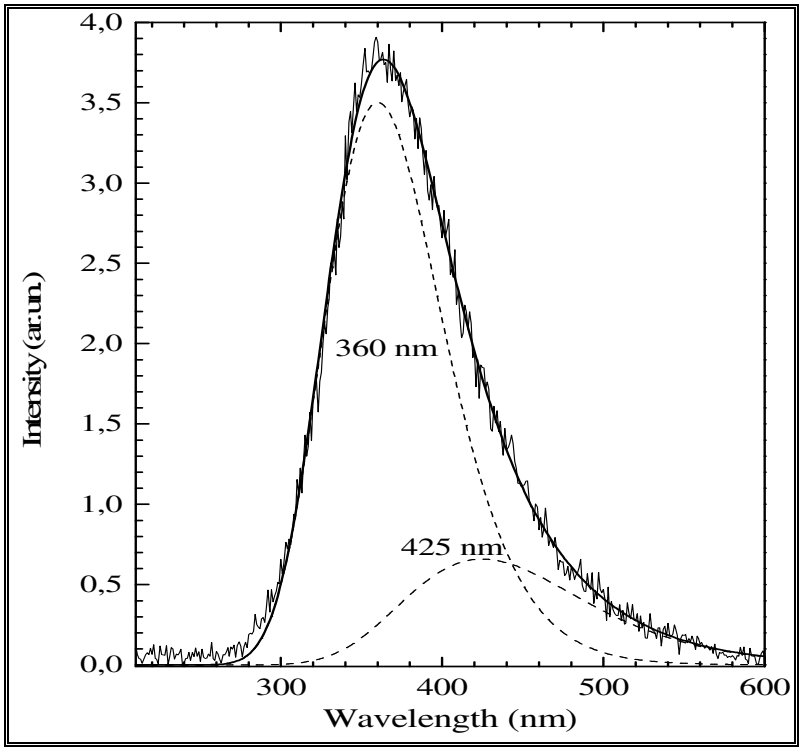

Figure 6.9. TL emission spectra of Ce-doped BaB_4O_7 measured at around 250 ^oC

In particular, it is well known that the Ce^{3+}-ions can efficiently capture holes owing to their strong tendency to the stable tetravalent state RE^{4+} corresponding to the empty and the half-filled 4*f* shell. Therefore, the capture of holes by the 4*f* level

of Ce^{3+}-ions forms Ce^{4+}-ions under ionizing irradiation. Upon heating, Ce^{4+}-ions can capture electrons thermally freed from traps in their 5*d* level to form an excited $(Ce^{3+})^{*}$-ion. Then, the subsequent radiative electron-hole recombination gives rise to the observed emission bands at 360 and 425 nm due to the transitions from 5*d* excited state to $^{2}F_{5/2}$ and $^{2}F_{7/2}$ ground states of Ce^{3+}, respectively. On the other hand, the emission spectrum of undoped sample measured at 190 ^{o}C is a broad band around 460 nm which its origin is unknown. It is possible that the emission observed in undoped sample is due to the intrinsic defects.

Evaluation of trapping parameters associated with the glow peaks of TSL glow curves is one of the most important aspects of studies in the field of condensed matter physics. Therefore, the trapping parameters of prominent glow peaks of both samples have been also studied using the CGCD method. This method has become very popular to obtain these parameters for the last two decades [101]. It has great advantages over the experimental methods (i.e. initial rise, peak shape and etc) owing to simultaneous determination of trapping parameters of all peaks without additional thermal treatments and experimental repetitions. Also, this method uses all data points in the whole glow curve rather than just a few points during the curve fitting procedures. It is apparent that if the number of data points used in the analysis increases, the potential for accurate determination of the trapping parameters gets better. The CGCD program is based on the least square minimization procedure and as mentioned in chapter 3 (Section 3.7.2). It was developed at the Reactor Institute at Delft, The Netherlands [101]. By using the Equation (3.23) and (3.24), the obtained trapping parameters were given

in Table 6.1 and Table 6.2. The statistical error of these parameters deriving from the analysis of glow peaks after different irradiation doses is of the order of 10%.

Table 6.1. The trapping parameters of undoped and BaB_4O_7 samples calculated by the CGCD method (β= 1 $^oC/s$)

Ce-doped BaB_4O_7					
	Peak 1	Peak 2	Peak 3	Peak 4	Peak 5
T_m(^{o}C)	90±3	135±2	195±2	250±2	331±2
E_a (eV)	0.6±0.05	0.5±0.05	0.97±0.1	1.04±0.1	1.01±0.1
Ln(s) (s^{-1})	18.65±1.8	13.3±1.3	23.5±2	22.0±2.2	18.3±1.7
B	1	1	1.41±0.15	1.31±0.1	1.12±0.1

Table 6.2. The trapping parameters Ce-doped BaB_4O_7 samples calculated by the CGCD method (β = 1 $^oC/s$)

Undoped BaB_4O_7				
	Peak 1	Peak 2	Peak 3	Peak 4
T_m(^{o}C)	117±4	195±2	255±4	365±4
E_a (eV)	0.41±0.04	0.79±0.08	0.32±0.04	0.91±0.09
Ln(s) (s^{-1}).	11.13±1.2	18.61±2	5.12±1	15.24±1.5
B	1	1.18±0.1	1	1

Comparison with data concerning undoped and Ce-doped BaB_4O_7 allows for identification of the contributions of impurities to the glow curves. A recent investigation showed that, besides metal impurities such as Cu and Ag ions, rare earth dopants (which are well known as very efficient activators in other materials, for example in alkali halide crystals or in oxides) originate good TL features in borate compounds [61]. In general, the undoped samples, whose emission can be related to intrinsic defects or to some unwanted impurity in the starting powder, exhibits a poor TL efficiency which seems to be insufficient for reliable

measurements in the low dose range measurements. On the other hand, the TL signal was steadily increased after incorporation of Ce-ions, as expected. In addition, the glow curve shape of BaB_4O_7 is highly changed after the doping of Ce-ions. This result indicates that there are large interactions between intrinsic defects and Ce-ions. However, further work is in progress to clarify details of the defect and glow curve structure.

In conclusion, this part of study describes preliminary investigations on the radiation dosimetry characteristics of undoped and Ce-doped BaB_4O_7 phosphors. The major TL peak in BaB_4O_7:Ce phosphor occurs at 250 ^oC and its TL sensitivity to beta radiation is approximately 1.8 times higher than that of TLD-100. The beta-dose response of this peak is linear in the dose range 1.5 mGy-1.3 kGy. The post irradiation fading of this peak at room temperature is also less than 5% in one month. The TL emission spectrum of this material has a broad peak at 360 nm and it is a promising characteristic which matches with the maximal efficiency of the most PM tubes. These some of the reported characteristics indicate that BaB_4O_7:Ce may be a new promising phosphor for the use in ionizing radiation dosimetry.

6.2. Investigation of TL Properties of Undoped and Al-Doped LiB_3O_5 Samples

As mentioned previously, the lithum borates benefit from better tissue equivalence as TL dosimeters whilst displaying a similar sensitivity to that of TLD-100. The doped lithium borate crystals have potential as new materials for neutron detection, due to the presence of Li and B, which both have large cross sections for neutron capture. Thus, efficient neutron capture is expected with high-energy

deposits. Since lithium borate has a low effective atomic number and low material density, it will have low efficiency for gamma ray background detection.

Lithium triborate (LiB_3O_5 or LBO) is an excellent nonlinear optical crystal discovered and developed by the Fujian Institute of Research on the Structure of Matter, Chinese Academy of Sciences. The LBO has found considerable use in the nonlinear conversion of light from infrared and visible lasers into the visible and UV spectral range. The LBO has also become the crystal of choice for harmonic conversion of infrared radiation to visible and/or ultraviolet wavelengths because of a fortuitous combination of linear optical properties and nonlinear parameters. Lithium triborate single crystals combine unusually wide transparency, good refractive index homogeneity, adequately large nonlinear coupling, extremely high damage threshold, a short wavelength UV absorption edge, low (but non-zero) absorption, a wide phase-matching acceptance angle and small walk-off angle for many interactions, and good mechanical/chemical properties. Its extremly high damage threshold make LBO crystal is very suitable for harmonic generation of high-intensity laser radiation in wide spectra.

However, the literature survey indicated that the TL processes in doped or undoped LiB_3O_5 have been insufficiently studied up to now when compared to $Li_2B_4O_7$ [126] . Ogorodnikov *et al.* detected two TL-peaks at about 143^oC and 33^oC in below room temperature in the glow curve of LiB_3O_5 [127-128]. These TL peaks have been previously associated with the B^{2+} and O^- trapping centers in LiB_3O_5 [129]. In other words, the TL-peak at 143 ^oC results from delocalization of electrons from the B^{2+}-centers and their recombination on the appropriate trapped hole centers. The O^- center seems to be the most likely candidate for such

recombination center. Further heating leads to delocalization of holes from the O^- centers (TL peak at -33 ^oC) and their recombination on the appropriate trapped electron centers. Above room temperature, the glow curve of polycrystalline pure lithium triborate showed a well-resolved glow peak at around 140 ^oC in (a) transparent, (b) translucent and (c) opaque samples. For the transparent samples, an additional glow peak at around 115 ^oC was also observed. On the other hand, for the translucent crystal samples, two humps at around 115 and 200 ^oC were also observed. The TL intensity is found to be minimum for the transparent region and about 10 times more intense for the opaque region. These results showed that TL glow curves of LiB_3O_5 are characteristic of its particular phase. Özdemir and her colleagues doped various activators such as Cu, Mn, Fe, Mg and Al into lithium triborate which was synthesized at 750 ºC for 14 hours to investigate the TL properties of them [130]. It was found that Cu and Al-doped LiB_3O_5 exhibit very significant thermoluminescence glow curves to be promising dosimetric materials. Ardıçoğlu and her co-workers studied the identification and characterization Gd-doped LiB_3O_5 which showed certain dosimetric response [131]. Keeping this in view, the TL dosimetric properties of undoped and Al-doped LiB_3O_5 compounds have been studied in the present work. The findings reported below show that this product may be a promising material for personal dosimetry.

In this study undoped and various impurities doped LiB_3O_5 samples are synthesized with solid-state diffiusion method as follows: Li_2CO_3 (99%, Merck) and H_3BO_3 (99.5%, Merck) were used as base materials. Li_2CO_3 and H_3BO_3 were mixed in the stoichiometric ratio and finely powdered in an agate mortar. Homogenized mixture was transferred into a convenient porcelain crucible and

preheated at 300 ^{o}C for 4 h to obtain CO_2 and H_2O release. Then, the mixture was heated in the at 750 °C for 16 h. Sufficient aqueous solution of desired dopant (Cu, Mn, Al in form of oxides) weighted separately, mixed with LB_3O_5 and finely powdered in an agate mortar and then mixture heated for 10 h in porcelain crucible. The resultant material rapidly cooled to room temperature in desicator and sieved to select particles of homogenous size (100-200 μm). The concentrations of Al-ions doped into LiB_3O_5 are given in Table 6.3.

Table 6.3. Concentrations of Al-ions in LiB_3O_5

Id.	*Al_2O_3 (wt.%)*	*Id.*	*Al_2O_3 (wt.%)*
Al-1	0.1	Al-6	0.6
Al-2	0.2	Al-7	0.7
Al-3	0.3	Al-8	0.8
Al-4	0.4	Al-9	0.9
Al-5	0.5	Al-10	1.0

According to Bétourné and Touboul lithium triborate crystallizes in the orthorhombic system with the space group $Pna2_1$ [132]. The unit cell parameters are: a = 8.44 Å, b = 7.36 Å and c = 5.11 Å, and unit volume of a cell is: 17.4 Å. The XRD patterns of the undoped LiB_3O_5 and Al-doped LiB_3O_5 are given in Fig. 6.10. In XRD patterns of Al-doped lithium triborates, Al_2O_3 peaks were not detected. There were no reflections associated with this activator. The phase of LiB_3O_5 did not change with doping process. According to the experimental results, it was observed that lithium triborate was produced successfully.

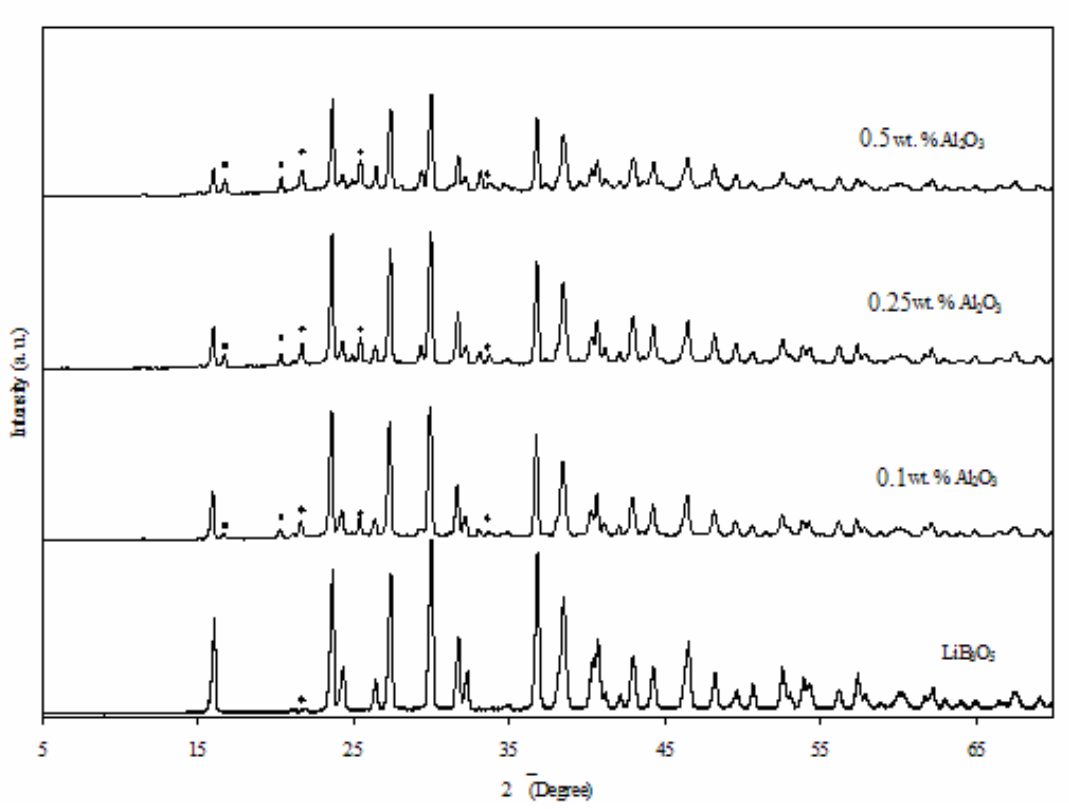

Figure 6.10. The X-ray diffraction pattern of undoped lithium triborate and Al-doped lithium triborates

Figure (6.11) shows a set of selected glow curves which were obtained from different amounts of Al-doped LiB_3O_5 powder samples. All the glow curves shown in the figure were measured after the application of same experimental procedures. After the production of samples, they were firstly read to obtain background signal in the TLD reader up to 400 ^oC and then irradiated for 5 min by β-ray at RT to obtain the glow curves. It can be seen that the shape of the TL peaks in the glow curve structures of all produced samples keep almost constant, showing a concentration-independent character. But, their intensities and temperatures are changed with the amount of dopant concentration of Al. As seen, the intensities of glow peaks are continuously increased with increasing the level of Al-concentration

(see the inset in Fig. 6.11). On the other hand, the peak temperature of main glow peak at about 200 ^{o}C was slightly shifted to the low temperature side with increasing the level of Al-concentration. From Fig. (6.11), it is also obvious that the TL intensity of %1 Al-doped phosphor is much stronger than that of the other samples; therefore, the following studies are focused on the TL property of 1% Al-doped samples.

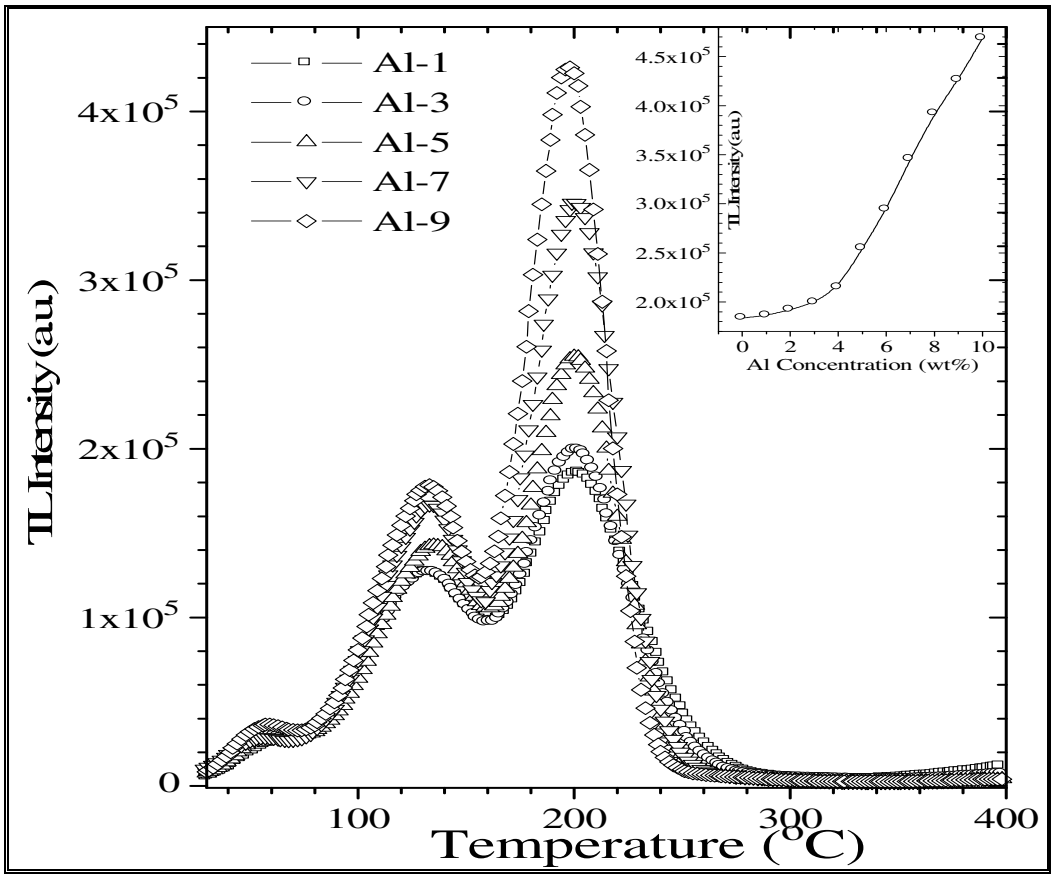

Figure 6.11. TL glow curves of various Al-doped LiB_3O_5 samples after the application of same experimental procedures. All glow curves were read out at 1^{o}C/s after the samples were exposed to the same dose level (≈4.5 Gy) at room temperature

Figure (6.12) shows one of the analyzed glow curves of 1% Al-doped LiB_3O_5 powder sample after irradiating the sample for 300 secs (≈4.5 Gy) by β-

rays. The TSL glow curves of Al-doped LiB_3O_5 sample exhibits two strong TL glow peaks at about 130 and 195 ^oC and a low intensity peak at around 60 ^oC when heated at a constant heating rate of 1 ^oC/sec. The ratio of peak intensity of glow peak at 195 ^oC to the lower temperature glow peak at 130 ^oC is ≈2.85 for the samples doped 1% Al-ion. But, it is interesting to note that this ratio decreases with decreasing the level of Al-concentration. No other peak was found at temperatures higher than 230 ^oC for irradiations of less than 10 Gy. However, a study devoted to determine the dose–response curve of the material gives an experimental evidence of another TL peak appearing at about 245 ^oC above 10 Gy.

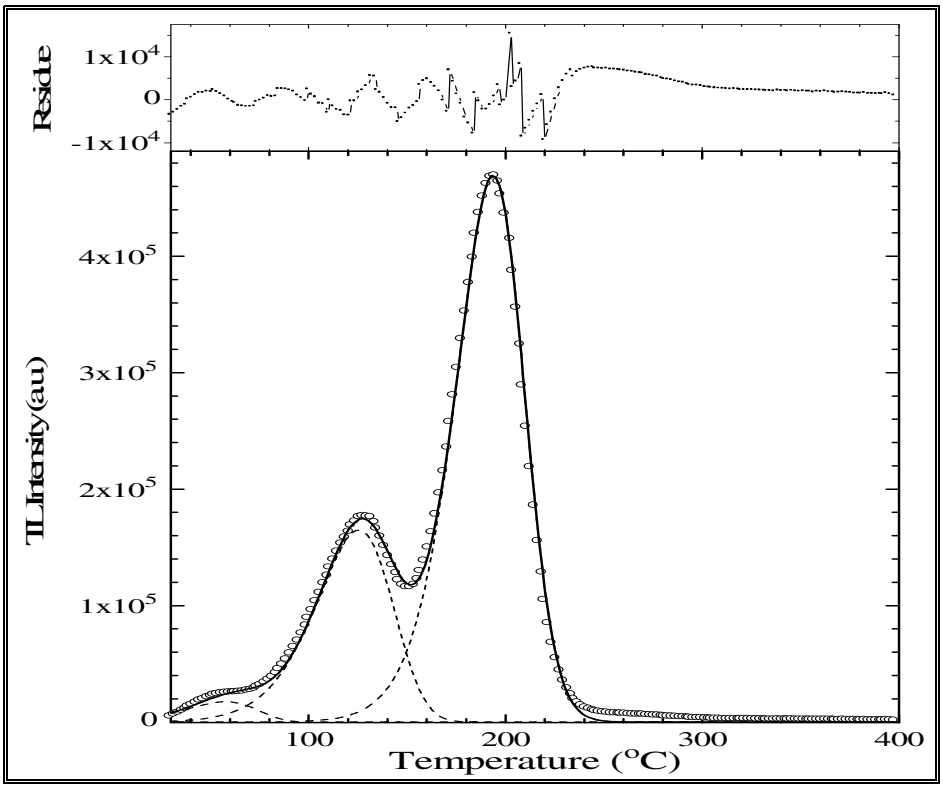

Figure 6.12**.** An analyzed glow curve of 1% Al Doped LiB_3O_5 obtained at a heating rate of 1 ^oC/sec following β-ray exposure at room temperature for 5 mins (≈4.5 Gy) (The open circles represent the experimental points, the full curve is the global fitting and broken curves represent fitted individual glow peaks)

Figure (6.13) shows some of the selected glow curves of Al-doped samples after different dose levels. Samples were read immediately after irradiation and it is seen that there are no great differences in the glow curve structures with increasing dose levels. Note that the difference is only the appearance of one glow peak at about 245 oC for high level of applied doses (D>10 Gy). The peak temperatures (T_m) of glow peaks at 130 and 195 ^{o}C slightly depend on the applied dose levels. As seen from Fig. (6.14a), the peak temperatures of both peaks were firstly shifted to the high temperature sides for the dose levels between 15 mGy and ≈30 Gy and then started to shift low temperature sides with increasing dose levels. The peak at about 60 ^{o}C is not clear at high doses (Fig. (6.13)) and it fades quickly and completely disappears in a few days after irradiation.

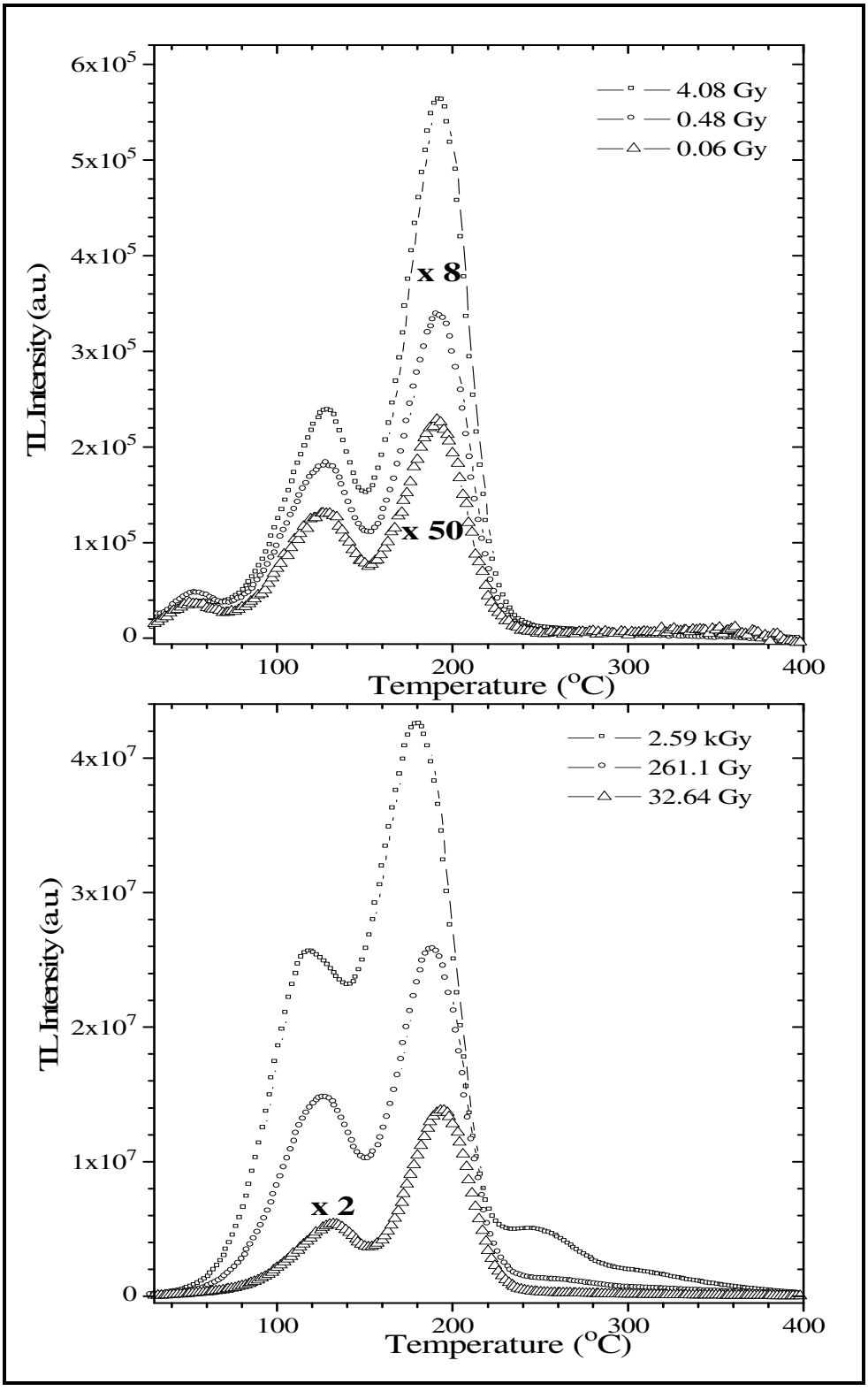

Figure 6.13. Some of the selected glow curves of Al-doped LiB_3O_5 measured at 1°C/s after different dose levels

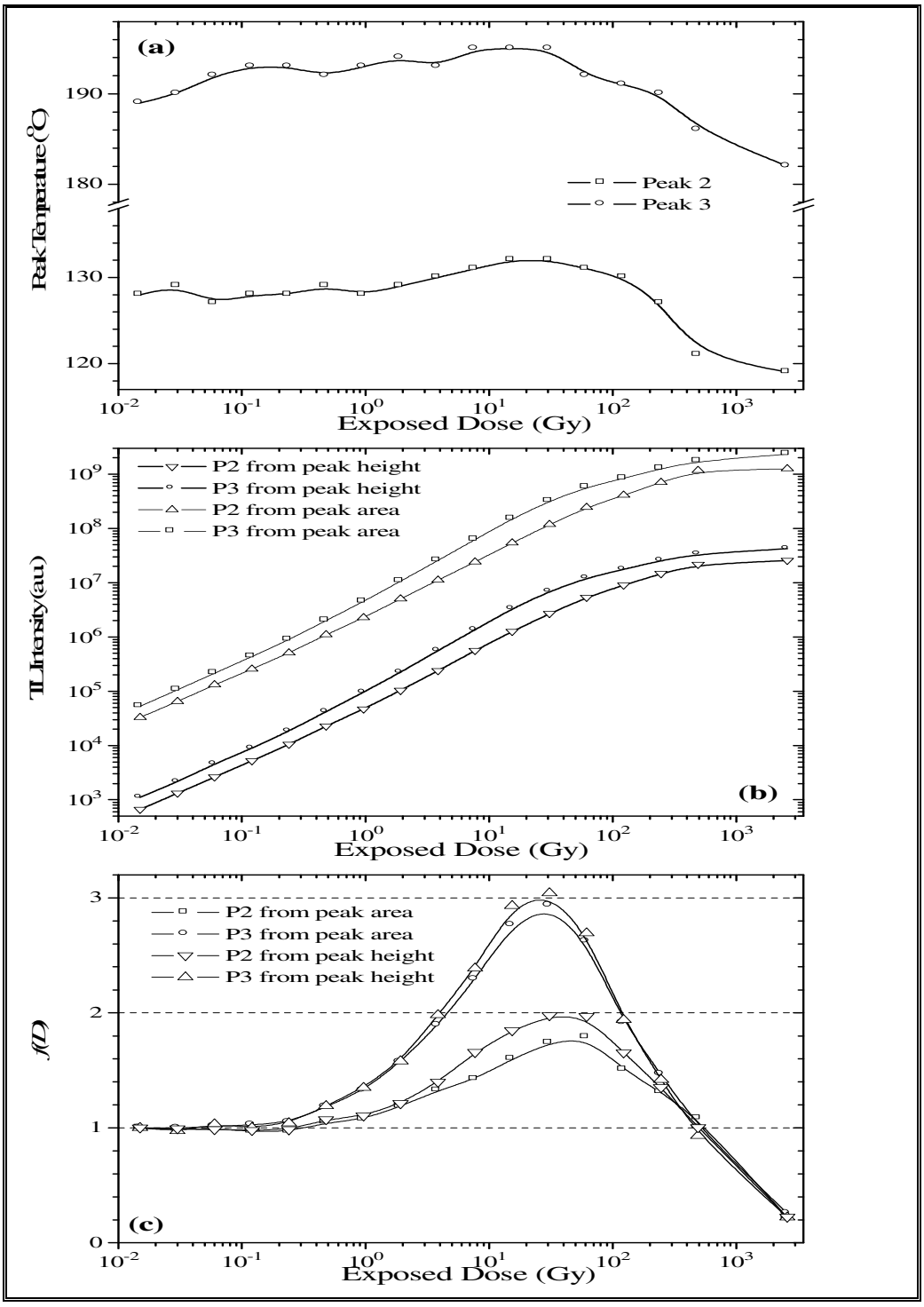

Figure 6.14. (a) The peak temperatures of glow peaks of Al-doped doped LiB_3O_5 as a function of exposed dose levels determined by from the maximum points of glow peaks. (b) The TL dose response curve of glow peaks in the glow curves of Al-doped LiB_3O_5 sample determined by the peak heights and area of glow peaks. (c) The TL dose response function ($f_{(D)}$) of glow peaks

In order to improve the performance of TL material, the pre-irradiation heat-treatment is usually utilized. Because, it is known that the pre-irradiation heat-treatment is generally reestablished the defect equilibrium that exists in the material before the irradiation and the heating can also empty the deep traps to avoid its influence on the TL sensitivity of a given peak since they can act as competitors. Therefore, one of the first problems investigated in the given study is the annealing procedure to be used in order to eliminate the effects of the previous irradiations. The experiment was carried out at 300, 350 and 400 ^{o}C for 15 min and the sample is rapidly cooled to room temperature after each heat treatment. The whole experiment was repeated at various dose levels. The intensity is obtained by the integral of the peak area of glow peak at 195 ^{o}C. The obtained results confirmed that an annealing treatment at 350 ^{o}C for 15 min was found sufficient to erase TL signal completely and restore the original TL sensitivity of the TL dosimeters. However, during routine applications of TL detectors for dose levels less than 0.5 Gy, a readout annealing appeared to be an optimal and very convenient procedure. For this reason, the comparison of TL sensitivity of TL detectors after oven and readout anneal was performed. Some samples after their background reading were irradiated to a test dose ≈0.45 Gy. The samples were subsequently readout up to 400 ^{o}C with a linear heating rate of 1 ^{o}C/s, and their glow curves were recorded. After this readout the samples were irradiated again at the same test dose and then readout. The glow curve shapes were seen to be identical in both cases, where the TL sensitivities were the same within less than 4%. However, for doses above 1 Gy (i.e., 4.5 Gy), it was found that readout annealing is probably insufficient to completely empty the deep traps in LiB_3O_5 and therefore an oven annealing is

necessary to get a stable TL response and the lowest background. In order to assess the reproducibility of the dose measurements attainable using Al-doped sample, the TL stability after repeated cycles of the both oven and readout annealing procedures was also tested at different dose levels (0.45 Gy, 4.5 Gy and 45 Gy). Repeated cycles of (i) oven annealing at 300, 350 and 400 ^{o}C for 15 min, irradiation, readout and (ii) irradiation, readout, were carried out (Fig. 6.15). The results showed that the readout and oven annealing procedures at 300 ^{o}C for 15 min show a very good stability within less than 2% based on standard deviation over more than 10 repeated cycles for the dose levels below 0.5 Gy. On the other hand, it was observed that when the samples are annealed in an oven at 400 ^{o}C for 15 min after irradiation with low or high doses, the intensity of all glow peaks is continuously decreased with increasing experimental cycles. Moreover, when the dose levels increased above 1 Gy (i.e for 4.5 or 45 Gy), it was observed that the readout annealing and oven annealing at 300 ^{o}C for 15 min are not sufficient to erase TL signal completely and restore the original TL sensitivity of the TL dosimeters (Fig. 6.15). As a result, it can be mentioned that the treatment at lower temperature below 350 ^{o}C is not able to release the electrons from all the deep traps, however, at higher temperature above the 350 ^{o}C with a long time it will decrease the sensitivity of the TL of the material. Consequently, if the previous history of the material is unknown, it is thus advantageous to anneal the sample at 350 ^{o}C for 15 (or at 300 ^{o}C up to 30 min) before putting it to any dosimetric use. It has been stressed that most of the commercially produced TL samples change color after repeated annealing and readout procedures and thus they lose their initial

sensitivity. On the contrary, the studied material (LiB_3O_5:Al) in the given study stayed unchanged in its color after its annealing and/or readout treatments.

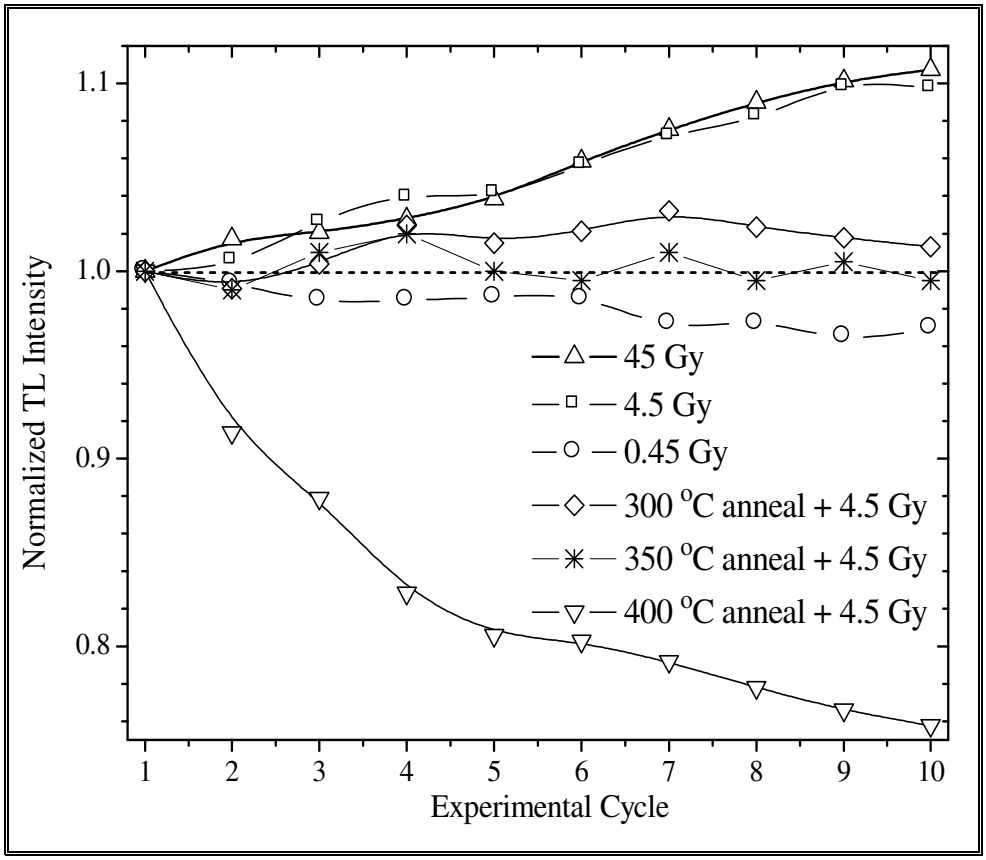

Figure 6.15. Reproducibility of deconvoluted area of peak 3 of Al-doped LiB_3O_5 through ten repeated cycles of irradiation-readout annealing

The dose response of Al-doped LiB_3O_5 was studied as a function of irradiation time between 1 sec and 48 hr using β-rays. Figure (6.13) shows some of the selected glow curves of 1% Al-doped samples after different dose levels. Samples were annealed at 350 ^oC for 15 min before each using and then read immediately after irradiation. All recorded glow curves were analyzed by CGCD program and the resulting dose response curve is shown in Fig. 6.14 (b) and (c). In here, all TL response values reported are an average of three measurements. As

seen from Fig. 6.14 (b), it likes as that the main glow peaks (P2 and P3) of Al-doped sample were linearly increased with increasing β-ray dose up to ≈10 Gy and then a saturation effects start to appear up to applied maximum dose level in the given present study. As seen, the peak area measurements using CGCD program and peak height measurements were given similar results. On the other hand, to clarify very well the dose-response curve of the glow peaks, they were also expressed by the supralinearity function, *f(D)*, given by the Equation (1.1). The behaviors of *f (D)* obtained for both peaks at 130 ^{o}C and 195 ^{o}C are presented in Fig. 6.14c. As clearly seen from this figure, the dose response of both peak are similar to each other which they are unity up to doses ≈0.5 Gy and greater than one (*f(D)*>1) for higher doses up to 500 Gy, where superlinearity starts. For additional doses, *f(D)* is less than 1, which means that sublinearity starts. So, as similar to the most common TL materials, Al-doped LiB_3O_5 compound shows extremely useful TL feature of perfect linearity in its TL response with dose up to 0.5 Gy. Generally supralinearity is a characteristic of a large variety of TL materials, so TL linearity in the high dose region, over 1 Gy, is exceptionally rare. As seen, the similar result was also obtained in the given present study. Therefore, the results suggest that the second peak at 195 ^{o}C can be safely used as a dosimetric peak in medical applications. The TL sensitivity of 1% Al-doped sample was also compared with TLD-100. They were given a test beta dose of 4.5 Gy and their sensitivities were compared. After the normalization to the same mass of both samples, the TL intensity of peak 3 of Al-doped sample was compared with intensity of peak 5 in TLD-100. It was found that the TL intensity of peak 3 in 1% Al-doped LiB_3O_5 is approximately 2 times less than the peak 5 of TLD-100.

For sample to be useful in dosimetry, the TL intensity of its dosimetric peaks should be stable and no fade upon storage after exposure. In order to investigate the fading characteristics of all peaks in Al-doped samples, the TLD samples were stored in dark conditions at room temperature, between 25-30 ^{o}C over a period of one month after beta-ray exposure. Figure 6.16 shows two of the selected glow curves from the glow curves of fading experiment of Al-doped sample.

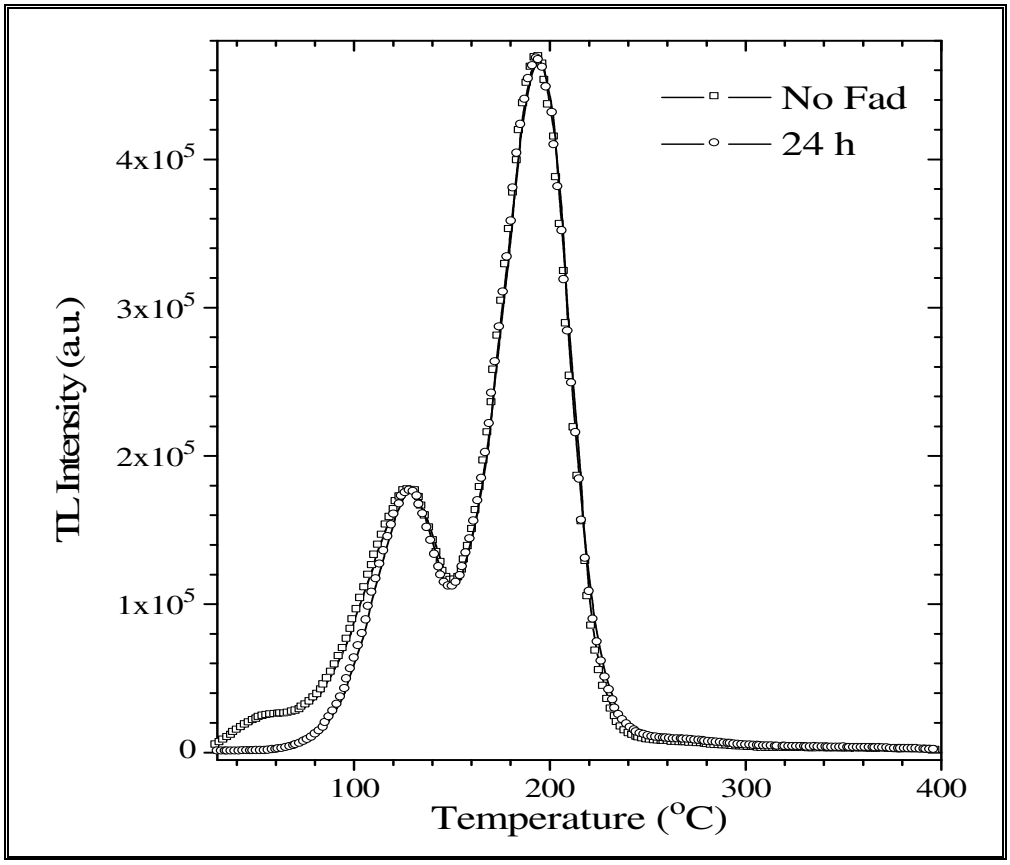

Figure 6.16.The recorded two glow curves of Al-doped LiB_3O_5 after no storage and storage 1 day at room temperature in the dark condition

The result of fading demonstrated a very small decrease of the TL response during the elapsed period of time in the main dosimetric peak (peak 3) of Al-doped samples (Fig. 6.17). The fading of this peak is less than 5% for 1 month if the

dosimeters were protected from direct room light. It is seen that the second peak at 130 ^{o}C fades approximately 35% of its original value after one month hence it is no dosimetric value. So, the influence of this peak in dosimetric measurements can be easily eliminated by making the TL measurements by incorporating a pre-read anneal at about 100 ^{o}C for a few seconds in the TL reader system. The initial peak (peak 1) which is close to room temperature and so it fades completely about 24 h after irradiation. It is known that most of the common TL materials are very sensitive to light. However, it was observed that room temperature fading of Al-doped LiB_3O_5 phosphor is less than 15% in one month even though the phosphor was not protected from room light.

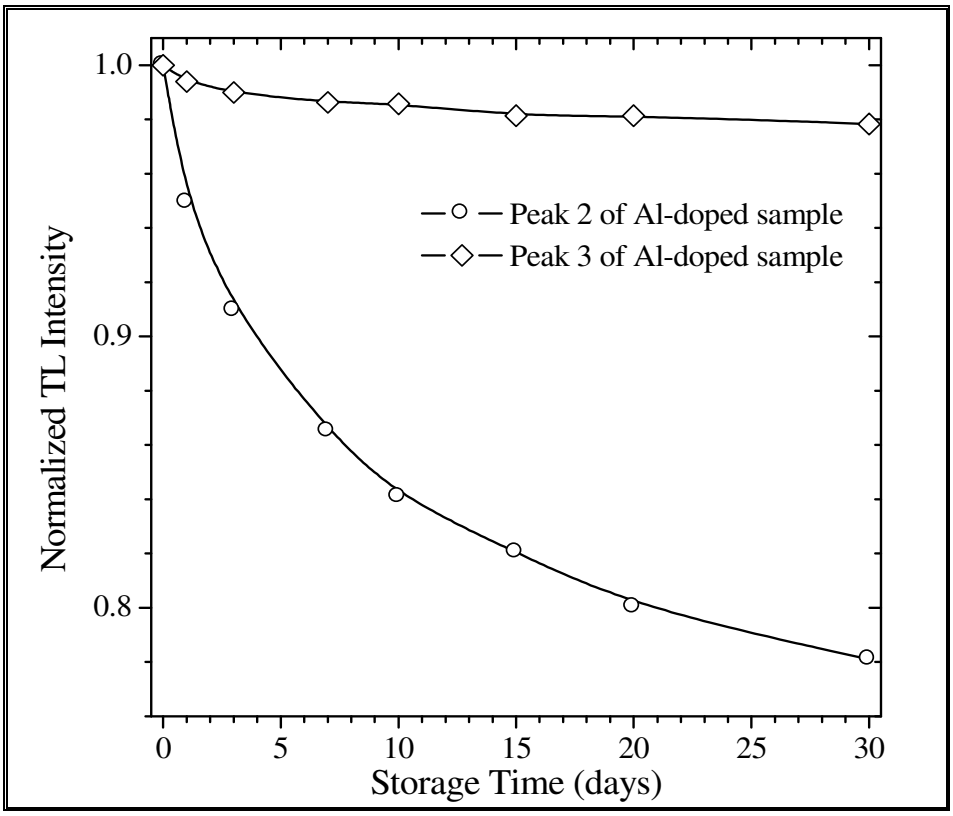

Figure 6.17. The obtained fading characteristics of glow peaks of Al-doped LiB_3O_5 using the CGCD program

The usable dose range of many phosphors is limited at the lower end of doses by the variability in the background signal from the undosed samples. In the given study, the experimentally determined minimum detectable dose defined as that dose which gives three times the standard deviation of the zero reading of the Al-doped LiB_3O_5 phosphors, is also estimated and it is found to be approximately 60 μGy.

The spectral composition of the TL emission leads to identify the recombination centers with undoped and doped samples. Therefore, the spectral composition of the TL was also investigated for undoped and Al-doped samples in the present study. Fig. 6.18 shows a set of selected emission spectra which were obtained from undoped and different amounts of Al-doped samples. As seen, the emission spectrum of undoped sample measured at about 200 ^oC is a broad band at around 550 nm. Its origin is unknown but it is probably due to the intrinsic defects. In general, Al included natural or synthetic TL materials gives an efficient emission in the violet to blue region of the spectrum and it acts as very efficient radiative recombination centre. In this work, it was observed that the relative intensity and maximum peak location of recorded emission spectrum are strongly dependent upon the Al-concentration. It can be seen that the peak wavelength of main emission band is continuously shifted to low wavelength sides with increasing dopant concentration and a new emission band starts to exist as a shoulder on the low wavelength side of main emission band. It can also be observed that the relative intensity of emission spectrum increases with increasing Al-concentration. An analyzed TL emission spectrum of 1% Al-doped LiB_3O_5 samples recorded at around 195 ^oC TL peak is shown in Fig. 6.19. It starts near 400 nm and extends up

to ≈700 nm. It can be very well fitted with two Gaussian shaped emission bands which main emission band is centered at around 520 nm and by a strong shoulder at around 460 nm (Fig. 6.18).

The trapping parameters of all glow peaks of Al-doped sample have been also studied using the CGCD method. By using the Equations (3.23) and (3.24), the obtained trapping parameters were given in Table 6.4. The statistical error of these parameters deriving from the analysis of glow peaks after different irradiation doses is of the order of 10%.

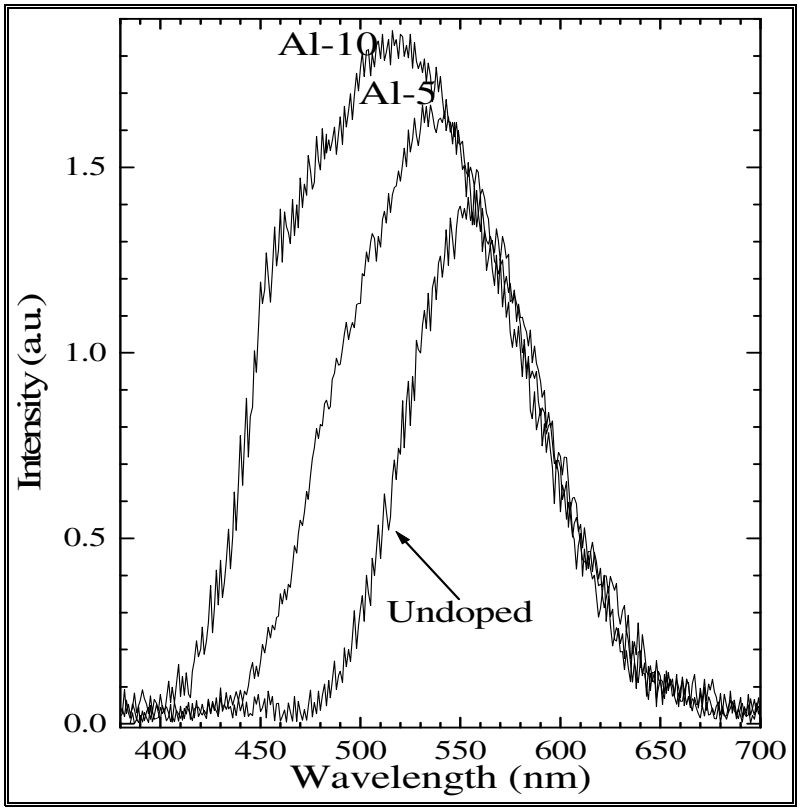

Figure 6.18. A set of TL emission spectrum of undoped and various Al-doped LiB_3O_5 samples after the application of same experimental procedures. All emission spectra were recorded after the samples were exposed to the same dose level (≈4.5 Gy) at room temperature

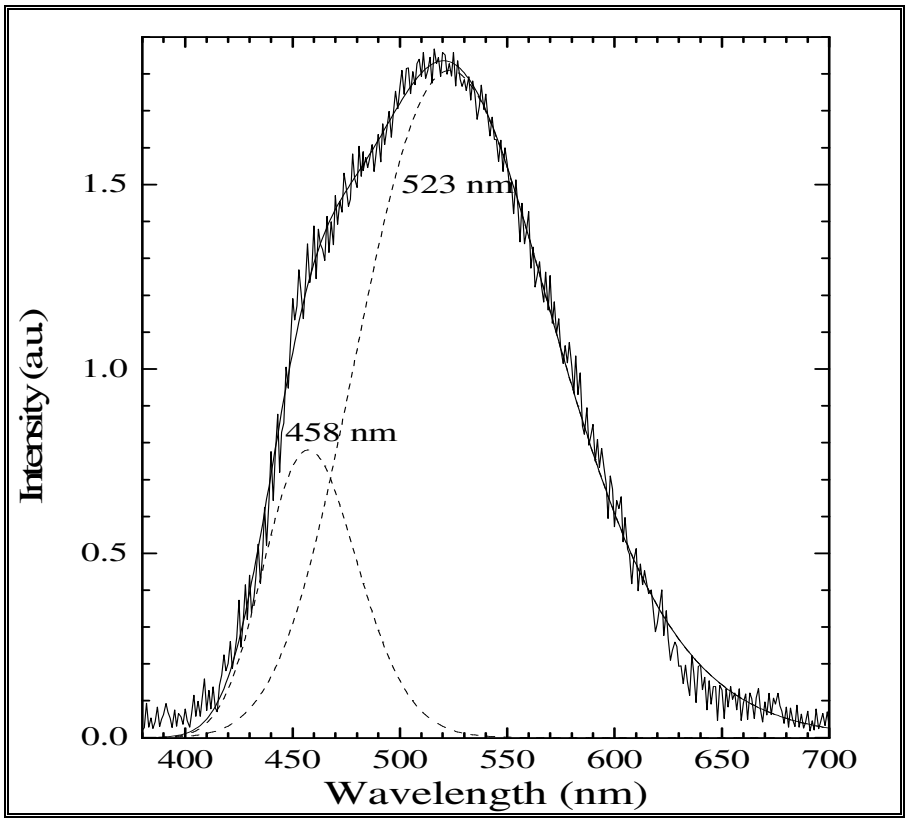

Figure 6.19. An analyzed TL emission spectra of 1%Al-doped LiB_3O_5 measured at around 195 ^oC

Table 6.4. The trapping parameters of Al-doped LiB_3O_5 samples calculated by the CGCD method (β= 1 $^oC/s$)

Al-doped LiB_3O_5			
	Peak 1	Peak 2	Peak 3
T_m (^oC)	58±2	126±3	194±2
E_a (eV)	0.5±0.02	0.7±0.02	1.18±0.02
$ln(s)$ (s^{-1})	14.6±0.3	17.3±0.4	26.5±0.3
B	1	1.07±0.03	1.24±0.04

In general, the undoped samples, whose emission can be related to intrinsic defects or to some unwanted impurity in the starting powder, exhibits a poor TL efficiency than the doped samples. On the other hand, as expected, the TL signal

was steadily increased after incorporation of metal impurities such as Al, Ag, and Cu or rare-earth impurities which are well known as very efficient activators in many materials, for example in alkali halide crystals or in oxides. However, the glow curve shapes of undoped samples can be changed after the doping of impurities. If the glow curve structure of undoped sample is changed after the doping, this result indicates that there are large interactions between intrinsic defects and doped impurities. On the other hand, the comparison of glow curves of undoped and Al-doped LiB_3O_5 samples in the given present study indicates that there is no great change in the glow curve structures of all samples. The difference is only in the relative intensities and peak temperature of glow peaks. As explained previously, the peak temperature of main peak is slightly decreased with increasing Al-concentration whereas its intensity increases. The result suggests that the activator aluminum ions are not related with the electron traps, while they play a predominant role in the luminescence centers. It seems also that between these centers and charge traps a radiative energy transfer takes place during the TL process. Further information about the trapping and recombination centers is not yet obtained in the given study with other techniques but some possible mechanisms can be indicated at this point.

By using only the result of TL emission data, the assignment of an emission band in the spectral range between 350 and 650 nm to a specific defect or dopant site is extremely difficult since electron–hole recombination tends to provide strong luminescence bands around this spectral range in most wide band gap insulators. From the data presented here, the comparison of undoped and Al-doped emission spectra of LiB_3O_5 show that Al-ions are responsible for the shift in the wavelength

of emission spectra and caused new emission band at the low wavelength side of main emission band of undoped sample.

The previous investigations have shown that the crystallographic structures of lithium borates consist predominantly of the oxygen vacancies neighboring alkali ions and other type of oxygen related defects throughout the crystal [133]. Much of the work done by EPR has indicated that aluminum is present in the Al^{3+} and Al^{+} states in most natural and synthetic samples. It is well known that EPR is only applicable to defects with unpaired electron spins. Therefore, the other charge states can also be possible that detected by other techniques, i.e. optical absorption. The inclusion of monovalent ions such as Al^{+} into the LiB_3O_5 lattice is feasible in terms of charge equilibrium if they enter the Li^{+} site. Nevertheless, this is only one factor to be considered and the second factor which should also be considered is the lattice distortions within the local region of lattice due to the differences in sizes of ionic radii of ions. Ionic radii are often cited as being similar at values near 0.068 and 0.075, 0.057 nm for Li^{+}, Al^{+} and Al^{3+}, respectively. The radius of Al^{+} differs from that of Li^{+} by 1.1 times, which does not suggest significant distortions in LiB_3O_5 lattice. Therefore, the Al^{+}-ions can enter the Li^{+} site into the LiB_3O_5. On the other hand, the Al^{3+}-ions occupy the interstitial voids of the appropriate network. If it represents a transition from Al^{3+} to Al^{4+} during hole capture then it suggests that the Al^{4+} state exists in the irradiated samples. On the other hand the liberated electrons during the irradiation can be trapped by oxygen related defects. During heating, electrons may be set free from these defects and recombine with intrinsic defects and Al^{4+} to yield $(Al^{3+})^{*}$ ion in the excited state. Therefore, the new TL emission is both characteristic of Al^{3+} emission when the Al^{3+} ion in the excited

state returns radiatively to the ground state and intrinsic defects. However, several other possibilities can also be suggested, and more experiments will be needed to identify the trapping and recombination centers.

As a result, this work describes the investigations on the radiation dosimetry characteristics of Al-doped LiB_3O_5 phosphor. The major TL peak in LiB_3O_5:Al phosphor occurs at 195±2^oC and its TL sensitivity to beta radiation is approximately 2 times lower than that of TLD-100. The beta-dose response of this peak is linear in the dose range 1.5 mGy-0.5 Gy which is very adequate for clinical and radiotherapy purposes. The post irradiation fading of this peak at room temperature is also less than 5% in one month. The TL emission spectrum of this material has a broad peak at 520 nm. Unfortunately the TL emission from the undoped or Al-doped samples is above the 450 nm, which is far from the ideal wavelength region of most photomultipliers. For TL dosimetry the most intense higher temperature signals span the region 375–475 nm, which is ideal for photomultiplier detection. Although, the Al-doped LiB_3O_5 samples were tested for beta radiation, the samples behave quite well for gamma and other ionizing radiations. In addition, LiB_3O_5 is remarkable advantageous in relation to medical and radiotherapy applications, since it is chemically inert to body fluids, non-toxic and tissue equivalent. These some of the reported characteristics make that LiB_3O_5:Al a promising TLD material for dosimetric purposes.

6.3. Thermoluminescence Properties of Undoped $Li_2B_4O_7$ Samples

$Li_2B_4O_7$ based phosphors for thermoluminescence dosimetry have been used in research and applications for several decades [134,135,136]. Important dosimetric properties such as responses to annealing procedures, simplicity of the glow curve, influence of humidity and fading, light sensitivity and photon dose response have been investigated by Prokic [137]. $Li_2B_4O_7$ TL dosimeters are particularly suited for applications in radiation dosimetry, especially radiation therapy and clinical applications, since they are tissue equivalent with an effective atomic number of 7.3, which is very close to that of soft biological tissue (Z_{eff} =7.4), making them convenient for measurements independent of the photon energy used in radiation treatments. Doped $Li_2B_4O_7$ crystals have also received attention in a role as efficient scintillators [137].

Nevertheless, there were still a number of problems to overcome to make copper-activated lithium borate feasible for routine dosimetry. Different methods of preparing this TL material have consequently been developed which result in rather different TL characteristics, i.e. the form of the glow curves, TL sensitivity, linearity, etc.

In this study, $Li_2B_4O_7$ were prepared by melting method. The preparation of lithium borate samples were made by mixing lithium carbonate (Li_2CO_3) (99%, Merck) with boric acid (H_3BO_3 (99.5%, Merck) and desired amount of dopant in stoichiometric ratio. In order to release H_2O and CO_2 from the mixture, samples were heated at furnace 300 ^oC for 10 hour. Then the mixture was melted at 950 ^oC in a plantinum crucible and then rapidly cooled to room temperature. The resultant glassy mass was ground. The glassy mass is reheated at 650 ^oC for 0.5 h, which

assures a complete crystallization, and then ground and sieved to obtain 100-200 mesh powder. After 1 h annealing at 400 ^{o}C, the phosphors were cooled rapidly to room temperature and ground in an agate mortar again [115,138]. The expected reaction is given below;

$$Li_2CO_3 + 4H_3BO_3 \rightarrow Li_2B_4O_7 + CO_2 + 6H_2O$$

X-Ray diffraction (XRD) examinations were performed to identify the produced samples. XRD patterns were recorded from $10^{o}<2\theta<80^{o}$ at a scanning rate of 4^{o} min^{-1} at RT by using a Rigaku MiniFlex X-ray Diffractometer with a Cu Kα (λ=1.5405Å) radiation source. $Li_2B_4O_7$ X-ray diffraction pattern of powder samples are recorded in Fig. 6.20. The sharp and single diffraction peaks of XRD patterns confirm the formation of new compounds.

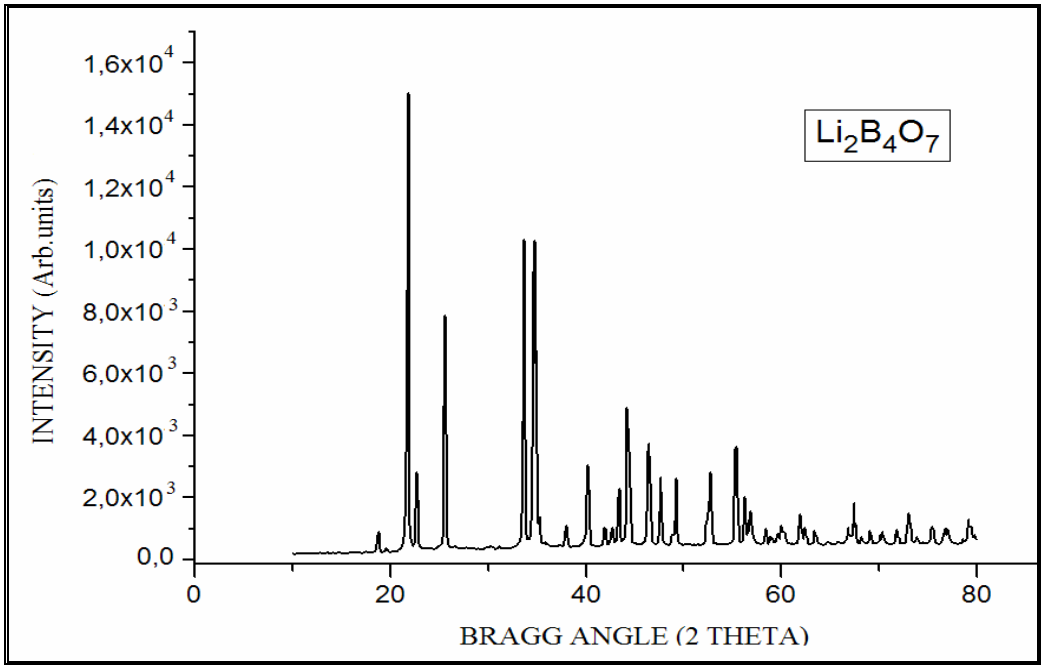

Figure 6.20. XRD pattern of $Li_2B_4O_7$ which synthesized with melting method

Inter plane spacing *(d),* lattice parameters of unit cell and miller indexes are found from *2θ* values by using a computer program package called ‘‘POWD’’ [120]. Diffraction lines are indexed by using Powd program and the crystal system found to be monoclinic unit cell. Crystal systems are tired and $\sum \Delta d (= d_{obs} - d_{cal})$ value was found to be minimum for monoclinic. The lattice parameters of unit cell were found to be *a= 4.22 Å. b= 6.95 Å, c= 3.49 Å* and unit cell volume *V=96,21Å*^{3}. The *(hkl)* values of the most prominent diffractions peaks are (100), (110), (-101), (101), (121) and (012). The data obtained from XRD pattern of $Li_2B_4O_7$ sample are given in Table. 6.5

Table 6.5. Comparison of observed and calculated *d*-values (Å) the most intensive reflections of $Li_2B_4O_7$ in room temperature

Peak No	$d_{obs.}$	d_{calc}	*h k l*	*Δd*
1	4.2267	4.2267	1 0 0	0.000
2	3.5588	3.5588	1 1 0	0.000
3	2.7120	2.7120	-1 0 1	0.000
4	2.6345	2.6345	1 0 1	0 .000
5	2.0562	2.0584	1 2 1	0.050
6	1.6681	1.6686	0 1 2	0.017

During this study, glow curves of synthesized $Li_2B_4O_7$ phospors was recorded for different times of β-irradiation. Some of the selected glow curves of $Li_2B_4O_7$ powder samples were shown in Fig. 6.21 after β-irradiating at room temperature between 5 min and 8 hour. The TL glow curves of $Li_2B_4O_7$ crystal exhibits one strong TL glow peak at around 200^{o}C. It is found that the intensities of the glow peaks of this sample were linearly increased with the increasing β-ray

dose. The TL dose response curve was studied as a function of irradiation time between 5 min and 8 h (0.1 Gy and 400 Gy) and the recorded glow curves were analyzed. The resulting dose response curve of $Li_2B_4O_7$ is shown in Figure 6.22. As seen, the integrated TL dose response curve of this material is approximately linear in the range of investigated region with no observed superlinearity and saturation effects. Note that the 400 Gy is particularly high value in the dosimetric investigations and therefore it takes possible to use this material in the fields other than clinical applications.

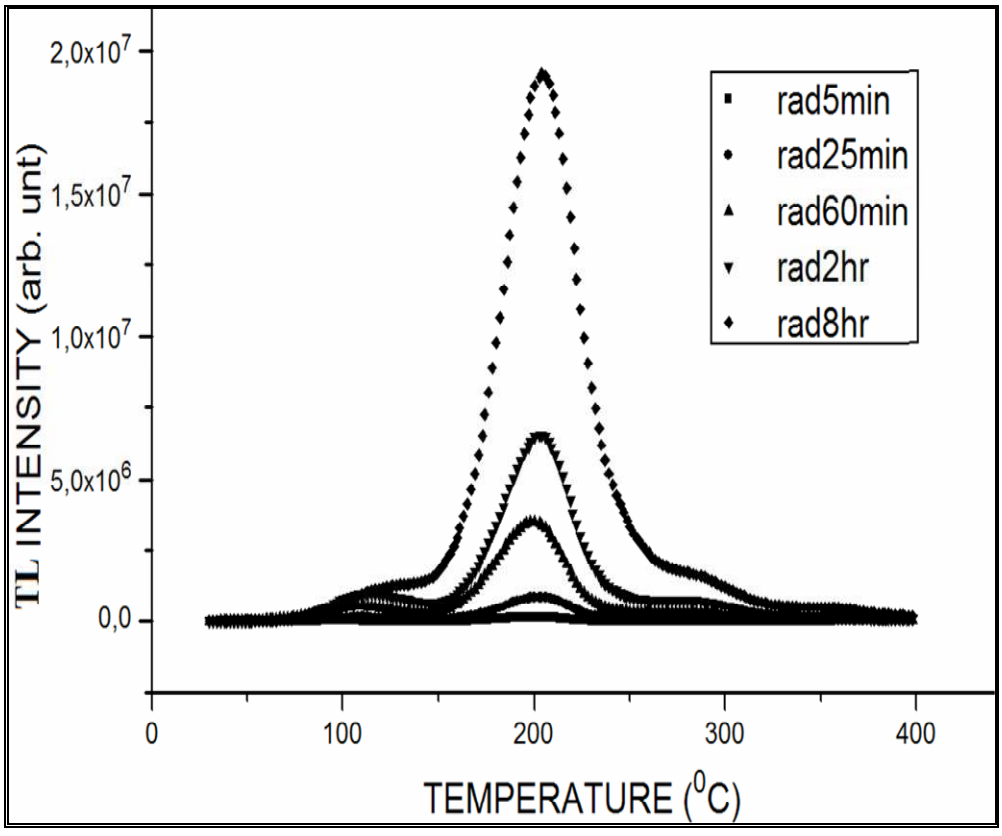

Figure 6.21. The influence of the ^{90}Sr-^{90}Y β (beta)-ray as a function of irradiation time on the of $Li_2B_4O_7$ phosphors at room temperature

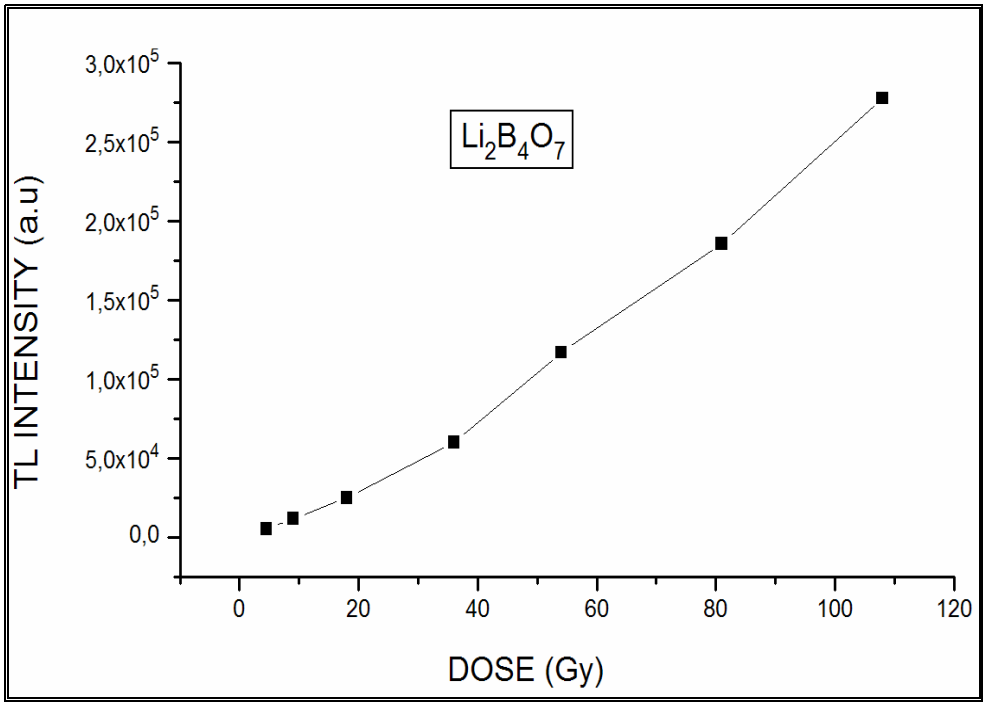

Figure 6.22. Linearity range of the TL responses of $Li_2B_4O_7$ phosphor versus absorbed doses

For sample to be useful in dosimetry, the TL intensity of the glow peaks, at least its dosimetric peak(s), should be stable and no fade upon storage after exposure. In order to investigate the fading characteristics of all peaks in the produced $Li_2B_4O_7$ phosphor, the samples were firstly irradiated with beta rays for 2 h at room temperature and then the irradiated samples were stored in the dark at room temperature for different periods of time up to one week. The dependence of the TL emission on the storage time was determined by peak height method but it was observed that the sensitivity of glow peak 200 ^oC has not affected during the storage period.

As indicated in previous parts, if the sensitivity of a sample does not change after several cycles of exposure and readouts, it can be considered as a good phosphor. Thus the produced $Li_2B_4O_7$ sample was also tested for reusability. The

reference sample was exposed to beta rays for 2 h and then its glow curve was recorded between room temperature and 400^{o}C. These procedures were repeated ten times and it was observed that the sensitivity of TL glow peaks have good stabilities during the successive readings. The obtained repeatability of the samples over ten cycles is always below 10%.

6.4. The Thermoluminescent Properties of Undoped, Al, Ce and Mn-Doped MgB_4O_7 Samples

The magnesium borates were prepared with melting point method at high temperature in air conditions. The polycrystalline sample of undoped MgB_4O_7 and 1% Ce, Al and Mn doped MgB_4O_7 are sensitized by melting method. The preparation of Ce, Al and Mn-doped magnesium tetraborateborate samples was made by mixing magnesium carbonate ($MgCO_3$) (99%, Merck) and boric acid (H_3BO_3 (99.5%, Merck) in stoichiometric ratio according to below reaction . The mixture was heated in oven at 400 ^{o}C in porcelain crucibles for 4 h to remove carbonates and water from the samples.

$$MgCO_3 + 4H_3BO_3 \rightarrow MgB_4O_7 + CO_2 + 6H_2O$$

The desired amount of impurities was added to mixture, then sample heated to 900 ^{o}C for 10 h which assures a complete crystallization. Then samples were cooled down up to 500 ^{o}C rapidly. After that the samples were taken out of furnace and dried in a desiccator. The resultant glassy mass was ground in an agate mortar again. The glassy mass is sintered at 400 ^{o}C for 4 h and then ground and sieved to obtain 100-200 mesh powder. Impurities doped MgB_4O_7 compound is synthesized according to the expected reaction is given below:

MgB_4O_7 + Impurity (CeO_2,Al_2O_3 or MnO_2) → (Ce, Al or Mn): MgB_4O_7

In order to analyze the structure of prepared undoped and doped MgB_4O_7 compounds, X-ray diffraction pattern of powder samples of were again recorded. Figure 6.23 shows the XRD pattern of 1% Ce-doped MgB_4O_7.

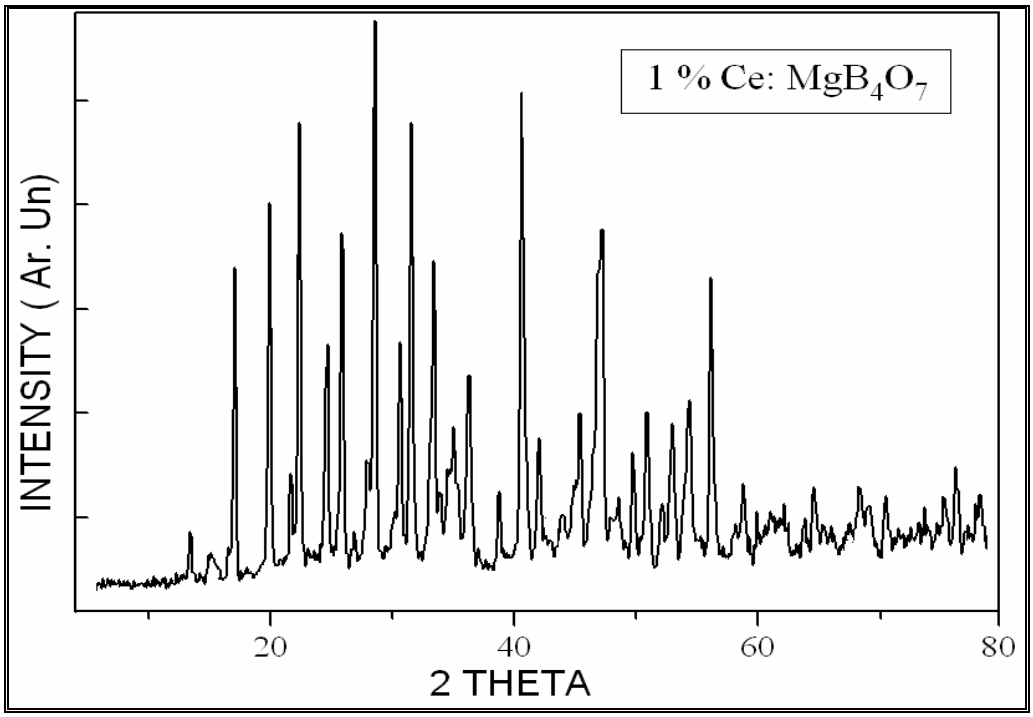

Figure 6.23. The XRD pattern of 1% Ce-doped MgB_4O_7

The XRD patterns were recorded from $10^o<2\theta<80^o$ at a scanning rate of 4^o min^{-1} at RT by using a Rigaku MiniFlex X-ray Diffractometer with a Cu K_α (λ=1.5405Å) radiation source. The interplanar spacing (d), lattice parameters of unit cell and miller indexes are found from 2θ values by using POWD. Crystal's systems are tried out and $\sum \Delta d (= d_{obs} - d_{cal})$ value was found to be minimum for monoclinic packing system. A good agreement between the absorbed and calculation d-values for monoclinic system, confirm the suitability of the crystal structure and unit cell parameters. The (hkl) values of the most prominent

diffractions peaks are (101), (200), (002),(012), (211), (112) and (-222). Obtained peaks of %1 Ce-doped MgB_4O_7 are in unison with JCDPS Cards [139]. The lattice parameters of unit cell were found to be a=6,43 Å, b=3.71Å, c=5.54Å and unit cell volume V=321.15 $Å^3$.

During the investigation of TL properties of undoped and various metal or rare elements doped MgB_4O_7, the glow curves of them were recorded for different times by β-irradiation. Some of the glow curves of undoped MgB_4O_7 powder samples were shown in Fig. 6.24 after irradiating at room temperature between 2.5 and 40 min with rate of 0.9 Gy/min. As seen it has been acquired two sharp peaks at about 170°C and 290°C. The intensity of 290 °C is the strongest. The appearance of different glow peaks indicates that different species of traps are being activated within the particular temperature, each its own value of activation energy and frequency factor. As seen, the intensity of glow peaks is linearly increased with increasing exposed beta doses.

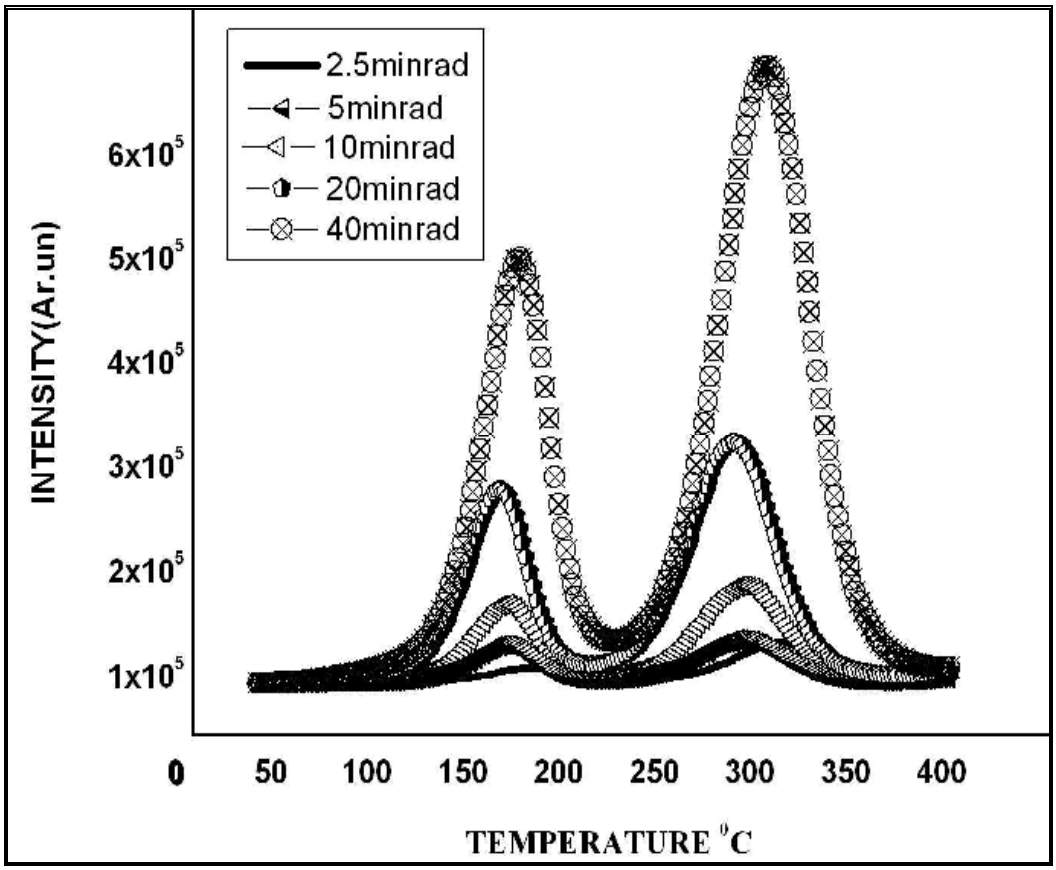

Figure 6.24. The influence of the ^{90}Sr-^{90}Y β (beta)-ray as a function of irradiation time on the of MgB_4O_7 phosphor at 293 K

The experimental glow curves acquired during fading study of pure MgB_4O_7 showed that the peak temperature at the maximum (290 ^oC) shifted towards higher values as the elapsed time from irradiation increased shown in Figure 6.25. This behavior probably suggest a more complex structure of traps than the usual one, based on one trap-one recombination centre. TL emission is due to a complex trap structure, namely a continuous trap distribution [81,140].

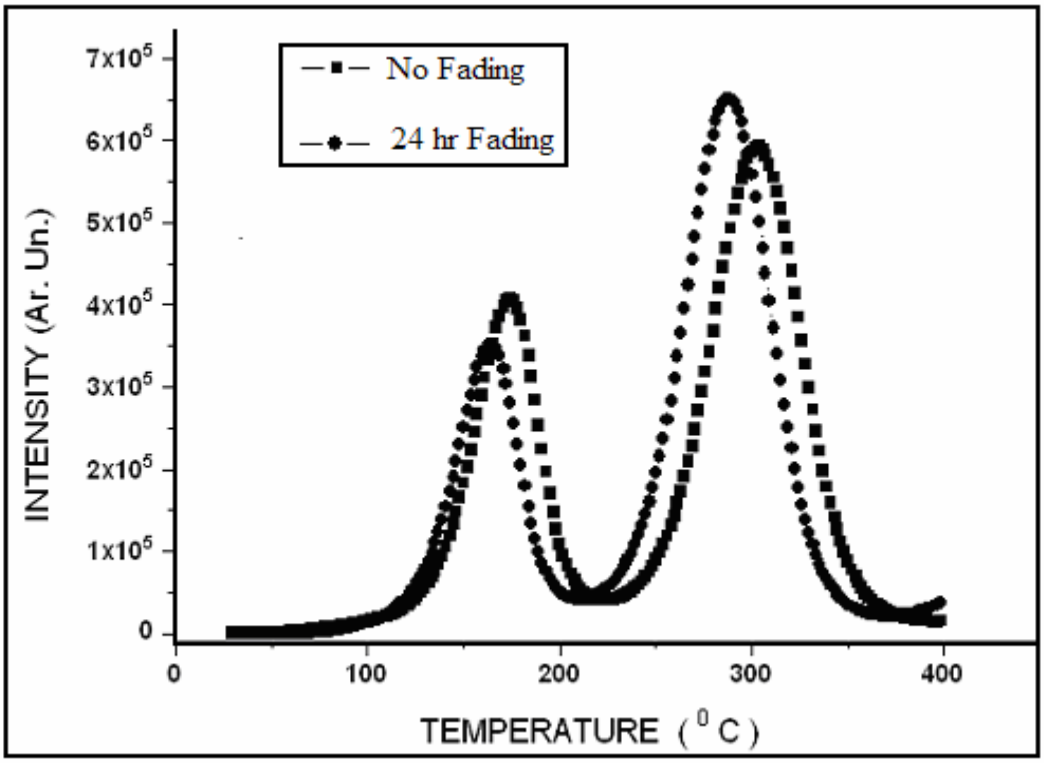

Figure 6.25. The comparison of glow peaks of 36 Gy irradiated undoped MgB_4O_7 phosphor and that of stored at dark room for 24 h

The TSL glow curves Ce-doped MgB_4O_7 crystal exhibits one strong TL glow peak at around 240 ^oC and a shoulder about 170 ^oC (Fig. 6.26). By doping 1% Ce to MgB_4O_7, the intensity of glow peaks are increased about three times and the small peak of MgB_4O_7 at 290 ^oC disappeared. On the other hand, the peak at 170^oC is seen as a shoulder. Therefore we can say that the concentrations of doped Ce^{3+}-ion can alters greatly the distributions of defects in MgB_4O_7 host material in studied concentration ranges. The TL dose response curve was studied as a function of irradiation dose between 2.25 Gy and 36 Gy. The resulting dose response curve of MgB_4O_7:1% Ce is also shown in the inset of Fig. 6.26. As seen, the integrated TL dose response curves of 1% Ce-doped MgB_4O_7 are approximately linear in the

range of investigated region with no observed super linearity and saturation effects (see inset of Figure 6.26).

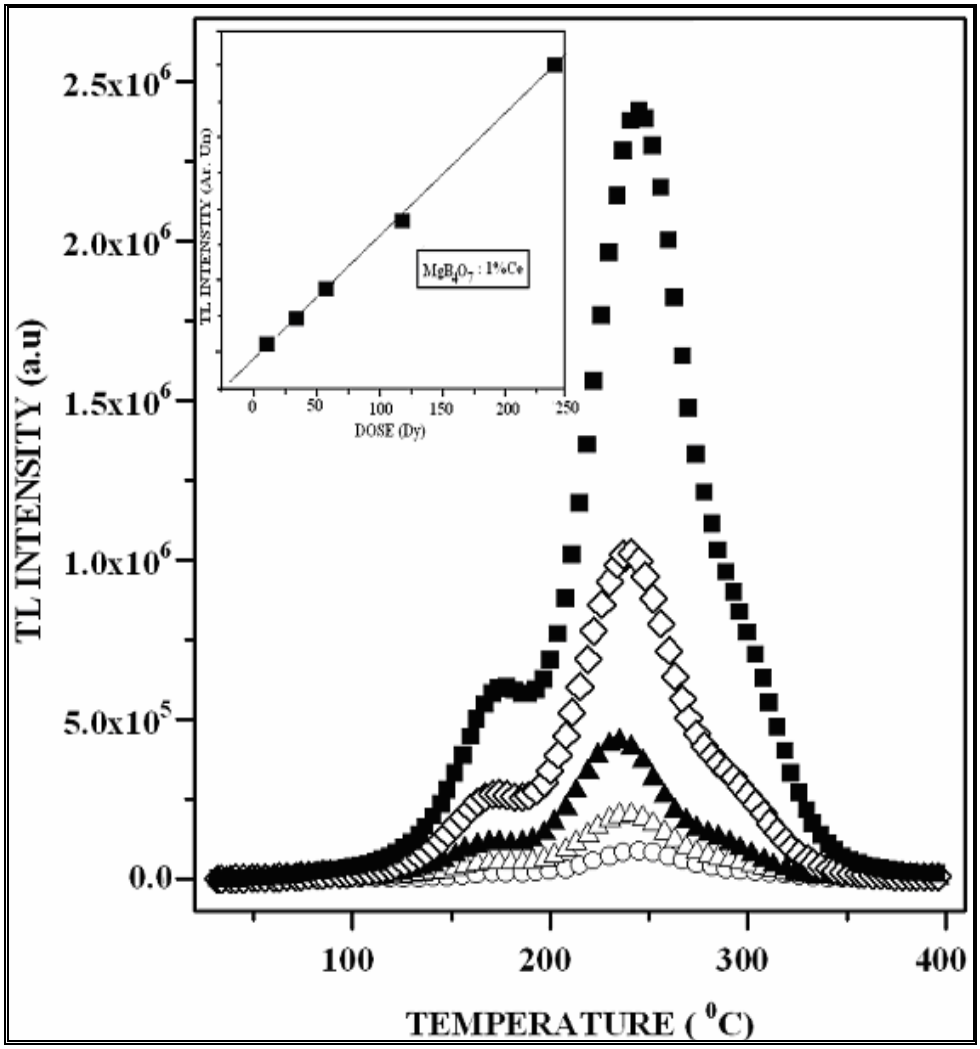

Figure 6.26. The influence of the ^{90}Sr-^{90}Y β (beta)-ray as a function of irradiation time on the 1% Ce-doped MgB_4O_7 phosphor at RT. The inset shape indicates linearity range of the TL responses of (TLD) 1 %Ce: MgB_4O_7 phosphor versus absorbed doses. [(○):2.25 Gy , (Δ) : 4.5Gy, (▼) 9 Gy, (◊) : 18 Gy, (■): 36 Gy]

The experimental glow curves of Ce-doped MgB_4O_7 acquired during fading study showed that a small fading acquired for the low temperature glow peak (T_m=170 ^{o}C) about 10 % but there isn't an important fading in the main peak

(T_m=240 ^oC) at ambient temperature of 25 ^oC in the dark (Fig. 6.27). This effect shows that MgB_4O_7 phosphor is useful for personal dosimetry.

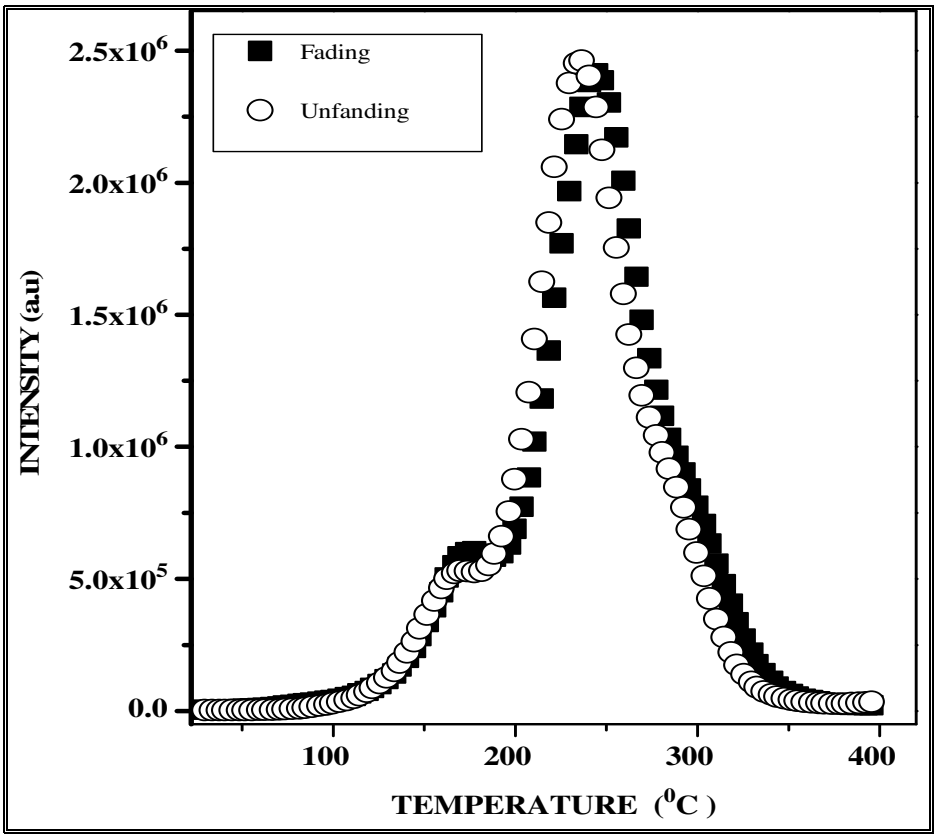

Figure 6.27. The comparison of glow peaks of 36 Gy irradiated MgB_4O_7:1%Ce phosphor (○) directly and (■) that of after stored at dark room for 24 hour (fading)

The all glow curves of Ce-doped MgB_4O_7 were also analyzed by the Computerized Glow Curve Deconvolution (CGCD) method to obtain the number of glow peaks and their kinetic parameters. To form an opinion about the *b* of all individual glow peaks in the glow curve structure of examined samples, the results of glow curves after different dose levels were firstly utilized in the current study. As mentioned previously, this is a simple test for the first-order kinetics. In TL theory, the peak temperatures of glow peaks are expected to change only with

heating rate for *b*=1. Hence, for a constant heating rate, the peak maximum should not be affected by other experimental parameters and should be fairly constant within the limit of experimental uncertainties. However, for b≠1 and below the trap saturation points {no(concentration of trapped electrons)<Nt (concentration of traps)}, it is generally received that the peak temperatures are shifted to the lower temperature side with increasing dose levels. It is seen from Fig.6.26 that the structures of the TL glow curves of Ce-doped MgB_4O_7 samples and the peak temperatures of glow peaks 1 and 2 were not changed with increasing dose levels. On the other hand, the peak temperature of glow peak 3 is slightly shifted to the low temperature side with increasing dose levels. These results indicate that the glow peaks 1 and 2 should be considered under the first-order kinetics whereas the peak 3 under the general-order kinetics. As a result, after many tries with different number of glow peaks, it was concluded that the glow curves of MgB_4O_7:Ce under different doses are well described by a linear combination of at least three closely overlapped glow peaks (P1, P2 and P3) corresponding to temperatures at around 170, 240 and 275^{o}C, respectively. Therefore, the glow curves of MgB_4O_7:Ce were always fitted with three components. An analyzed glow curve of Ce-doped MgB_4O_7 measured after 36 Gy irradiation at RT is shown in Figure 6.28 along with the components obtained from CGCD. The obtained kinetic parameters were given in Table 6.6.

Table 6.6. The trapping parameters of Ce-doped MgB_4O_7 samples calculated by the CGCD method (Heating Rate= 1 $^oC/s$)

Trapping Parameters	Glow peaks		
	Peak 1	Peak 2	Peak 3
T_m (^oC)	170	240	275
E_a (eV)	0.863	1.06	0.983
$Ln(s)$ (s^{-1})	19.6	20.8	17.44
b	1.00	1.00	1.45

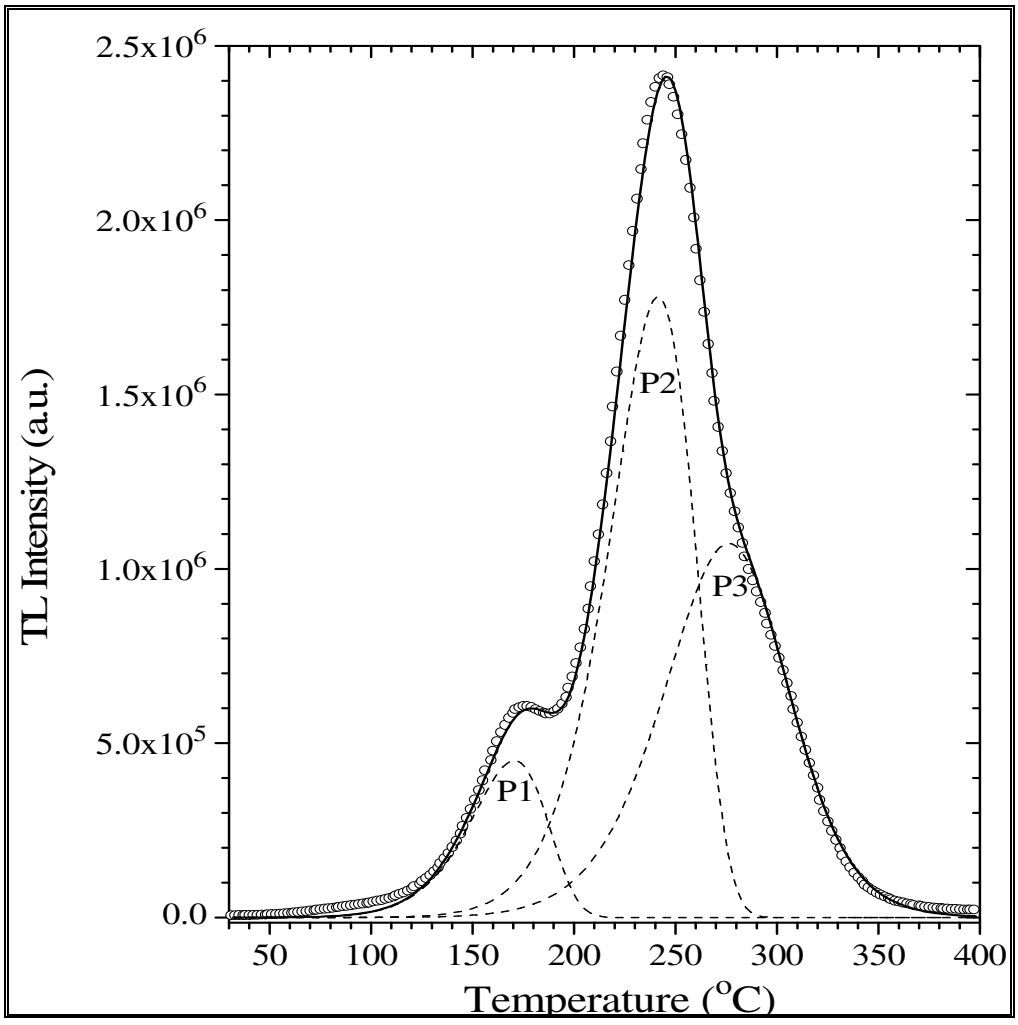

Figure 6.28. An analyzed glow curve of Ce-doped MgB_4O_7 (D=36Gy; β=1°Cs^{-1})

It is well known that if the sensitivity of a sample does not change after several cycles of exposure and readouts, it can be considered as a good phosphor. Thus, the produced pure and Ce-doped MgB_4O_7 samples were also tested for

reusability. The reference samples were exposed to beta rays for 10 min and then their glow curves were recorded between room temperature and 400 ^{o}C. These procedures were repeated seven times and it was observed that the sensitivity of TL glow peaks have good stabilities during the successive readings. The obtained repeatability of the samples for seven cycles is always below 10% (Fig. 6.29).

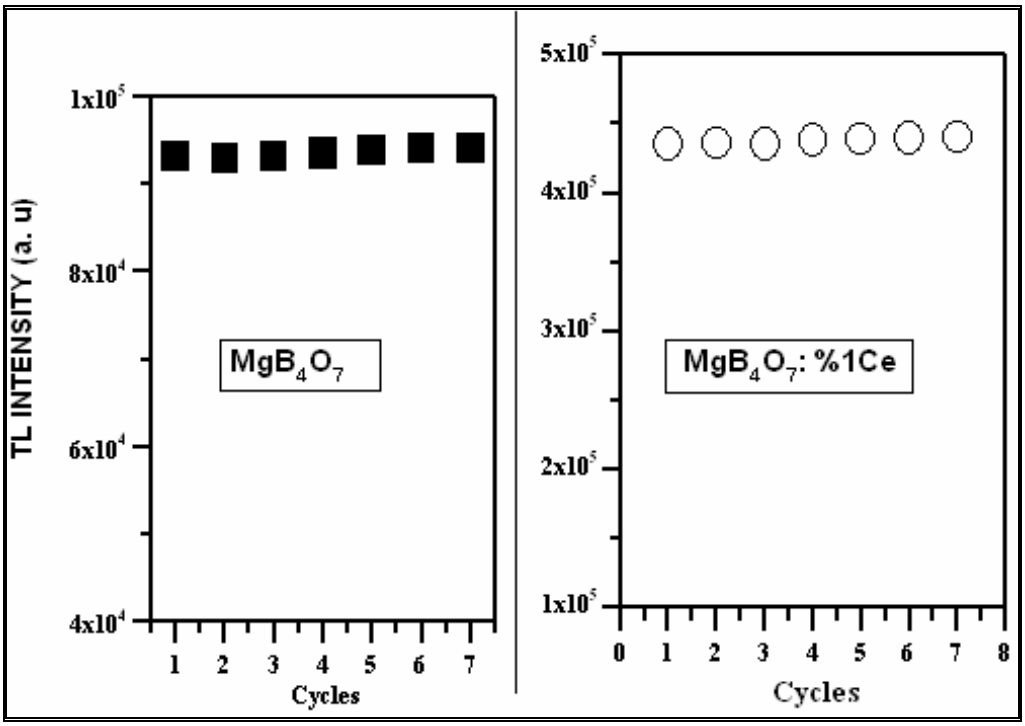

Figure 6.29. Reproducibility of undoped (■) and 1%Ce doped MgB_4O_7 (○) samples throught seven times repeated annealing-irradition-readout.

The influence of the ^{90}Sr-^{90}Y β (beta)-ray as a function of irradiation time on the 1% Al and Mn-doped MgB_4O_7 phosphors are shown in Figures (6.30) and (6.31), respectively. It is useful to indicate that the TL output of 1% Al-doped MgB_4O_7 phosphor is 1.5 times higher from undoped MgB_4O_7 phosphor at the same dose. The glow curve 1% Al doped MgB_4O_7 consisted of two well separated TL peaks. The main and maximum peak situated at about 302 ^{o}C and low temperature

peak at about 172 ^{o}C. Samples were read immediately after irradiation and it is seen that there are no great differences in the glow curve structures with increasing dose levels. By doping 1% Al to MgB_4O_7, the TL main peak shifts 10 ^{o}C toward high temperature side. Therefore we can say that the concentrations of doped Al^{2+} ion sligtly alters the distributions of defects and trapped electrons produced by β-ray irradiation in MgB_4O_7 host materials.

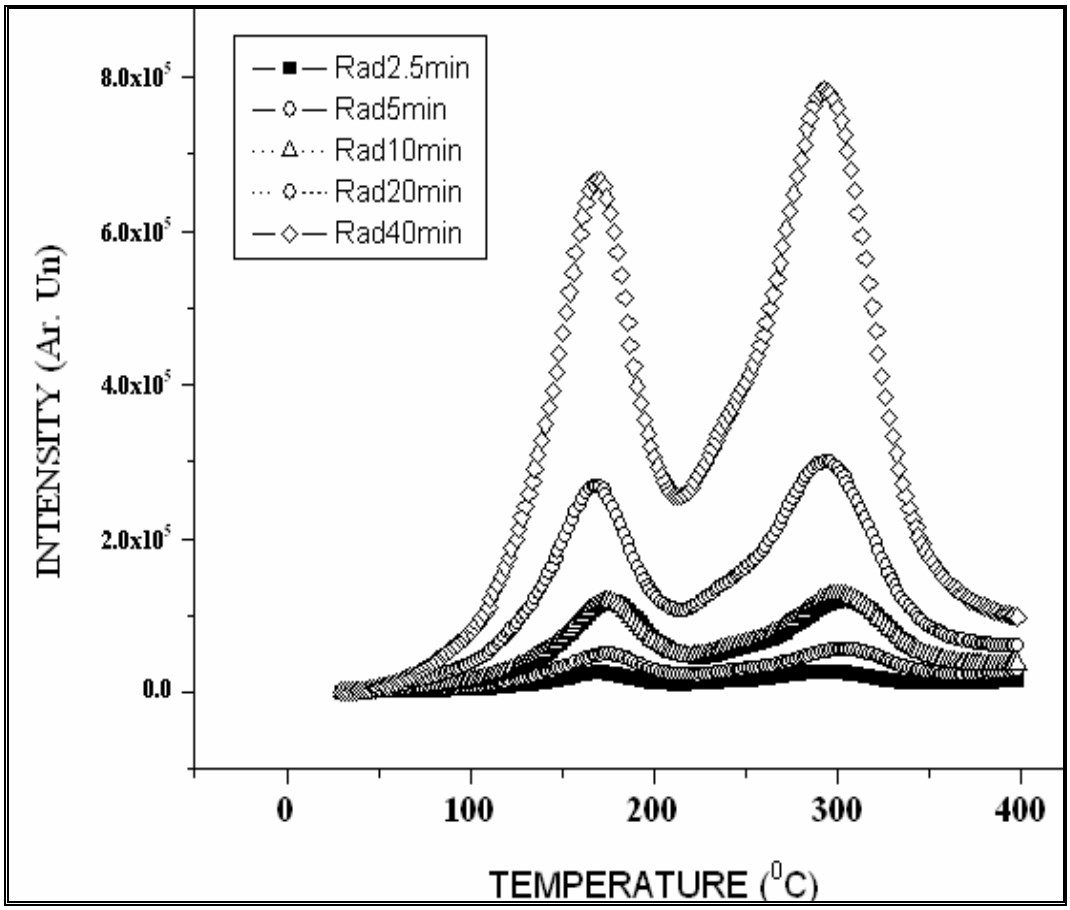

Figure 6.30. The influence of the ^{90}Sr-^{90}Y β (beta)-ray as a function of irradiation time on the 1% Al doped MgB_4O_7 phosphor at rate of 0.9 Gy/min

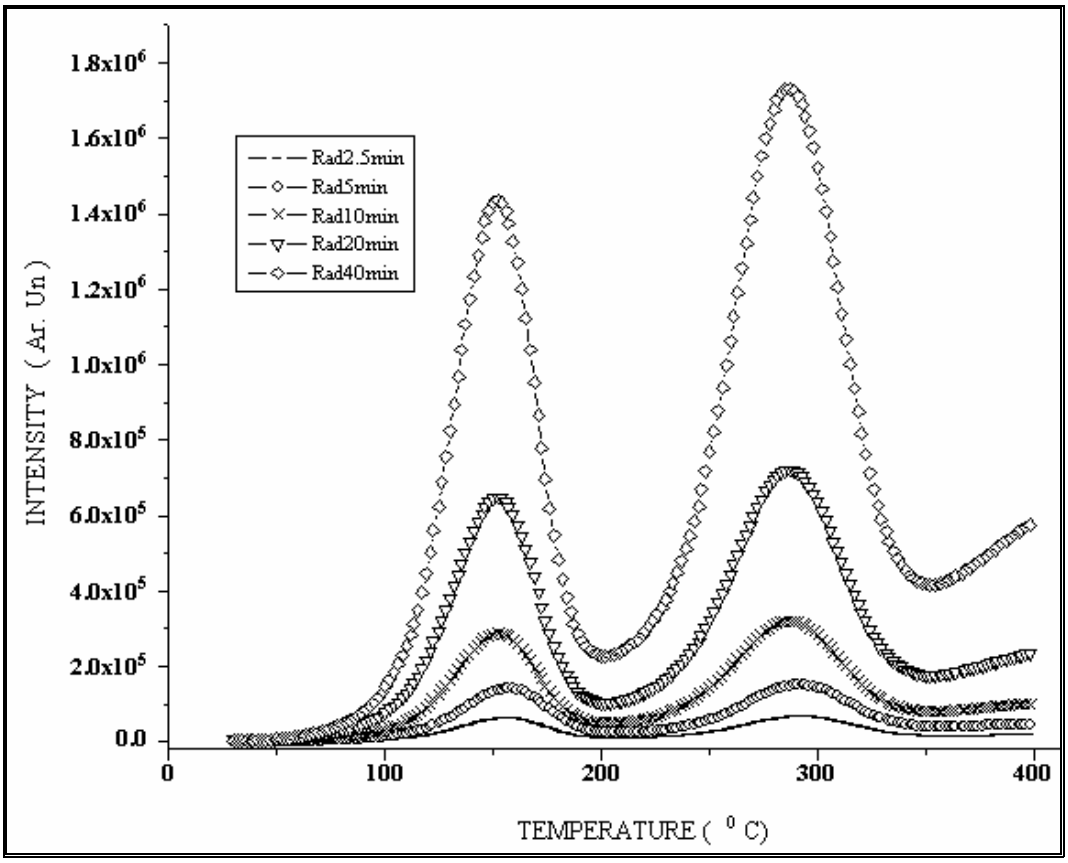

Figure 6.31. The influence of the ^{90}Sr-^{90}Y β (beta)-ray as a function of irradiation time on the 1% Mn-doped MgB_4O_7 phosphor at 293 K

The glow curve 1% Mn doped MgB_4O_7 consisted of two well separated TL peaks. The main and maximum peak situated at about 290 ^oC and low temperature peak at about 150 ^oC.

The dose response curves were obtained by taking the mean value of five measurements. As seen, the integrated TL dose response curves of prepared both materials are approximately linear in the range of investigated region with no observed superlinearity and saturation effects see figure 6.32. The TL-dose dependence curve was observed to be almost linearity in studied dose range from 2.25 Gy to 36 Gy for radiation processing dose levels.

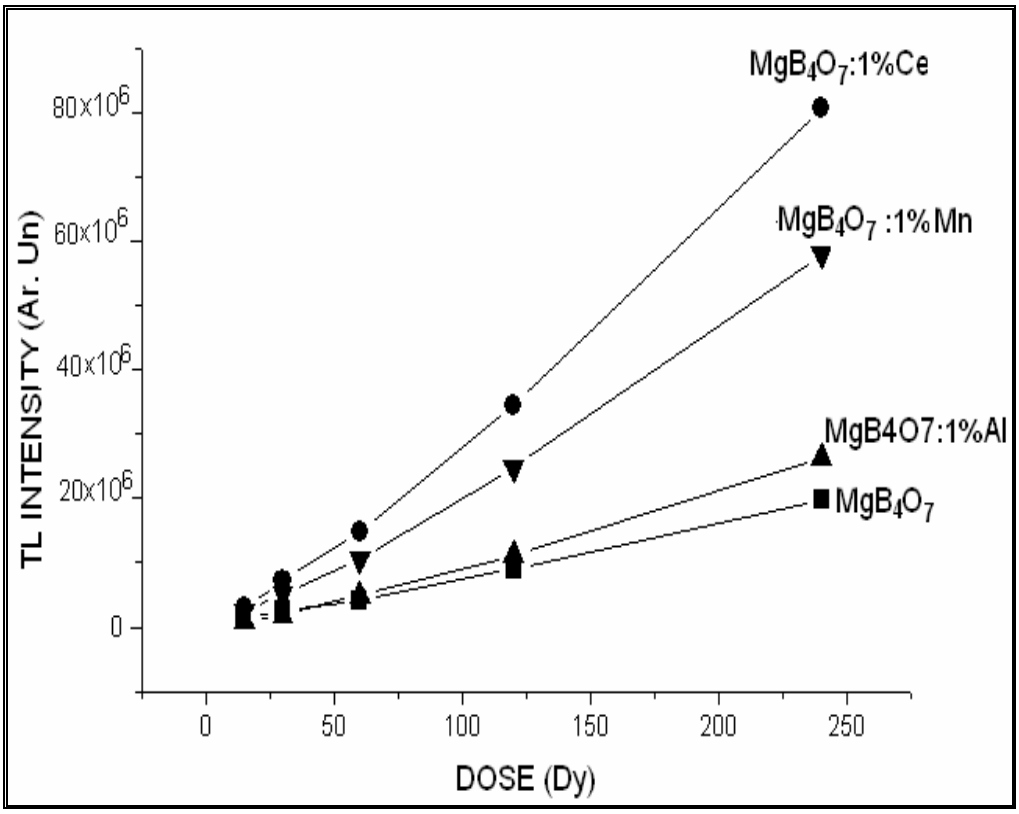

Figure 6.32. Linearity range of the TL responses of 1% Ce (●) Al (▲), Mn (►) doped and undoped MgB_4O_7 (■) phosphors versus exposed doses

By comparison of Ce and Al-doped MgB_4O_7 samples, it can be seen that Ce activator enhances the TL properties more than Al activator. As seen from Figure 6.32, 1% Ce-doping to MgB_4O_7 increases its TL output about three times but the same condition Al-doping increases its intensity approximately 1.5 times. Therefore, it is interpreted that Ce-doping is better than Al doping for MgB_4O_7 samples. However, much more research is still needed to strengthen this comment.

6.5. The Thermoluminescent Properties of Undoped CaB_4O_7

CaB_4O_7 sample was prepared by melting method in our thermoluminescence laboratories. Calcium tetraborateborate sample was made by mixing Calcium carbonate ($CaCO_3$) (99%, Merck) and boric acid (H_3BO_3) (99.5%, Merck) in stoichiometric ratio and the mixture was heated at 400 ^oC in a porcelain crucibles for 4 hour to remove carbonates and water from the samples. Then sample was heated to 900 ^oC for 10 hour which assures a complete crystallization. After this stage, sample was cooled down rapidly up to 500 ^oC. Then the samples are taken out of furnace and dried in a dessicator. The resultant glassy mass was ground in an agate mortar again. The glassy mass is sintered at 400 ^oC for 4 hour and then ground and sieved to obtain 100-200 mesh powder. One of synthesized sample CaB_4O_7 and X -ray analyze has taken by using a Rigaku X-ray Diffractometer with a Cu K_α (λ=1.5405Å) radiation source. Inter plane spacing (d), lattice parameters of unit cell and miller indexes are found by using previously explained computer program [120]. X-ray diffraction pattern of powder samples of CaB_4O_7 is seen in Fig. 6.33. Crystals systems are tired and $\sum \Delta d (= d_{obs} - d_{cal})$ value was found to be minimum for monoclinic. There are seven predominant peaks which used in calculation unit cell. Without the addition of activators, the presence of the activators has no effect on patterns. A good agreement is obtained between the observed and calculated d-values as seen in (Table 6.7), confirm the suitability of the crystal structure and unit cell parameters. The lattice parameters of unit cell were found to be a=6,45 Å, b=3.74 Å, c=5.59 Å and unit cell volume V=125,8 $Å^3$.

Table 6.7. Comparison of observed and calculated *d*-values (Å) of the most intensive reflections of CaB_4O_7 in room temperature

Peak No	$d_{obs.}$	$d_{calc.}$	h k l	Δd
1	4.2267	4.2267	1 0 1	0.000
2	3.5588	3.5588	2 0 0	0.000
3	2.7120	2.7120	0 0 2	0.000
4	2.6345	2.6345	0 1 2	0 .000
5	2.0562	2.0584	2 1 1	0.050
6	1.6681	1.6686	1 1 2	0.017
7	1.8241	1.8239	-2 2 2	-0.020

A good agreement between the absorbed and calculation *d*-values for monoclinic system, confirm the suitability of the crystal structure and unit cell parameters.

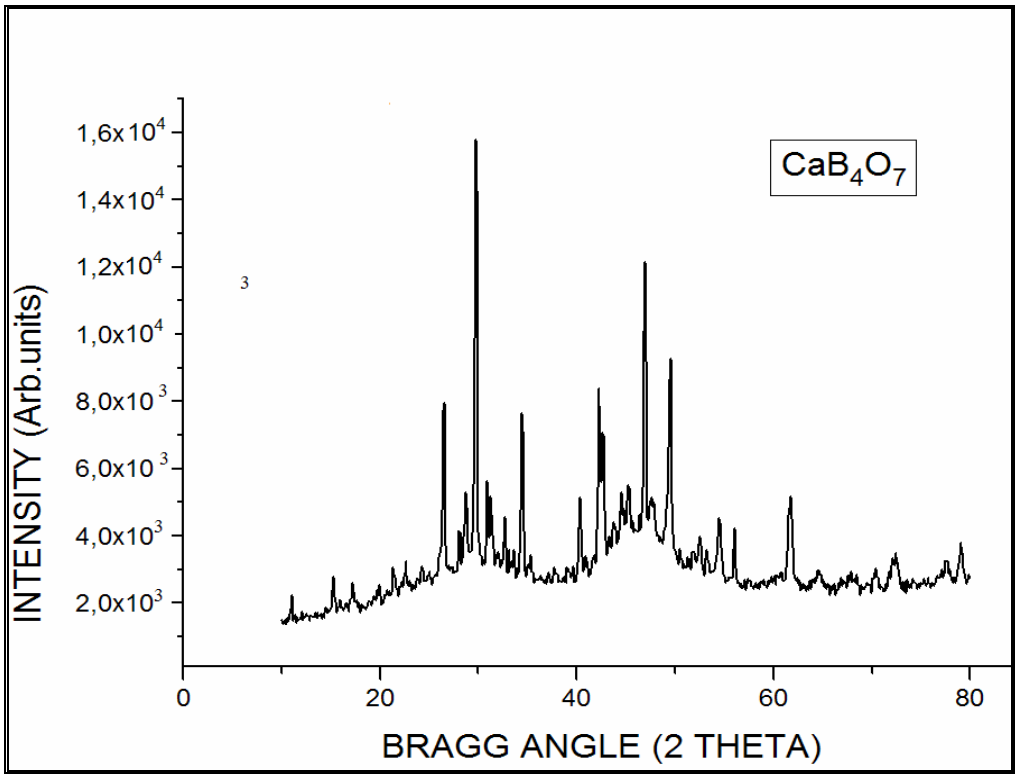

Figure 6.33. The XRD pattern of CaB_4O_7 which synthesized with melting method

During the study of TL properties of undoped CaB_4O_7, the glow curves of them were again recorded for different times of β-irradiation. Some of the selected glow curves of CaB_4O_7 powder samples were shown in Figure 6.34, β-irradiating at room temperature between 5 min and 120 min.

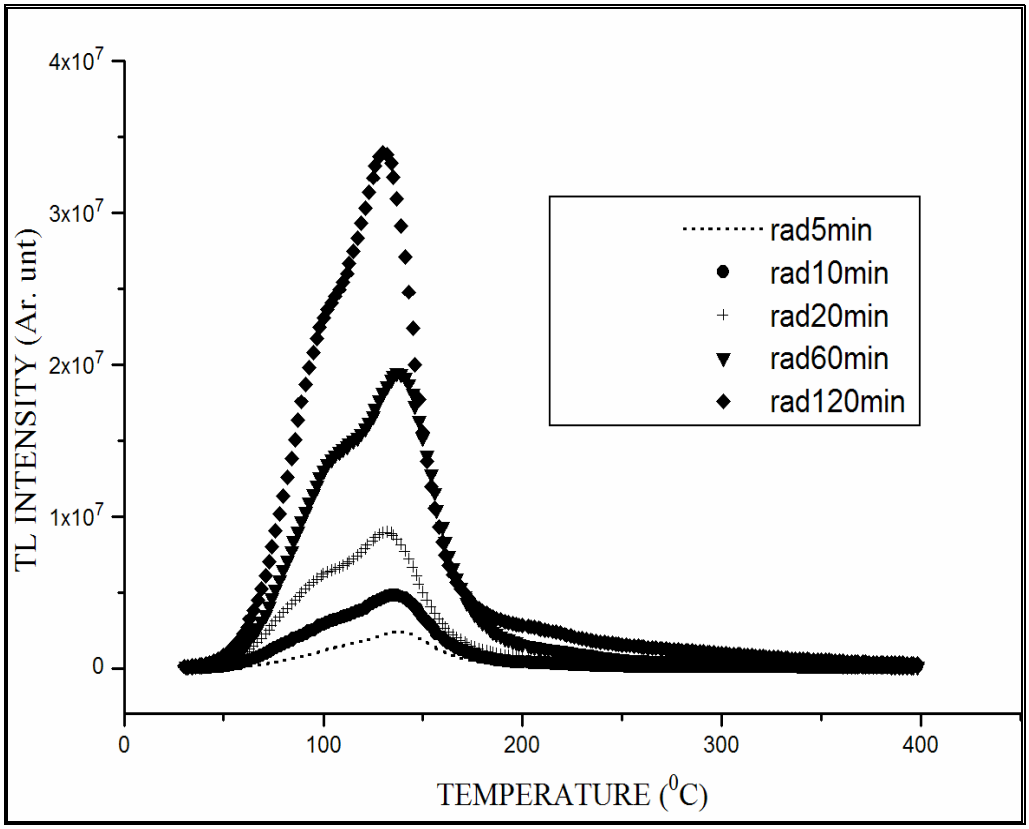

Figure 6.34. The influence of the ^{90}Sr-^{90}Y β (beta)-ray as a function of irradiation time on the CaB_4O_7 phosphor at 293K

The peak temperature of main peak situated at about 138 ^oC and low temperature shoulder at about 86 ^oC. Samples were read immediately after irradiation and it is seen that there are no great differences in the glow curve structures with increasing dose levels. But maximum peak temperature shifts toward low temperature side with increasing exposed dose level. The main peak of this sample is not suitable for radiation dosimetry, because the temperature is not

high enough to preserve the TL intensity when stored at room temperature. And sample is too hygroscopic to be used in air.

In order to check the reproducibility of the dose measurements using the CaB_4O_7 phosphor a number of repeated readouts were carried out for the same β-ray dose. Figure 6.35 shows the results obtained after five repeated cycles of annealing-irradiation-readout. The slight variation in the maximum TL intensity during the five cycles indicates that phosphor is reusable in the TL studies.

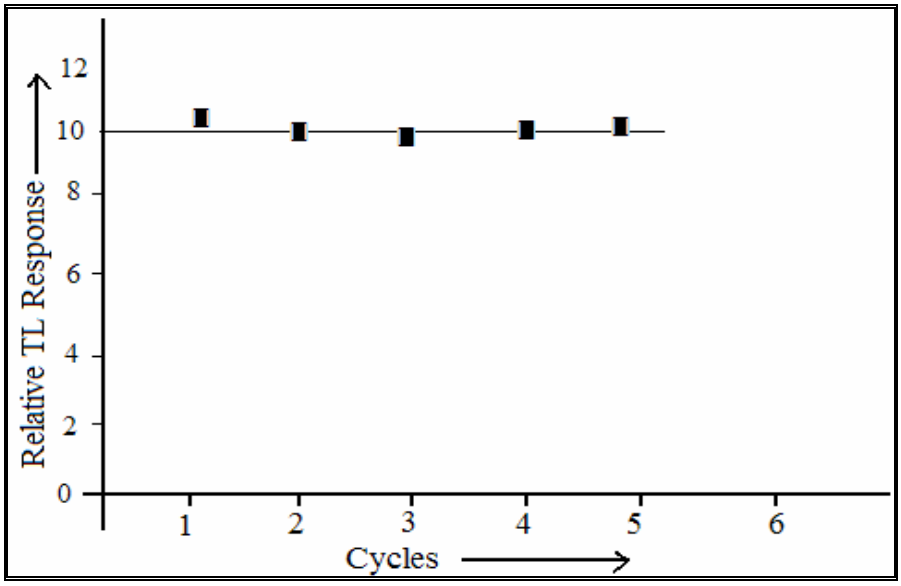

Figure 6.35. Reproducibility of CaB_4O_7 sample through five repeated cycles of annealing-irradiation-readout

The TL properties of several borates doped with different activators such as Ce, Mn, Al, Cu and ascertained that the sintered samples always show a better TL reponse than of undoped. The above study was undertaken to discover whether some other borates doped with activators my show more suitable TL responses that may be used for dosimetry.

CHAPTER VII

CONCLUSION

The thermoluminescence dosimetry is rapidly gaining acceptance as standard dosimetric technique in fields' radiation protection, personnel, environmental and clinical dosimetry. Despite of its well known and its broad application TLD is often regarded as mystic phenomena. Some users achieve astonishing results with great accuracy, while for others all attempts seem to fail. The aim of this study is to develop new TL materials that based on alkaline erath borates which can be used as a radiation dosimetry. In this manner, it was attempted to focus on methods of crystal growth and characterizing growth TL materials. At the end of this study, it was observed that;

1) The undoped and Ce-doped polycrystalline BaB_4O_7 powder samples were prepared by a melting method and the formation of the compounds were confirmed by an X-ray diffraction study. The TSL studies of undoped sample show a prominent glow peak at 195 °C and three small peaks at 117, 255 and 365 °C whereas Ce-doped sample show three prominent TL glow peaks at 195, 250, 331 °C and two small peaks at around 90 ^{o}C and 135 °C when heated at a constant heating rate of 1 °C/s. Comparative TSL studies of these two compounds show that the Ce-doped BaB_4O_7 compound is approximately five times more sensitive than

undoped compound. The obtained Ce-doped BaB_4O_7 crystal is quite suitable for use in high dose measurements in medical or industrial area between 0.01 Gy and 30 Gy due to its good linear dose response during this range and its low fading, but much more research is still needed to increase the sensitivity of this sample due to its low sensitivity when compared TLD-100. The TL emission spectra of Ce-doped showed a maximum peak at 360 nm for all measurements during TL measurements which is attributed to the characteristic emission from 5d to 4f transitions of Ce^{3+} ion [141].

2) The polycrystals of undoped and metal elements doped LiB_3O_5 compounds were synthesized with solid state method in air condition successfully. The TL out signals of these compounds were steadily increased after incorporation of impurities such as Al, Mn, and Cu or rare-earth impurities which are well known as very efficient activators in many materials, for example in alkali halide crystals or in oxides. As explained previously, after the investigation of TL properties of Al, Mn and Cu-doped samples, it was found that Al-doped LiB_3O_5 samples have much more sensitivity then the others. Therefore, the TL properties of Al-doped samples were studied in detail in the given present study. It was observed that the intensity of glow peaks of this material is increased with increasing Al-concentration. This result indicates that Al-ion behaves as a recombination center in the doped samples. The TSL studies of undoped and Al-doped LiB_3O_5 samples show similar glow curve structures which have three TL glow peaks at about 60±2 ^oC, 120±2 ^oC and 195±2 ^oC when heated at a constant heating rate of 1 $^oC/s$. Whereas their comparative TSL studies indicates that 1% Al-doped LiB_3O_5 compound is approximately 2.5 times more sensitive than undoped compound. The

TL emission spectra of Al-doped showed a maximum band at around 520 nm. The main dosimetric characteristics, which are namely the TL dose response, TL sensitivity, fading, minimum detectable dose, reproducibility, precision of dose measurement and annealing procedure, were shown that Al-doped LiB_3O_5 sample could be used in dosimetric applications. In addition, it was observed that the TL sensitivity of this material to beta radiation is approximately 3 times lower than that of TLD-100. Moreover, LiB_3O_5 tissue equivalent absorption coefficient is about Z_{eff} ≈7.4 and this value is very near to human tissue equivalent which is equal to Z_{eff} ≈7.42. Therefore, the results suggest that the main peak at approximately 200 ^{o}C can be safely used as dosimetric peaks in medical applications.

3) The polycrystalline of undoped, Ce, Al, and Mn activators doped MgB_4O_7 compounds were also synthesized with melting method in air condition. After the investigation of TL properties of Ce-doped MgB_4O_7 samples, it seems as a promising TL detector of different dosimetric applications. By comparison of Ce, Mn and Al-doped MgB_4O_7 samples, it was found that Ce activator enhances the TL properties more than Al and Mn activator. 1% Ce-doping to MgB_4O_7 increases its TL output about three times and the same condition Al-doping increases its intensity approximately 1.5 times and Mn doing increases about 1.2 times.

4) The polycrystallized lithium tetraborate ($Li_2B_4O_7$) are generally used as TLD materials. The solid state method which used in this study was found to give rise to a moisture resistant property for this phosphor. The dosimetric characteristics of $Li_2B_4O_7$ are like linearity, fading, and reusability were found very well so it is one of the most promising phosphors for TLD. $Li_2B_4O_7$ phase formation is quite slow and its melt solidifies into a glassy state unless very slow cooling rate are maintained.

5) As a result, it can be considered that, the developed two samples (BaB_4O_7:Ce and LiB_3O_5:Al) seems promising as a TL detector of different dosimetric applications owing to their simple glow curves with high sensitivity, the absence of thermal fading even at elevated temperatures, reduced light sensitivity, re-usability with good reproducibility and chemical stability.

REFERENCES

[1] Horowitz (Ed), Y.S., (1984), *Thermoluminescent and Thermoluminescent Dosimetry,* Vols. 1–3, CRC Press, Boca Raton, FL.

[2] McKeever, S.W.S., Moscovitch, M. and Townsend, P.D., (1995), *Thermoluminescence Dosimetry Materials: Propeties and Uses, Nuclear Technology Publishing*, Kent .

[3] Bos, A.J.J., (2001), *Nuc.Inst. And Meth. in Phy. Res.* ***B*** 184 3-28.

[4] Kleinert H., (1989), *Gauge Fields in Condensed Matter*, Vol. II, "STRESSES AND DEFECTS",743-1456, World Scientific (Singapore).

[5] Meyer, G., (1982), *Prog. Solid St. Chem*, **14**, 141.

[6] Azorin, J., Furetta, C., and Gutierrez, A., (1993), *Phys. Stat. Sol. a* **138**, 9.

[7] Townsend, P.D. and Kelly, J.C., (1993), *Colour Centres and Imperfections in Insulators and Semiconductors*, Sussex University Press, London, 70.

[8] Vij, D.R., (1993), Editor, *Thermoluminescent Materials,* PTR Prentice-Hall, New Jersey.

[9] Chen, R., and McKeever, S.W.S.,(1997) *Theory of Thermoluminescence and Related Phenomena*, World Scientific, Singapore, page; 286-287.

[10] Berker, K.,(1970), *Solid-State Dos.*, CRC Crit. Rev.Radiol. Sci.,**1 (3)**, 363.

[11] Kathren, R.L, in : Kase, K.R, Bjårngard, Attix, F.H., (1987), *The Dosimetry of Ionizing Radiation*, Vol. II, Academic Press, Orlando, , p.303.

[12] Wiedemann, E. And Schmidt, G.C., (1895),*Uber Liminsecenz, Ann, Phys. Chem.*, **54**, 604.

[13] Przibram, K. *et al.,* (1923), *Akad. Wiss. Wien [Ila]*, **132,** 262, 285. 3.

[14] Randall, J.T. and Wilkins, M.H.F. (1945),*Proc*. R. Soc., London Ser. A 184.

[15] Garlick, G.F.J. and Gibson, A.F. (1948), *Proc. Phys. Soc.* **60**, 574.

[16] Johnson, N.M., (1960), *Journal Of Sedimentary Research* **30**, 305-313.

[17] Daniels, F., Boyd, C.A. and Saunders, D.F., (1953), *Science* **117**, 343.

[18] McKeever, S.W.S., (1985), *Thermoluminescence of Solids*, Cambridge University Press, Cambridge .

[19] Mosisek, M., (1966), *Therm. of Some Irradiated Polymers, Proc. 2nd Tihany Symp.Radiat.Chem*., DoboJ. And Hedvig P., Eds, Budapest.

[20] Mosisek, M., (1968), *Thermoluminescence of Some Irradiated Polymers*, Jaderna Energ., 14, 198.

[21] Fleming, S.J., (1969), *Thermoluminescence from Irradiated Polymers, Proc. R. Aust. Chem. Inst.* 36, 199.

[22] Partridge, R.H., (1972), *Thermoluminescence. in polymers, in Radiation Chemistry of Polymers*, vol.1. Dole, M. Ed., Acad. Pres, New York, 194.

[23] Tomita, A., (1970), *J. Phys. Soc. Jap*., **28**, 731.

[24] Mozisek, M., (1970), *J.Appl. Radiat. Isotopes*, **21**,11.

[25] Lyman, T., (1935), *Phys. Rev*. **48**, 149.

[26] Tousey, R., (1951), *Phys. Rev*. **83**, 792.

[27] Watanabe, K., (1951), *Phys. Rev*. **83**, 785.

[28] Kossel, W, Mayer, V., and Wolf, H.C., (1954), *Sim. Von. Str. Am leb Ob Naturwissenschaften,* **41**,209.

[29] Wick, F.G. and Slattery, M.K., (1928), *J.Opt. Soc. Am*.**16**, 398.

[30] Ginther , R.J., (1954), *Electrochem. Soc*.,101, 248.

[31] Ginther, R.J. and Kirk, R.D., (1957), *J. Electrochem. Soc.* **104**,365.

[32] Gorbics, S.G. *et al*, (1968), *Int. J.Appl, Radiat. Isotopes*, **19**, 81.

[33] Morehead, F.F. and and Daniels, F., (1952), *J.Phys.Chem.**56***, 546.

[34] Schulman, J.H., et al. (1963), *Thermoluminescent Methods in Personnel Dosimetry*, Proc.Symp.Pers. Dos. Techn., Madrid, OECD/ENEA, Paris, 319.

[35] Mandeville , C.E. and Albrecht, H.O., (1954), *Phys. Rev.* **94**, 44.

[36] Becker, K., Cheka, J.S., and Oberhofer, M., (1970), *Health Phys*.**19**,391.

[37] Scarpa, G., (1970), *Phys. Med. Biol*., **15**, 667.

[38] Yamashita, T., Nada, N. Onishi, H. Kitamura, S., (1971), *Health Phys.*,**1**, 295.

[39] Spurny, Z., (1972), *Thermalox 995 (BeO) as Thermoluminecent Dosimeter of Gamma Component in Field of Neutrons*, Paper IAEA/SM-160/52 Proc. Symp. Dosimetry Techniques Applied to Agriculture, Industry, Biology, and Medicine, IAEA, Vienna, 1.

[40] Luchner, K., (1957), *Ann. Phys*.,**149**,435.

[41] Schayes, R. *et al.*, (1963), *La Dosimetrie par Thermoluminescence, Rev. MBLE 6*, 33 MBLE, Brussels. Belgium.

[42] Botshvar, I.A., *et al*., (1963), *At. Energ*,**15**,48.

[43] Ginther, R.J., (1965), *Therbium-Activated Thermoluminescent Glass for Dosimetry, in Luminescence Dosimetry*, CONF-650637,118.

[44] Garrett, D.E.,(1998), *Borates, Handbook of Deposits, Processing and Use*, Academic Press, London

[45] Boss, A.J.J., (1998), *Radiat. Meas.*, **29** (3-4), 319-322.

[46] Boss, A.J.J., Piters, T.M., Gomez Ros, J.M., And Delgado, A., (1993), *Iri-Ciemat Report,* **131**-93-005 (Iri,Deltt).

[47] Kazanskaya, V.A., Kuzmin V.V, Minaeva, E.E. and Sokolov, A.D., (1974), *in procceding 4th international conference on Luminescence Dosimetry*, Krakow, poland, 581.

[48] Manam, J. and Sharma, S. K., (2004), *J. Mat.Science* **39**, 6203 – 6208.

[49] Sangeeta, S.C. Sabharwal, (2004), *Journal of Luminescence*.

[50] Juan, L. *et al*, (2004), *Nuclear Instr. and Meth. in Phy. Res. B.*

[51] Hitomi, T. (1971). *Rad. Dos. And Mat.Therfor*.U.S.Pat. Filed n_0 **213,** 950.

[52] Prokic, M. (1980)*, Nucl. Instrum. Meth.* 175, 83-86.

[53] Karali, T., Rowlands A.P, Prokic M, Townsend P.D, Halmagean E, (2002). *Radiat Prot Dosimetry.* **100** (1-4):333-6.

[54] Adrovic, F, Prokić M, Ninković, M.M, Glisić, R. (2004), *Rad. Prot. Dosimetry* .**112**(3),439-42.

[55] Furetta, C., Prokic, M., Salamon, R., Kitis, G., (2000), *Appl. Radiat. Iso*t.**52** (2), 243-50.

[56] Driscoll, C.M.H., Mundy, S.J., and Eliot, J .M., (1981), *Radiation Protection Dosimetry*, 135-137.

[57] Furetta, C.*et al*., (1999), *Nucl. Inst. Meth. In Phys. Res. A* **420**, 441-445.

[58] Pradhan, A.S., (1981), *Radiation Protection Dosimetry*,**1**, 153.

[59] Campos, L.L. and Fernandes, F., (1990), *Radiation Protection Dosimetry*, 111-113.

[60] Souza, J.H, Ferrari, V.A., And Freitas de L.C., (1993), *Radiation Protection Dosimetry,* 239-242.

[61] Fukuda, Y., Okuno, T., and Takeuchi N.,(1983), *Radiation Protection Dosimetry,* 309-312.

[62] Fukuda, Y.**,** Okuno, T., and Takeuchi, N., (1986), *Radiation Protection Dosimetry* **17**,97-401.

[63] Prokic, M., (2000), *Applied Radiation and Isotopes* **52**, 97-103.

[64] Rojas, S.S, Yukimitu, K., A.S.S. de Camargo, Nunes, L.A.O. and Hernandes, A.C., (2006), *Journal of Non-Crystalline Solids* Vol. **352**, Issues 32-35, 3608-3612 .

[65] Mazzetti, C., Carli, F.D., (1926), *Gazetta Chimica Italiana,* **56**, 23.

[66] Rollet, A.P., Bouaziz, R., (1955), *Comptes Rendus*, **240**, 2417.

[67] Moryc, U., Ptak W.S., (1999), *Journal of Mol. Structure*, **241**,511-512.

[68] Ogorodnikova, I.N., Isaenkob, L.I., Kruzhalova, A.V., Porotnikova, A.V., (2001), *Radiation Measurements,* **33**, 577–581.

[69] Senguttuvana, N. *et al*., (2002), *Nuc. Ins.and Meth.in Phys.Res.A,* **486**, 264-267.

[70] El-Faramawy *et al*., (2000), *Radiation Phyiscs and Chemistry*, 8.

[71] Furetta, C., Sanipoli C., Scacco, A., Somaiah, K., (1996), *Radiation Protection Doimetry*, 339-342.

[72] Danilkina, M., Kerikmäea, M., Kirillova A., Lusta, A., (2006), *Proc. Estonian Acad. Sci. Chem.*, **55**, 3, 123–131.

[73] Zhengye, X. Qiang, T. Zhang, Z. *Science in China Series G: Physics, Mechanics and Astronomy*, 311-320.

[74] Prokić, M. (2002), *Radiat Prot Dosimetry*. **100.**

[75] Wall, B .F, Driscoll, C.M .H., Strong, J.C. and Fisher, E.S. (1982), *Phys. Med. Biol.*1023-1034.

[76] Miljanić ,S. Ranogajec-Komor M, Knezević, Z. Stuhec, Prokić, M., (2006), *Radiat Prot Dosimetry.* **119**, 191-196.

[77] Laksmanan, A.R., Chandra, B., and Rhatt, C.H., (1981), *Rad .Proc. Dos.*191-198

[78] Ronogajec-Komor, M., (2002), *Thermoluminescence dosimetry-Appl. in Monitoring Radiation Safety Management,* **2** (1), 2-16.

[79] Bos, A.J.J. and Piters, T.M. (1993), *Radiat. Prot. Dosim.* **47**, 41.

[80] Boss, A.J.J, Dielhot J.B.,(1991), *Radition Prot. Dos.* **36,** 23.

[81] Chen, R., in: Horowitz, (Ed)Y.S., (1984), *Therm. and Thermoluminescent Dosimetry*, Vol. **1**, CRC Press, Boca Raton, FL, 81.

[82] Randall, J.T. and Wilkins, M.H.F. (1945), *Proc. R. Soc. Lon. Ser. A* **184**, 366.

[83] Randall, J.T. and Wilkins, M.H.F. (1945), *Proc. R. Soc. London Ser. **A*** **184**, 390.

[84] Randall,J.T. and. Wilkins, M.H.F. (1945), *Proc. R. Soc. London Ser.* **A 184**, 367.

[85] Kitis, G., Gomez, J.M. -Ros and Tuyn, J.W.N. (1998), *J. Phys. D* **31**, 2636–2641.

[86] Pagonis, R.V., Mian, S.M. and Kitis, G. (2001), *Rad. Prot. Dosim.* 93, 11.

[87] Garlick, G.F.J. and Gibson, A.F. (1948), *Proc. Phys. Soc.* **60,** 574.

[88] Randall, J.T. and Wilkins M.H.F., *(1945), Proc R.Soc. London Ser. A **184,*** 392.

[89] May, C.E. and Partridge, J.A., (1964), *J. Chem. Phys.* **40**, 1401.

[90] Chen, R., and McKeever, S.W.S. (1997), *Theory of Thermoluminescence and Related Phenomena*, World Scientific, Singapore.

[91] Chen, R., and Winer, A.A., (1970), *J.Appl. Phys*. **41**,5227.

[92] Kelly, P.J., Laubitz, M.J.and Bräunlich, P., (1960), *Phys. Rev. **B*** **4**.

[93] Piters, T.M. and Bos A.J.J., (1993), *J. Phys. D* **26,** 2255.

[94] Chen, T-C., and Stoebe, T.G. (1998), *Radiat. Meas.* **29**, 39.

[95] Chen, R. (1969). *J.Appl.Physics* **40**, 570.

[96] Grossweiner, L.I, (1953), *J. Appl. Physics* **24,** 1306.

[97] Bunghkbardt, B., Singh, D. and Piesch E. (1977). *Nuclear Instrumentatio and Methods*, 142.

[98] Halperin, A., and Braner, A.A., (1960), *Phys. Rev.* **117,** 405.

[99] Hoogenboom, *et al*., (1988), *Journal of Applied Physics*, 3193-3198.

[100] Yazıcı, A.N. and Öztürk, Z., (1998), *Turk J. Phys*. **22**(1) 1-8.

[101] Boss A.J.J., Piters, T.M., Gomez, Ros J.M., And Delgado, A., (1993), *Iri-Ciemat Report 131-93-005 (Iri,Deltt).*

[102] Yazici, A.N. Chen, R., Solak, S.and Yegingil, Z., (2002), *J. Phys .D. Appl. Phys*., **35**, 2526.

[103] Horowitz ,Y.S. and Yossian, D., (1995), *Radiat. Protect. Dosim.,* **60**,1.

[104] Daniels, F., Boyd, C.A. and Saunders, D.F. (1953), *Science **117***, 342.

[105] Mohan, N.S. and Chen, R., (1970), *J.Phys.: Appl. Phys.*, **3**, 243-247.

[106] Hoogenboom, J.E. de Varies W., Dielhof, J.B., and Boss, A.J.J., (1988), *Journal of Applied Physics*, 3193-3200.

[107] Akselrod, M.S., Kortov, V.S., Kravetsky, D.J. and Gotlib, V.I., (1990), *Radiat. Prot. Dosim.* **32**, 15.

[108] Akselrod, M.S., Kortov, V.S.,. Kravetsky, D.J and Gotlib, V.I., (1990), *Radiat. Prot. Dosim. 33*, 119.

[109] Akselrod, M.S.,. Kortov, V.S and Gorelova, E.A. (1993), *Radiat. Prot. Dosim.* **47**, 159.

[110] Rosenflanz, A., Frey, M, Endres, B., Anderson, T, Richards, E., & Schardt, C., (2004), *Nature* **430**, 761–764.

[111] Yamashita, Y., Yasuna,Y. and Ikeda ,M., (1974), *Health Phys*. **27**, 201.

[112] Yamashita, et al, (1974), *Health Phys*. **27**, 202.

[113] Boss, A.J.J. (1998), *Radiat. Meas.,* **29** (3-4),319-322.

[114] Azorin, J., Furetta,C., and Gutierrez, A., (1993), *Phys. Stat. Sol. a* **138**, 9.

[115] Manam, J. Sharma S.K., (2004), *Nucl. Instr. And Meth. B* **217**, 314.

[116] Schipper , W.J., Blaase G., Leblans P., (1994), *Chem. Matter***. 6,** 1784.

[117] Mckeever, S.W.S., (1993), *Therm. of sol., At. En Press,* 12 .

[118] Danby, R.J., (1988), *J. Phys. C. Solid State Physics,* **21**, 485–494.

[119] Yazıcı, A. N., (1993), *Thermal and optical Charateristics of Radiation Induced Defect Centers in Alkali Halide Crystal, PhD Thesis.*

[120] Flinders, E.Wu., *Powd-an interactive Powder diffraction Data interpretation and indexing program version 2.* by University Bedford Australia.

[121] Kazanskaya, V.A., Kuzmin, V.V., Minaeva, E.E. and Sokolov, A.D., (1974), *in proc. 4th intern. Conf. on Lum. Dos.*, Krakow, poland, 581.

[122] Laksmanan, A.R. Chandra, B. and Rhatt, C.H. (1982), *Rad .Proc. Dos.***2**(4) 231.

[123] Furetta, C., Prokic, M., Salamon, R., and Kitis, G., (2000), *Apll. Radiation and isotopes* **52,** 243.

[124] Fukuda, Y., Mizuguchi, K., and Takeuchi, N., (1990), *Rad. Protect. Dosimetry* **33**, 111.

[125] Kowatari, M., Koyama, D., Satoh, Y., Linuma, K., Uchida, S, (2002), *Nucl. Instr. And Meth.* **B** 480, 431.

[126] Prokic, M., (2001), *Radiat. Meas.* **33,** 393.

[127] Ogorodnikov, I.N., Kuznetsov, A.Y., Kruzhalov, A.V.,.Maslov, V.A, (1995), *Radiat.Meas.*, **24**, 423.

[128] Ogorodnikov, I.N., Kruzhalov, A.V., Kuznetsov, A.Y., (1996), *Radiat. Protect .Dosim.*, **65**, 109.

[129] Sabharwal, S.S.C., (2006), *J.Crystal Growth*, **289**, 703.

[130] Özdemir, Z., Özbayoglu, G., Yılmaz, A, (2007), *J.Mater.Sci*., 42, 8501.

[131] Ardiçoğlu, B., Özbayoğlu, G., Özdemir Z., and Yilmaz, (2006), A., J.Alloys and Compd. 418, 77.

[132] Bétourné, E., Touboul, M., (1997), *J. Alloys Compd.,* **255,** 91.

[133] Radaev, S.F. Sorokin, N.I., Simonov, V.I., (1991), Fiz. Tverd.Tela., 33, 3597.

[134] Ishii, M. *et al.(* 2004), *Radiat. Meas.* **38,** 571–4.

[135] Kitis, G., Furetta C., Prokic, M. and Prokic, V. (2000), *J. Phys. D: Appl.Phys.* 33, 1252–62.

[136] Takenaga, M., Yamamoto, O., Yamashita, T. (1980), *Nucl. Instr.. Methods* 175, 77–8.

[137] Prokic, M., (2002), *Radiat. Prot. Dosim.* **100,** 265–8.

[138] Zhang, T.Z., Su, Q. (2000), *J.SID* **8,** 27.

[139] Powder diffraction file No.32-0549 JCPDS-ICDD, USA.

[140] May, C.M., Partridge, J.A., (1964), *Chem. Phys*. **40,** 1401.

[141] Yazici, A.N., Doğan, M., Kafadar, V. E., Toktamis, H., (2006), *Nuclear Instruments and Methods in Physics Research* B **246**, 402–408.

CURRICULUM VITAE

PERSONAL INFORMATION

Surname, Name : Doğan Mehmet
Nationality : Turkish (TC)
Date and Place of Birth : 1972 , ŞANLIURFA
Marital Status : Married
Phone : +90 532 695 04 65
Fax : +90 414 511 00 15
Email : mhdogan@hotmail.com

EDUCATION

Degree	Institution	Year of Graduation
MS	Inonu Un. Nat. & Appl Sc.Ins. Phys Dept.	2000
BS	Inonu Un. Sc. And Art fac. Phys. Dept	1997
High School	Gaziantep Anadolu Lisesi	1993

WORK EXPERIENCE

Year	Place	Enrollment
2003-Present	DOĞANLAR PAMUK SAN. AŞ.	Owner of the firm and Manager

FOREIGN LANGUAGES

ENGLISH

PUBLICATIONS

1. Yazici, A. N., Doğan, M., Kafadar, V. E. and Toktamış, (2006), *Thermoluminescence of undoped and Ce-doped BaB_4O_7, Nucl. Enst.and meth. In Phys. Res. Sec.B. vol.* **246,** page;402-408,

2. Doğan, M. Balcı, Y, Yakıncı, M.E., Aksan M.A., ve Ateş H., (1999), HgBaCaCuO Sistemine Pb katkılanmasının Etkilerinin incelenmesi, I. Ulusal Yüksek Sıcaklık Süperiletkenler Kongresi, Trabzon/TÜRKİYE,

3. Aksan, M.A., Yakıncı, M.E., Balcı, Y., Ateş, H. ve Doğan, M., (1999) "Daldırma Yöntemi ile Hazırlanmış Bi-Sr-Ca-Cu-O Süperiletken Kalın Filmlerde Manyetik Yönlendirme" I. Ulusal Yüksek Sıcaklık Süperiletkenler Kongresi, Trabzon/TÜRKİYE.

4. Yakıncı, M.E., Balcı Y., Aksan, M.A., Ateş H. ve Doğan M., (1999), "Cam-Seramik $Bi_2Sr_2Ca_2Cu_3O_{10+x}$ H *T c* Süperiletken Çubukların Termal İletkenlik Özellikleri" I. Ulusal Yüksek Sıcaklık Süperiletkenler Kongresi, Trabzon/TÜRKİYE.

5. Balcı Y., Yakıncı, M.E., Aksan M.A., Ateş H. ve Doğan M., (1999), "BSCCO (n=3) Sistemine Titanyum Katkılanmasının Etkisi" I. Ulusal Yüksek Sıcaklık Süperiletkenler Kongresi, Trabzon/TÜRKİYE.

6. Yakıncı, M.E., Balcı Y., Aksan, M.A., Ateş, H. ve Doğan, M., (1999), "In-Situ DC Arc Sputtering" Yöntemi ile Üretilen $Y_{0.8}Cd_{0.2}Ba_2Cu_3O_7$ Süperiletken İnce Filmlerin Elektriksel ve Mikroyapısal Özellikleri" I. Ulusal Yüksek Sıcaklık Süperiletkenler Kongresi, Trabzon/TÜRKİYE.

7. Yazici, A.N, Doğan, M., Khaidukov, N.M. Makho*v,* V.N., (2004), Ce^{3+}, Tb^{3+}, Dy^{3+} ve Tm^{3+} ile ayrı ayrı katkılanmış çift potasyum yttrium florit' in α ve β ışımasının karşılığındaki termoluminasans özellikleri, Türk Fizik Derneği 22. Fizik Kongresi, Bodrum, Türkiye

8. Doğan, M. (2000), M.Sc Thesis, Senthesize of the $HgB_2Ca_{n-1}Cu_nO_{2n+2+\delta}$ Sperconductors and investigating of the Pb Substitution effects on the electrical and Physical Properties, Inonu University.